PHILOSOPHICAL TRANSACTIONS OF THE ROYAL SOCIETY A MATHEMATICAL, PHYSICAL & ENGINEERING SCIENCES

Steep Gravity Waves in Water of Arbitrary Uniform Depth

E. D. Cokelet

Phil. Trans. R. Soc. Lond. A 1977 **286**, 183-230
doi: 10.1098/rsta.1977.0113

STEEP GRAVITY WAVES IN WATER OF ARBITRARY UNIFORM DEPTH

By E. D. COKELET
Institute of Oceanographic Sciences, Wormley, Godalming, Surrey

(*Communicated by M. S. Longuet-Higgins, F.R.S. – Received* 21 *October* 1976)

CONTENTS

Modern applications of water-wave studies, as well as some recent theoretical developments, have shown the need for a systematic and accurate calculation of the characteristics of steady, progressive gravity waves of finite amplitude in water of arbitrary uniform depth.

In this paper the speed, momentum, energy and other integral properties are calculated accurately by means of series expansions in terms of a perturbation parameter whose range is known precisely and encompasses waves from the lowest to the highest possible. The series are extended to high order and summed with Padé approximants.

For any given wavelength and depth it is found that the highest wave is not the fastest. Moreover the energy, momentum and their fluxes are found to be greatest for waves lower than the highest. This confirms and extends the results found previously for solitary and deep-water waves.

By calculating the profile of deep-water waves we show that the profile of the almost-steepest wave, which has a sharp curvature at the crest, intersects that of a slightly less-steep wave near the crest and hence is lower over most of the wavelength.

Vol. 286. A 1335. 24 [Published 18 July 1977

An integration along the wave profile cross-checks the Padé-approximant results and confirms the intermediate energy maximum.

Values of the speed, energy and other integral properties are tabulated in the appendix for the complete range of wave steepnesses and for various ratios of depth to wavelength, from deep to very shallow water.

1. Introduction

An accurate knowledge of the field of motion in progressive, irrotational water waves is essential for many applications in coastal engineering, offshore structures, ship hydrodynamics, open-channel flows and air–sea interaction. Since the pioneering work of Airy (1845), Stokes (1847, 1880*b*), Rayleigh (1876) and others, most applications have relied on approximations, based on the assumptions that the wave slopes are small or that the particle accelerations are negligible compared to gravity – assumptions no longer valid for waves of finite steepness. These approximations lead to motions that are either sinusoidal or cnoidal in form.

More recently practical demand for better accuracy has led to the use of higher-order approximations such as the Stokes fifth-order series for waves in finite-depth water (De 1955) or the ninth-order Rayleigh–Boussinesq series for solitary waves (Fenton 1972). However two difficulties have arisen. First, it was discovered by Schwartz (1974) that the Stokes small-amplitude expansion for deep-water waves is not convergent beyond a certain wave steepness, less than the maximum. This means that to sum these series use must be made of Padé approximants or other summation techniques; in any case it is impossible to follow Stokes in using the amplitude of the first harmomic as the expansion parameter. Secondly, it was discovered by Longuet-Higgins & Fenton (1974) for solitary waves and also by Longuet-Higgins (1975) for deep-water waves that many characteristics of gravity waves, such as the speed, energy and momentum, are not monotonic functions of the wave amplitude, as had always been assumed, but in fact increase up to a certain wave amplitude and then diminish before the wave of greatest amplitude (for a given wavelength) is reached. Thus the highest waves are not necessarily the fastest or the most energetic.†

These discoveries emphasized the need for a reliable calculation of the form and characteristics of even the simplest, symmetric progressive waves in water of uniform depth for all amplitudes up to the highest. It is this which the present paper aims to provide. In point of fact the calculations were first begun in order to provide an accurate check on the general numerical method of calculating time-dependent free-surface flows described by Longuet-Higgins & Cokelet (1976).

In §2 we formulate the problem and assume a solution in the form of a Fourier series whose coefficients must be determined (Stokes 1847, 1880*b*).

In §3 following Schwartz (1974) we represent the Fourier coefficients as series in terms of a perturbation parameter. Recursion relationships are derived between expansion co-efficients at various orders which provide for their efficient calculation on a digital computer. In the manner of Longuet-Higgins (1975) we define a perturbation parameter in terms of the fluid speed at the wave crest in such a way that its range is known *ab initio*. The procedure for determining the expansion coefficients is outlined, and the practical computational limitations are discussed.

The series for the wave height and speed are summed in §4 by using $[N/N]$ Padé approximants. Some examples of the degree of numerical convergence are given. We find that for all depths the highest wave is not the fastest. A comparison of our results with those of other researchers shows

† There is evidence of this also in a paper by Sasaki & Murakami (1973). For solitary waves confirmation has been provided by a quite independent method of calculation (Byatt-Smith & Longuet-Higgins 1976).

good agreement in some cases. In others it is suggested why adequate results for highest waves have not previously been obtained.

In § 5 the mass, momentum, energy and their respective fluxes are calculated for various depths. It is found that they too achieve maximum values for waves somewhat lower than the highest and then decrease as the highest wave is approached. These results are supported by Padé approximating different series and combining them by using relations between the integral properties.

We demonstrate in § 6 that the profile of an almost-highest wave intersects that of a slightly lower wave near the wave crest, and consequently the higher wave is on average *less extreme*. This helps to explain the intermediate maxima in the integral properties. Finally we integrate along the wave profile directly to *confirm* the maxima in the potential energy for near-highest waves.

Tables of the integral properties of the waves as functions of the perturbation parameter are presented in the appendix for relative fluid depths ranging from deep-water to about $\frac{1}{60}$ of a wavelength.

2. Formulation of the problem

Consider two-dimensional, periodic, surface waves of wavelength λ and wavenumber $k = 2\pi/\lambda$ propagating under the influence of gravity, g, in a fluid of constant density, ρ. Take units of mass, length and time such that $\rho = k = g = 1$ and hence $\lambda = 2\pi$. Assume that the fluid is inviscid and incompressible and that the motion is irrotational. The waves are assumed to propagate from left to right over a horizontal bottom without change of form. By a choice of reference frame the fluid velocity at any fixed depth always within the fluid averaged over one wave cycle may be taken as zero. The frame of reference so defined is unique as is the propagation speed, c, of the waves with respect to that frame.

Choose rectangular coordinates (x, y) such that the x-axis is horizontal and the y-axis is directed vertically upwards. Locate the free surface at $y = \eta$ and the bottom at $y = -d$. The mean elevation of the free surface is $\overline{\eta}$ where an overbar denotes an average over one wave cycle. Therefore the mean depth is $D = d + \overline{\eta}$ and does not in general equal d. Since the fluid is irrotational and incompressible a velocity potential, ϕ, and stream function, ψ, can be defined such that the velocity, (u, v), may be written

$$\left.\begin{aligned} u &= \frac{\partial \phi}{\partial x} = \frac{\partial \psi}{\partial y}, \\ v &= \frac{\partial \phi}{\partial y} = -\frac{\partial \psi}{\partial x}, \end{aligned}\right\} \tag{2.1}$$

and both ϕ and ψ satisfy Laplace's equation, $\nabla^2\phi = \nabla^2\psi = 0$.

Now consider a second rectangular coordinate system (X, Y) moving in the positive x-direction with the waves at speed c. In this reference frame the motion is independent of time, t. The velocity potential, Φ, stream function, Ψ, and velocity, $(\mathscr{U}, \mathscr{V})$, in this frame are related to similar quantities in the (x, y)-frame by

$$\left.\begin{aligned} &X = x - ct, \quad Y = y, \quad \Phi = \phi - cx, \quad \Psi = \psi - cy, \\ &\mathscr{U} = u - c = \frac{\partial \Phi}{\partial X} = \frac{\partial \Psi}{\partial Y}, \\ &\mathscr{V} = v = \frac{\partial \Phi}{\partial Y} = -\frac{\partial \Psi}{\partial X}. \end{aligned}\right\} \tag{2.2}$$

PHILOSOPHICAL TRANSACTIONS OF THE ROYAL SOCIETY A MATHEMATICAL, PHYSICAL & ENGINEERING SCIENCES

It is convenient to define the complex variables $Z = X + \mathrm{i}Y$ and $W = \Phi + \mathrm{i}\Psi$ which are analytic functions of one another. The Z-plane is shown in figure 1.

The boundary conditions to be imposed on the flow are that the free surface and bottom are streamlines, that is

$$\left.\begin{aligned} \Psi &= 0 \quad \text{on} \quad Y = \eta, \\ \Psi &= Q \quad \text{on} \quad Y = -d. \end{aligned}\right\} \tag{2.3}$$

Also the pressure along the free surface is assumed to be equal to the constant atmospheric pressure ($p = 0$) with the effects of surface tension neglected. This condition can be related to the fluid velocity and surface displacement through the Bernoulli equation applied at the free surface

$$\mathscr{U}^2 + \mathscr{V}^2 + 2\eta = K \quad \text{on} \quad \Psi = 0, \tag{2.4}$$

where K is the Bernoulli constant.

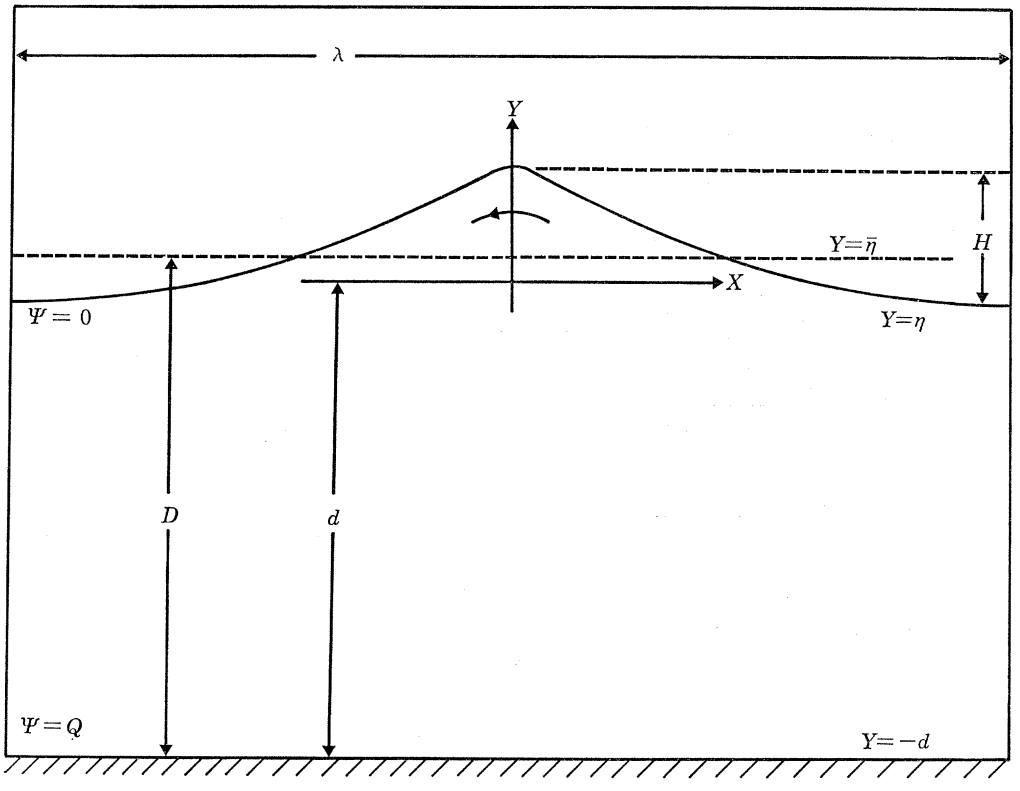

FIGURE 1. The Z-plane.

Stokes (1847) first solved this problem by taking the complex velocity potential W as essentially a Fourier series in the complex coordinate Z of the form

$$\frac{W}{c}(Z) = A_0 Z + B_0 + \sum_{j=1}^{\infty} (A_j \mathrm{e}^{\mathrm{i}jZ} + B_j \mathrm{e}^{-\mathrm{i}jZ}). \tag{2.5}$$

The complex constants A_j and B_j are then determined by satisfying the boundary conditions. Later Stokes (1880*b*) realized that the problem could be considerably simplified if he took Z as a Fourier series in W of the form

$$Z(W) = A_0 \frac{W}{c} + B_0 + \sum_{j=1}^{\infty} (A_j \mathrm{e}^{\mathrm{i}jW/c} + B_j \mathrm{e}^{-\mathrm{i}jW/c}) \tag{2.6}$$

since the boundary conditions are to be satisfied along lines of constant Ψ (the imaginary part of W). Stokes (1847) also showed that the profile of a steady wave must be symmetric about the crest (later proved by Levi-Civita (1925)) which in terms of the complex variables means

$$Z(W) = -Z^*(-W^*). \tag{2.7}$$

Here the asterisks denote complex conjugation, and the origin has been placed beneath the wave crest. Applying the bottom boundary condition of (2.3), the symmetry condition (2.7) and the fact that $\overline{\mathscr{U}} = -c$ to (2.6) yields

$$Z(W) = -\frac{W}{c} + \mathrm{i}\sum_{j=1}^{\infty}\frac{a_j}{j}(\mathrm{e}^{\mathrm{i}jW/c} - \mathrm{e}^{-2jd}\mathrm{e}^{-\mathrm{i}jW/c}), \tag{2.8}$$

where the height of the origin above the bottom has been defined such that $d \equiv Q/c$. The depth d is sometimes referred to as the undisturbed fluid depth and represents the depth of a uniform stream flowing with speed c whose mass flux equals that of the wave. The real and imaginary parts of (2.8) give

$$X = -\frac{\Phi}{c} - \sum_{j=1}^{\infty}\frac{a_j}{j}(\mathrm{e}^{-j\Psi/c} + \mathrm{e}^{-2jd}\mathrm{e}^{j\Psi/c})\sin\left(j\frac{\Phi}{c}\right), \tag{2.9a}$$

$$Y = -\frac{\Psi}{c} + \sum_{j=1}^{\infty}\frac{a_j}{j}(\mathrm{e}^{-j\Psi/c} - \mathrm{e}^{-2jd}\mathrm{e}^{j\Psi/c})\cos\left(j\frac{\Phi}{c}\right). \tag{2.9b}$$

From equation (2.9a) it is apparent that a change in Φ/c of 2π is equivalent to traversing one wave cycle in the Z-plane. The real constants a_j in (2.8) are determined by satisfying the Bernoulli equation (2.4) on the free surface. The complex velocity, q, is given by

$$q = \mathscr{U} - \mathrm{i}\mathscr{V} = \frac{\mathrm{d}W}{\mathrm{d}Z} = \left(\frac{\mathrm{d}Z}{\mathrm{d}W}\right)^{-1} = \frac{-c}{1 + \sum_{j=1}^{\infty} a_j(\mathrm{e}^{\mathrm{i}jW/c} + \mathrm{e}^{-2jd}\mathrm{e}^{-\mathrm{i}jW/c})}. \tag{2.10}$$

Substitution of (2.9) and (2.10) into (2.4) gives

$$c^2 + \left(2\sum_{j=1}^{\infty}\frac{a_j}{j}\delta_j\cos\left(j\frac{\Phi}{c}\right) - K\right)\left\{\left[1 + \sum_{j=1}^{\infty}a_j\sigma_j\cos\left(j\frac{\Phi}{c}\right)\right]^2 + \left[\sum_{j=1}^{\infty}a_j\delta_j\sin\left(j\frac{\Phi}{c}\right)\right]^2\right\} = 0, \tag{2.11}$$

where two parameters depending only on d and defined by

$$\left.\begin{aligned}\sigma_j &= 1 + \mathrm{e}^{-2jd},\\ \delta_j &= 1 - \mathrm{e}^{-2jd},\end{aligned}\right\} \tag{2.12}$$

have been introduced.

Expanding equation (2.11) as a cosine series and equating the harmonic coefficients to zero we have

$$\left.\begin{aligned} c^2 + 2\sum_{l=1}^{\infty}\frac{a_l\delta_l f_l}{l} &= Kf_0,\\ \sum_{l=1}^{\infty}\frac{a_l\delta_l}{l}(f_{|l-j|} + f_{l+j}) &= Kf_j \quad (j = 1, 2, \ldots),\end{aligned}\right\} \tag{2.13}$$

where the f_j have been introduced for convenience and are defined in terms of the a_j by

$$\left.\begin{aligned} f_0 &= 1 + \sum_{l=1}^{\infty}a_l^2\sigma_{2l},\\ f_j &= a_j\sigma_j + \sum_{l=1}^{\infty}a_l a_{l+j}\sigma_{2l+j} + \frac{1}{2}\sum_{l=1}^{j-1}a_l a_{j-l}(\sigma_l - \delta_{j-l}) \quad (j = 1, 2, \ldots).\end{aligned}\right\} \tag{2.14}$$

In all summations each term is taken to be identically zero if the lower limit exceeds the upper.

The notation adopted here is the same as that of Schwartz (1974) who, following Nekrasov (1921), transformed one cycle of the Z-plane into an annular region in the ζ-plane by the mapping $\zeta \equiv r\,e^{ix} = e^{iW/c}$. (Note that due to the opposite direction of wave propagation Z and W are equal to $-z^*$ and w^* as defined by Schwartz.) The free surface maps to a circle of radius $r = 1$ and the bottom to a circle of radius $r = r_0 = e^{-d}$. Therefore Schwartz's σ_j and δ_j are equal to those defined in (2.12). Although useful in some instances the ζ-plane mapping obscures the simple form of the Fourier series (2.6). Since it is not a necessary step in the solution we will not consider it further.

3. The perturbation solution

Equations (2.13) and (2.14) are a set of nonlinear algebraic equations which determine the Fourier coefficients a_j completely. These can be solved in a consistent manner by a perturbation expansion technique. Let ϵ denote a global perturbation parameter which is zero for infinitesimal waves and is positive for higher waves.

Following Schwartz we assume expansions of the form

$$a_j = \sum_{k=0}^{\infty} \alpha_{jk}\,\epsilon^{j+2k} \quad (j = 1, 2, \ldots), \tag{3.1a}$$

$$f_j = \sum_{k=0}^{\infty} \beta_{jk}\,\epsilon^{j+2k} \quad (j = 0, 1, \ldots), \tag{3.1b}$$

$$c^2 = \sum_{l=0}^{\infty} \gamma_l \epsilon^{2l}, \tag{3.1c}$$

$$K = \sum_{l=0}^{\infty} \Delta_l \epsilon^{2l}. \tag{3.1d}$$

Substitution of (3.1) into (2.13) and (2.14) and equating coefficients of equal powers of ϵ yield the following recurrence relations:

$$\gamma_l + 2\sum_{j=0}^{l-1} \frac{\delta_{l-j}}{l-j} \sum_{m=0}^{j} \alpha_{l-j,\,j-m}\,\beta_{l-j,\,m} = \sum_{k=0}^{l} \Delta_{l-k}\,\beta_{0k} \quad (l = 0, 1, \ldots), \tag{3.2a}$$

$$\sum_{l=1}^{j} \frac{\delta_l}{l} \sum_{k=0}^{p} \alpha_{l,\,p-k}\,\beta_{j-l,\,k} + \sum_{l=1}^{p} \frac{\delta_{l+j}}{l+j} \sum_{k=0}^{p-l} \alpha_{l+j,\,p-l-k}\,\beta_{lk}$$
$$+ \sum_{l=0}^{p-1} \frac{\delta_{p-l}}{p-l} \sum_{k=0}^{l} \alpha_{p-l,\,l-k}\,\beta_{j+p-l,\,k} = \sum_{l=0}^{p} \Delta_l \beta_{j,\,p-l} \quad (j = 1, 2, \ldots;\ \ p = 0, 1, \ldots), \tag{3.2b}$$

$$\beta_{00} = 1, \quad \beta_{0k} = \sum_{l=1}^{k} \sigma_{2l} \sum_{p=0}^{k-l} \alpha_{lp}\,\alpha_{l\ k-l-p} \quad (k = 1, 2, \ldots), \tag{3.2c, d}$$

$$\beta_{jk} = \alpha_{jk}\,\sigma_j + \sum_{l=1}^{k} \sigma_{2l+j} \sum_{p=0}^{k-l} \alpha_{lp}\,\alpha_{l+j,\,k-l-p}$$
$$+ \frac{1}{2}\sum_{l=1}^{j-1} (\sigma_l - \delta_{j-l}) \sum_{p=0}^{k} \alpha_{lp}\,\alpha_{j-l,\,k-p} \quad (j = 1, 2, \ldots;\ \ k = 0, 1, \ldots). \tag{3.2e}$$

Equations (3.2a–e) are of order ϵ^{2l}, ϵ^{j+2p}, ϵ^0, ϵ^{2k} and ϵ^{j+2k} respectively. This system of equations is not closed until the expansion parameter ϵ has been specified.

Stokes (1847, 1880b) applied the method of successive approximation to this problem and found that the coefficients at any order can be determined solely in terms of those at lower orders.

The algebraic manipulation actually involved in finding the coefficients is exceedingly laborious, but Schwartz (1974) made a great advance. He was the first to derive equations (3.2) and using them was able to program the manipulations on a modern digital computer. This has allowed the Stokes expansion to be carried out to a very high order thus greatly increasing its usefulness.

(*a*) *The expansion parameter*

The choice of the expansion parameter ϵ is of considerable importance to this problem. A parameter whose range encompasses waves from the lowest to the very highest and which gives rapid convergence in the various perturbation series (3.1) is most desirable. Stokes chose for his parameter the first Fourier coefficient, a_1. This is zero for infinitesimal waves and increases initially with the wave height. To the order to which Stokes carried his approximation ($O(a_1^3)$ for general depths, $O(a_1^5)$ for deep water) this parameter proved satisfactory. With it he showed that the phase speed, c, increases with the wave height, H.

Schwartz (1974) carried Stokes's expansion out to order a_1^{70}. Using Domb–Sykes plots (a graphical version of the ratio test) and Padé approximants (rational fractions), he found that a_1 is not a monotonically increasing function of H. That is, for any given depth a_1 first increases with H, reaches a maximum and then decreases until H attains its peak value. Therefore, a_1 is not a suitable expansion parameter for waves near the highest since a single value of a_1 can correspond to *two different* wave heights.†

In order to remove the ambiguity in Stokes's expansion Schwartz chose a new expansion parameter

$$\epsilon = a = \tfrac{1}{2}H, \tag{3.3}$$

where a is the wave amplitude. He carried the expansions in (3.2) out to $O(a^{48})$ for general depths and to $O(a^{117})$ for deep water. The resulting series were summed with Padé approximants thus greatly increasing their domain of convergence.

The maximum value of a is not known *a priori*, and to determine it Schwartz made use of Stokes's (1880*a*) *conjecture* that the fluid velocity in the (x, y)-frame at the crest of the *highest* wave must equal the phase speed. In the moving (X, Y)-frame the crest is a stagnation point. What Stokes actually showed was that for a wave with a crest stagnation point the profile must become sharply pointed with an included angle of 120°. This solution is a *local* solution valid only at the stagnation point. Such a profile represents a *limiting* wave in the sense that any symmetric wave whose crest velocity in the (x, y) frame exceeds the phase speed cannot be steady. Stokes did not prove that such a *limiting* wave is a *highest* wave, but it turns out to be the case.

Therefore, accepting Stokes's conjecture equations (2.10) and (3.1*a*) give for the highest wave

$$\frac{c}{1+\sum_{j=1}^{\infty}\sigma_j a_j} = \frac{c}{1+\sum_{j=1}^{\infty}\sum_{k=0}^{\infty}\sigma_j \alpha_{jk}\epsilon^{j+2k}} = 0. \tag{3.4}$$

Taking c as finite and nonzero the denominator of (3.4) must be infinite. By $[N/N]$ Padé approximating the denominator of (3.4) and considering the limit of the smallest positive pole as N increased, Schwartz calculated the maximum wave amplitude for any given depth. He was then able to determine the wave speed as a function of wave height for waves from the lowest to

† An indication of this for deep-water waves is given in Table 3 of Monkmeyer & Kutzbach (1966), who iteratively solved a set of nonlinear algebraic equations for the first 15 Fourier coefficients. However, they do not mention the non-monotonicity of a_1 in their text, nor do their results indicate a maximum in the phase speed for the almost-highest wave.

near the highest for a variety of water depths. However the convergence of Schwartz's series deteriorated for very high waves and for very shallow depths.

A new expansion parameter has been introduced by Longuet-Higgins & Fenton (1974) in their study of solitary waves. The parameter ω' is defined by

$$\omega' = 1 - \frac{q_{\text{crest}}^2}{c_0^2}, \tag{3.5}$$

where q_{crest} is the fluid speed at the wave crest in the reference frame moving with the wave and c_0 is the phase speed of infinitesimal solitary waves. This parameter has the advantage that its range, $0 \leqslant \omega' \leqslant 1$, is known *ab initio*. For a linear wave the crest speed equals the phase speed ($q_{\text{crest}} = c_0$, $\omega' = 0$), and for the limiting wave the crest is a stagnation point ($q_{\text{crest}} = 0$, $\omega' = 1$). An added advantage is that the Padé-approximated perturbation series converge better with this parameter than with the wave amplitude as in the usual Rayleigh–Boussinesq expansion for solitary waves.

For a perturbation solution of periodic waves in deep water Longuet-Higgins (1975) used a similar expansion parameter

$$\omega = 1 - \frac{q_{\text{crest}}^2 q_{\text{trough}}^2}{c^2 c_0^2}, \tag{3.6}$$

where q_{trough} is the fluid speed at the wave trough. This parameter reduces to that used by Longuet-Higgins & Fenton for solitary waves and has a similar range, $0 \leqslant \omega \leqslant 1$. The q_{trough} term was introduced so that ω could be expressed by a series in even powers of Schwartz's parameter a. Taking Schwartz's series whose coefficients were supplied by the present author, Longuet-Higgins reverted to obtain series in ω which converged more rapidly than those in a. However this series reversion process was prone to the rapid loss of significant figures with increasing order.

We shall choose the expansion parameter ϵ defined as

$$\epsilon^2 = 1 - \frac{q_{\text{crest}}^2 q_{\text{trough}}^2}{c^4}. \tag{3.7}$$

This has the following attributes:

(1) its range, $0 \leqslant \epsilon \leqslant 1$, is known *ab initio*,

(2) most physical properties of the flow are expressable as series in even powers of ϵ,

(3) the perturbation expansion can be carried out initially in terms of ϵ without having to resort to series reversion, and

(4) the resulting series in ϵ can be readily summed with Padé approximants giving rapid convergence in a wider range of fluid depths and wave heights than previously possible.

(*b*) *Solving for the perturbation coefficients*

Now that the perturbation parameter has been specified the system of equations (3.2) and (3.7) is closed. The fluid speeds at the wave crest and trough are obtained from (2.10) with $\Psi = 0$ and $\Phi/c = 0$ and π respectively. Expanding the right hand side of (3.7) in powers of ϵ, we have

$$\epsilon^2 = 1 - \frac{1}{\left(1 + \sum_{j=1}^{\infty}\sum_{k=0}^{\infty} \sigma_j \alpha_{jk} \epsilon^{j+2k}\right)^2 + \left(1 + \sum_{j=1}^{\infty}\sum_{k=0}^{\infty} (-1)^j \sigma_j \alpha_{jk} \epsilon^{j+2k}\right)^2} \tag{3.8}$$

and after some rearrangement and reduction

$$\left(\frac{1}{1-\epsilon^2}\right)^{\frac{1}{2}} = 1 + 2\sum_{j=1}^{\infty}\sum_{k=0}^{j-1}\alpha_{2(j-k),\,k}\,\sigma_{2(j-k)}\,\epsilon^{2j} + \sum_{j=2}^{\infty}\sum_{l=1}^{j-1}\sum_{k=0}^{j-l-1}\sum_{m=0}^{j-l-k-1}\alpha_{2(j-l-k-m),\,k}\,\alpha_{2l,\,m}\,\sigma_{2(j-l-k-m)}\,\sigma_{2l}\,\epsilon^{2j} - \sum_{j=1}^{\infty}\sum_{l=0}^{j-1}\sum_{k=0}^{j-l-1}\sum_{m=0}^{j-l-k-1}\alpha_{2(j-l-k-m)-1,\,k}\,\alpha_{2l+1,\,m}\,\sigma_{2(j-l-k-m)-1}\,\sigma_{2l+1}\,\epsilon^{2j} \quad (j = 0, 1, \ldots). \tag{3.9}$$

Expansion of the left-hand side and equating powers of ϵ gives

$$\frac{(-1)^j\,(-\frac{1}{2})!}{j!\,(-\frac{1}{2}-j)!} = 2\sum_{k=0}^{j-1}\alpha_{2(j-k),\,k}\,\sigma_{2(j-k)} + \sum_{l=1}^{j-1}\sum_{k=0}^{j-l-1}\sum_{m=0}^{j-l-k-1}\alpha_{2(j-l-k-m),\,k}\,\alpha_{2l,\,m}\,\sigma_{2(j-l-k-m)}\,\sigma_{2l} - \sum_{l=0}^{j-1}\sum_{k=0}^{j-l-1}\sum_{m=0}^{j-l-k-1}\alpha_{2(j-l-k-m)-1,\,k}\,\alpha_{2l+1,\,m}\,\sigma_{2(j-l-k-m)-1}\,\sigma_{2l+1} \quad (j = 1, 2, \ldots), \tag{3.10}$$

where the equation is of order ϵ^{2j}.

The calculation procedure is as follows:

(1) specify the maximum order, N, of the perturbation expansion,

(2) specify the undisturbed fluid depth, d, and calculate $\delta_j = 1 - \mathrm{e}^{-2jd}$ and $\sigma_j = 1 + \mathrm{e}^{-2jd}$ ($j = 1, 2, \ldots, N$),

(3) calculate the coefficients at order ϵ^p in terms of the previously determined coefficients with $p = 0, 1, \ldots, 2M, 2M+1, \ldots, N$,

(a) within any even order, $2M$,

(i) calculate α_{ij} and β_{ij} by solving equations (3.2b) and (3.2d) simultaneously proceeding in the sequence $(i,j) = (2M, 0), (2M-2, 1), \ldots, (4, M-2)$,

(ii) calculate $\alpha_{1,M-1}$, $\beta_{1,M-1}$, $\alpha_{2,M-1}$ and $\beta_{2,M-1}$ by simultaneously solving equations (3.2d) with $j = 1$, $k = M-1$, (3.2b) with $j = 2$, $p = M-1$, (3.2d) with $j = 2$, $k = M-1$, and (3.10) with $j = M$,

(iii) calculate β_{0M} from equation (3.2c) with $k = M$,

(b) within any odd order, $2M+1$,

(i) calculate Δ_M from (3.2b) with $j = 1$, $p = M$,

(ii) calculate α_{ij} and β_{ij} by simultaneously solving (3.2b) and (3.2d) proceeding in the sequence $(i,j) = (2M+1, 0), (2M-1), \ldots, (3, M-1)$,

(4) and, finally, calculate γ_l from (3.2a) with $l = 0, 1, \ldots, \frac{1}{2}N$.

Notice that the odd-order coefficients $\alpha_{1,M-1}$ and $\beta_{1,M-1}$ cannot be determined until the next higher even order, and also that the even-order Δ_M cannot be determined until the next higher odd order. Table 1 shows a schematic representation of part 3 of the calculation scheme. The first column gives the order of the equations involved and the calculation proceeds from left to right, row by row through the remainder of the table.

(c) *Limits to the maximum order of the expansion*

The radius of convergence of a series is restricted by the location of the nearest singularity, but it can often be extended by using such analytical tools as Padé approximants. These are most

effective if the series can be calculated to a very high order with great accuracy. Such calculations are possible if the algebraic manipulations are handled by a modern digital computer. Of course, such computations are limited by the availability of computer time and space, the loss of significant figures, and the existence of computational overflow.

The calculation scheme was programmed in FORTRAN IV on Cambridge University's IBM 370/165 digital computer. The computations were done for specific depths with e^{-d} ranging from 0 to 0.9 in increments of 0.1. In double precision (approximately 17 significant figures) the required computer execution time ($\sim N^4$) for one value of d was 40 s to order ϵ^{110}. The storage space required ($\sim N^2$) was 90 K bytes where 1 byte equals 8 bits, a double precision word is 8 bytes and 1 K equals 1024.

TABLE 1. THE COEFFICIENT CALCULATION SCHEME: THE CALCULATION PROCEEDS LEFT TO RIGHT, ROW BY ROW

order						
0	$\beta_{0,0}$					
1	Δ_0					
2	$\alpha_{1,0}\beta_{1,0}\alpha_{2,0}\beta_{2,0}$	$\beta_{0,1}$				
3	Δ_1	$\alpha_{3,0}\beta_{3,0}$				
4	$\alpha_{4,0}\beta_{4,0}$	$\alpha_{1,1}\beta_{1,1}\alpha_{2,1}\beta_{2,1}$	$\beta_{0,2}$			
5	Δ_2	$\alpha_{5,0}\beta_{5,0}$	$\alpha_{3,1}\beta_{3,1}$			
6	$\alpha_{6,0}\beta_{6,0}$	$\alpha_{4,1}\beta_{4,1}$	$\alpha_{1,2}\beta_{1,2}\alpha_{2,2}\beta_{2,2}$	$\beta_{0,3}$		
.	.	.	.	.		
.	.	.	.	.		
.	.	.	.	.		
$2M$	$\alpha_{2M,0}\beta_{2M,0}$	$\alpha_{2M-2,1}\beta_{2M-2,1}$	$\alpha_{2M-4,2}\beta_{2M-4,2}$	. . .	$\alpha_{1,M-1}\beta_{1,M-1}\alpha_{2,M-1}\beta_{2,M-1}$	$\beta_{0,M}$
$2M+1$	Δ_M	$\alpha_{2M+1,0}\beta_{2M+1,0}$	$\alpha_{2M-1,1}\beta_{2M-1,1}$	. . .	$\alpha_{5,M-2}\beta_{5,M-2}$	$\alpha_{3,M-1}\beta_{3,M-1}$

The rate of loss of significant figures can be ascertained by comparing the results of the same calculation carried out at two different computer 'precisions', for example at single precision (approximately 7 significant figures) and double precision. Figure 2 is a plot of the number of significant figures lost against the order of the expansion for $e^{-d} = 0, 0.3, 0.5, 0.7, 0.9$. The loss-rate is about the same for each of the series in (3.1). The $e^{-d} = 0.5$ case was done in quadruple precision (approximately 35 significant figures). From the figure it is concluded that above moderate values of N the loss-rate increases with decreasing d until $e^{-d} = 0.5$ and then decreases. By extrapolation it appears that the $e^{-d} = 0.5$ double precision calculations would become useless past order ϵ^{90} or ϵ^{100}.

The presence of singularities is usually indicated by an increase in the magnitudes of the expansion coefficients with increasing order. Figure 3 is a plot of the magnitude of the largest $|\alpha_{ij}|$ against N for various d. The size of the coefficients increases with N and decreases with d, a result first noted by Stokes (1880*b*). Since the maximum physically allowable value of ϵ is 1, this would preclude the convergence of the sequence of partial sums of the series for high waves; however, it will be shown in §§4–6 that the $[N/N]$ Padé approximants give self-consistent convergence. The largest number which the IBM 370/165 can hold without overflow is of order 10^{75}. Therefore, by extrapolation from figure 3 we conclude that the computations will be limited at about $O(\epsilon^{120})$ for $e^{-d} = 0.9$ and at higher orders for greater depths.

Extrapolation of the curves for $e^{-d} = 0$ in figures 2 and 3 indicates that the deep-water results will be limited first by the loss of significant figures. In quadruple precision all 35 significant

figures will not be lost until order ϵ^{250} or ω^{125}. However Longuet-Higgins (1975) found that by reverting from series in a to series in ω no gain in accuracy was possible past order ω^{40}. This discrepancy is due to the large rounding errors inherent in reverting the series. These errors will become more pronounced as d decreases.

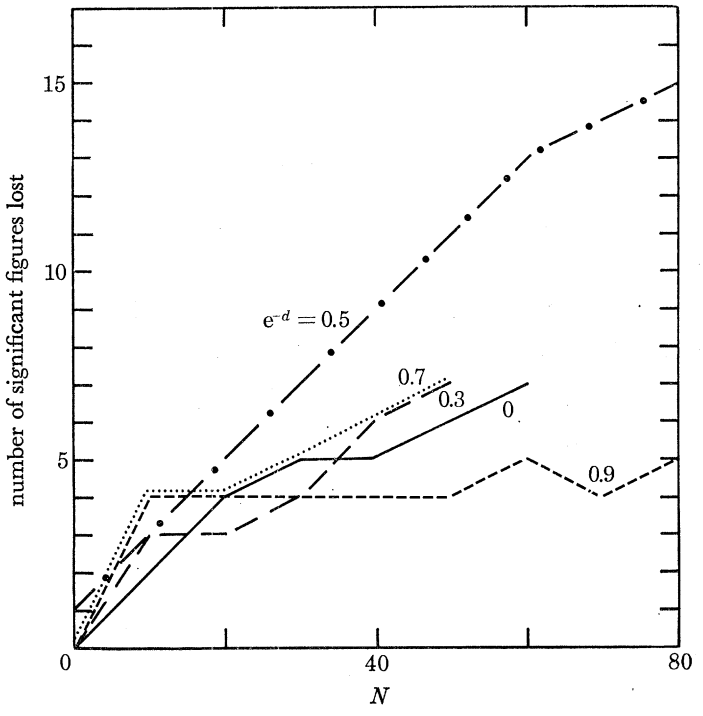

FIGURE 2. The number of significant figures lost plotted against the order of the expansion, N, for various fluid depths, d.

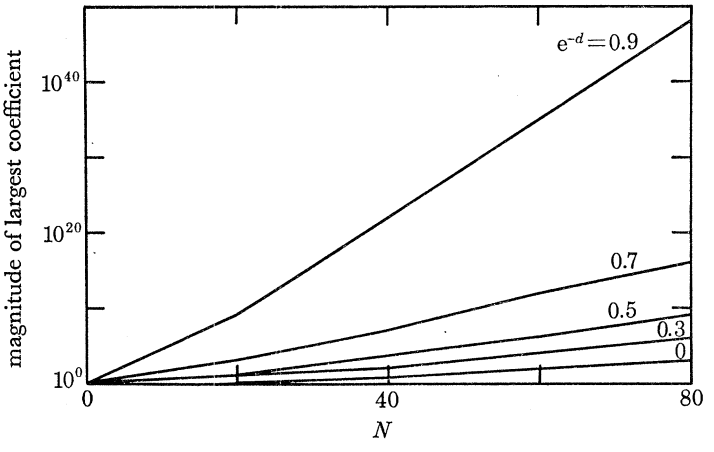

FIGURE 3. The magnitude of the largest expansion coefficient plotted against the order of the expansion, N, for various fluid depths, d.

4. The wave height and speed

The nonlinear behaviour of water waves traditionally has been illustrated by the dependence of the phase speed on the wave height. To express a as a series in ϵ similar to (3.1c) for c^2 we have from (2.9b) evaluated at the wave crest and trough

$$\begin{aligned} a = \tfrac{1}{2}H &= \sum_{j=1}^{\infty} \frac{a_{2j-1}\delta_{2j-1}}{2j-1} \\ &= \sum_{j=1}^{\infty}\sum_{l=1}^{j} \frac{\alpha_{2l-1,j-l}\delta_{2l-1}}{2l-1}\epsilon^{2j-1}. \end{aligned} \tag{4.1}$$

Thus a may be found in terms of the α_{ij} as determined in §3b.

For deep water the expansions to tenth order are

$$\left.\begin{aligned} a = {} & 4.08248\times10^{-1}\epsilon + 4.72510\times10^{-2}\epsilon^3 + 8.97681\times10^{-3}\epsilon^5 \\ & - 2.50178\times10^{-4}\epsilon^7 - 2.83082\times10^{-3}\epsilon^9 + \ldots, \\ c^2 = {} & 1 + 1.66667\times10^{-1}\epsilon^2 + 5.24691\times10^{-2}\epsilon^4 + 1.71496\times10^{-2}\epsilon^6 \\ & + 3.40850\times10^{-3}\epsilon^8 - 2.32940\times10^{-3}\epsilon^{10} + \ldots \end{aligned}\right\} \tag{4.2}$$

correct to 6 significant figures. With a few exceptions the order of magnitude of the coefficients decreases uniformly to 10^{-5} at order ϵ^{110} (beyond which we have not carried the expansion). Thus it seems likely that the series will converge even for the highest wave ($\epsilon^2 = 1$). An expansion in Longuet-Higgins's (1975) parameter, ω, behaves similarly, but this is in marked contrast to Schwartz's (1974) expansion in the wave amplitude, i.e.

$$\left.\begin{aligned} a &= a, \\ c^2 &= 1 + a^2 + 5\times10^{-1}a^4 + 2.5\times10^{-1}a^6 \\ &\quad - 4.88889\times10^{-1}a^8 - 4.56623a^{10} + \ldots. \end{aligned}\right\} \tag{4.3}$$

The order of magnitude of the coefficients in the c^2 series increases to 10^7 at order a^{30} (Schwartz 1972, table A-1). Using the maximum value of a of about 0.44 as determined by Schwartz, we find that the ratio of successive terms in the series exceeds 1 which implies that the simple sequence of partial sums will not converge for waves of maximum amplitude.

For $e^{-d} \leqslant 0.5$ our coefficients behave in a manner similar to those for deep water, but for shallower depths the coefficients begin increasing with order past some critical order (< 110) dependent on d.

(a) *The Padé-approximant results*

We shall use $[N/N]$ Padé approximants to sum the series for a and c^2 taking advantage of their ability to provide automatic analytic continuation. Briefly, the $[M/N]$ Padé approximant of a function $f(z)$ whose series expansion is known to order z^{M+N}, i.e.

$$f(z) = f_0 + f_1 z + \ldots + f_{M+N} z^{M+N} + \ldots, \tag{4.4}$$

can be defined by

$$[M/N]f(z) = \frac{p_0 + p_1 z + \ldots + p_M z^M}{1 + q_1 z + \ldots + q_N z^N}. \tag{4.5}$$

The p_j and q_j can be found in terms of the f_j by equating coefficients of powers of z in (4.4) and (4.5) to order z^{M+N}. The original series and the Padé approximants are thus equal to order z^{M+N}, but the Padé approximant has an infinite number of terms as can be shown by expanding

the reciprocal of the denominator as a series in z and multiplying by the numerator. $[M/N]f(z)$ is often much more useful than the truncated series (4.4) since the Padé approximant has at its disposal N poles corresponding to the N roots of the denominator.

When the number of poles of $f(z)$ is not known *a priori* the Padé approximant with the same order is both numerator and denominator, denoted $[N/N]f(z)$, is the most useful since it is invariant under Euler transformations. This means that in theory it is equal to the approximant obtained by first locating the successive poles of the function, mapping them away to infinity and then $[N/N]$ Padé approximating. (However, it should be pointed out that in practice fewer significant figures may be lost by first Euler transforming and then Padé approximating.)

TABLE 2*a*. SUMMED $[N/N]$ PADÉ APPROXIMANTS OF THE WAVE AMPLITUDE, a, AND THE WAVE SPEED SQUARED, c^2, FOR $e^{-d} = 0$

	$10a$			c^2		
N	$\epsilon^2 = 0.9$	$\epsilon^2 = 0.95$	$\epsilon^2 = 1$	$\epsilon^2 = 0.9$	$\epsilon^2 = 0.95$	$\epsilon^2 = 1$
1	4.35962	4.51298	4.66581	1.20930	1.22589	1.24324
2	4.64281	4.70608	4.82943	1.20952	1.22614	1.24354
3	4.23876	4.32868	4.37613	1.18673	1.18485	1.15968
4	4.24233	4.33712	4.39709	1.18983	1.19332	1.18666
5	4.24343	4.34059	4.40862	1.19004	1.19393	1.18864
6	4.24391	4.34296	4.42326	1.19010	1.19420	1.18981
7	4.24395	4.34325	4.42636	1.19013	1.19435	1.19104
8	4.24396	4.34331	4.42715	1.19013	1.19440	1.19170
9	4.24397	4.34468	4.42386	1.19013	1.19441	1.19212
10	4.24397	4.34356	4.41862	1.19013	1.19442	1.19249
11	4.24396	4.34333	4.42691	1.19013	1.19442	1.19268
12	4.24397	4.34341	4.43054	1.10913	1.19442	1.19248
13	4.24397	4.34342	4.43103	1.19013	1.19442	1.19280
14	4.24397	4.34344	4.43711	1.19013	1.19442	1.19297
15	4.24397	4.34342	4.43121	1.19013	1.19442	1.19280
16	4.24397	4.34342	4.43110	1.19013	1.19442	1.19284
17	4.24397	4.34342	4.43137	1.19013	1.19442	1.19283
18	4.24397	4.34342	4.43138	1.19013	1.19442	1.19289
19	4.24397	4.34342	4.43138	1.19013	1.19442	1.19286
20	4.24397	4.34342	4.43133	1.19013	1.19442	1.19284
21	4.24397	4.34342	4.43134	1.19013	1.19442	1.19284
22	4.24397	4.34342	4.43153	1.19013	1.19442	1.19270
23	4.24397	4.34342	4.43159	1.19013	1.19442	1.19257
24	4.24397	4.34342	4.43157	1.19013	1.19442	1.19257
25	4.24397	4.34343	4.43079	1.19013	1.19442	1.19345
26	4.24397	4.34342	4.43125	1.19013	1.19442	1.19453
27	4.24397	4.34342	4.43078	1.19013	1.19442	1.19323

Padé approximants were introduced into water-wave theory by Schwartz (1974) and were later employed successfully by Longuet-Higgins & Fenton (1974) and Longuet-Higgins (1975). Some useful references on Padé approximants and series singularities are Baker (1965), Graves-Morris (1973) and Van Dyke (1974).

Bearing in mind the limitations of § 3*c* we have carried out the series expansions to order ϵ^{110} in double precision for $e^{-d} = 0, 0.1, 0.2, \ldots, 0.9$. This maximum order is a compromise between order ϵ^{100} at which all significance will be lost for $e^{-d} = 0.5$ and order ϵ^{120} at which computational overflow will occur for $e^{-d} = 0.9$. More importantly, for most fluid depths and wave heights this is a sufficiently high order for the sequence of Padé approximants to converge to at least six figures.

Table 2 shows the sequence of summed $[N/N]$ Padé approximants of a and c^2 for values of ϵ^2 near 1 and for three fluid depths, $e^{-d} = 0$, 0.5, 0.9. It will be noted that the deep-water results, $e^{-d} = 0$, converge rapidly for $\epsilon^2 \leqslant 0.95$. For the highest wave the Padé approximants appear to converge up to $N = 21$ and then begin to fluctuate. This is due to the loss of significant figures during the calculation of the approximants themselves which is in turn influenced by the nearness of singularities. The convergence of the Padé approximants with N is a play-off between two factors – the increase of information about the series against the attendant loss of significant figures. Inspection of the results for the two shallower depths reveals the decrease in the rate of

TABLE 2*b*. SUMMED $[N/N]$ PADÉ APPROXIMANTS OF THE WAVE AMPLITUDE, a, AND THE WAVE SPEED SQUARED, c^2, FOR $e^{-d} = 0.5$

	$10a$			$10c^2$		
N	$\epsilon^2 = 0.9$	$\epsilon^2 = 0.95$	$\epsilon^2 = 1$	$\epsilon^2 = 0.9$	$\epsilon^2 = 0.95$	$\epsilon^2 = 1$
1	2.38913	2.49600	2.60386	7.83084	7.97585	8.12751
2	2.40153	2.51090	2.62160	7.80392	7.94315	8.08809
3	2.33264	2.38790	2.38113	7.83055	7.97384	8.12358
4	2.33154	2.38501	2.37197	7.62450	7.61918	7.44588
5	2.34206	2.41300	2.45649	7.64046	7.66434	7.59241
6	2.34281	2.41518	2.46305	7.64311	7.67257	7.61980
7	2.34321	2.41663	2.46863	7.64310	7.67254	7.61969
8	2.34343	2.41783	2.47605	7.64380	7.67563	7.63460
9	2.34348	2.41816	2.47939	7.64401	7.67711	7.64844
10	2.34348	2.41822	2.48027	7.64401	7.67709	7.64827
11	2.34348	2.41820	2.47998	7.64403	7.67745	7.65669
12	2.34349	2.41828	2.48166	7.64403	7.67738	7.65417
13	2.34348	2.41823	2.48055	7.64403	7.67734	7.65295
14	2.34349	2.41831	2.48255	7.64403	7.67737	7.65382
15	2.34349	2.41831	2.48272	7.64403	7.67743	7.65594
16	2.34349	2.41830	2.48250	7.64403	7.67740	7.65469
17	2.34349	2.41831	2.48317	7.64403	7.67748	7.65938
18	2.34349	2.41833	2.48629	7.64403	7.67748	7.65889
19	2.34349	2.41832	2.48334	7.64404	7.67751	7.66478
20	2.34349	2.41834	2.50526	7.64404	7.67753	7.67704
21	2.34349	2.41832	2.48364	7.64403	7.67749	7.66036
22	2.34349	2.41833	2.48559	7.64403	7.67749	7.66055
23	2.34349	2.41832	2.48356	7.64403	7.67749	7.66051
24	2.34349	2.41831	2.48298	7.64403	7.67749	7.66022
25	2.34349	2.41833	2.48594	7.64403	7.67750	7.66128
26	2.34349	2.41832	2.48387	7.64403	7.67748	7.65920
27	2.34349	2.41828	2.48176	7.64403	7.67748	7.65929

convergence with decreasing d. In general, convergence is better for greater depths and smaller wave heights; thus the $e^{-d} = 0.9$ values of table 2*c* represent the worst convergence encountered. Even in this extreme case, based on the consistency of the Padé approximants, a and c^2 are good to 2 and 3 significant figures respectively.

The main results are plotted in figures 4 and 5 and are tabulated in the appendix. Figure 4 which is a plot of a against ϵ^2 shows that for each water depth the wave amplitude is a monotonically increasing function of ϵ^2. Therefore a limiting wave for which $\epsilon^2 = 1$ is also a highest wave. Figure 5 is the graph of $(c^2 - c_0^2)/c_0^2$ against ϵ^2 where c_0 is the phase speed of an infinitesimal wave, i.e.

$$c_0^2 = \tanh d = \frac{1 - e^{-2d}}{1 + e^{-2d}}. \tag{4.6}$$

The dashed lines in these figures represent the uncertainty in the values of a and c^2 associated with the incomplete convergence of the Padé approximants. The curve for $e^{-d} = 1$ is from the work of Longuet-Higgins & Fenton (1974) for solitary waves.

The important thing to notice in figure 5 is that for the entire depth range the highest wave is not the fastest, but instead the wave speed reaches a maximum for waves somewhat lower than the highest! This is a generalization of the solitary-wave results of Longuet-Higgins & Fenton (1974) and the deep-water results of Longuet-Higgins (1975). The intermediate depth curves lie between the two limits of zero and infinite depth and behave in a similar manner.

TABLE 2c. SUMMED $[N/N]$ PADÉ APPROXIMANTS OF THE WAVE AMPLITUDE, a, AND THE WAVE SPEED SQUARED, c^2, FOR $e^{-d} = 0.9$

	$100a$			$10c^2$		
N	$\epsilon^2 = 0.9$	$\epsilon^2 = 0.95$	$\epsilon^2 = 1$	$\epsilon^2 = 0.9$	$\epsilon^2 = 0.95$	$\epsilon^2 = 1$
1	1.72246	1.77950	1.83497	0.93365	0.93564	0.93738
2	1.69137	1.74707	1.80122	1.55824	1.59182	1.62603
3	2.70747	2.83116	2.95259	1.84846	1.93911	2.04019
4	3.50182	3.72339	3.94703	1.75933	1.82862	1.90360
5	3.47095	3.68775	3.90625	1.77830	1.85876	1.93172
6	3.78807	4.06188	4.34325	1.72886	1.79113	1.85771
7	4.06412	4.40435	4.76334	1.72085	1.78112	1.84530
8	4.00135	4.32460	4.66321	1.72215	1.78274	1.84732
9	4.04073	4.37492	4.72672	1.70152	1.75570	1.81227
10	4.10505	4.46140	4.84128	1.68429	1.73074	1.77668
11	4.06266	4.40359	4.76366	1.68454	1.73112	1.77725
12	4.06276	4.40372	4.76383	1.65773	1.68554	1.69958
13	4.05562	4.39406	4.75100	1.61687	1.59017	1.43854
14	4.07627	4.42104	4.78583	1.63824	1.64503	1.61031
15	4.08822	4.43557	4.80349	1.63619	1.64028	1.59815
16	4.08780	4.43507	4.80289	1.63593	1.63969	1.59662
17	4.05927	4.39863	4.75662	1.63916	1.64714	1.61565
18	4.09130	4.43919	4.80776	1.64007	1.64922	1.62083
19	4.09560	4.44419	4.81364	1.63831	1.64520	1.61080
20	4.12885	4.48033	4.85406	1.63848	1.64559	1.61179
21	4.08275	4.42916	4.79594	1.63780	1.64403	1.60784
22	4.08212	4.42840	4.79503	1.63960	1.64813	1.61811
23	4.11403	4.46480	4.83717	1.64083	1.65092	1.62496
24	4.09605	4.44472	4.81428	1.63916	1.64715	1.61571
25	4.11211	4.46280	4.83501	1.64051	1.65021	1.62326
26	4.13391	4.48575	4.86010	1.63931	1.64748	1.61650
27	4.09312	4.44144	4.81054	1.63906	1.64692	1.61511

Figure 6 is a graph of the wave height divided by the undisturbed fluid depth, H/d, against the Froude number squared, c^2/gd, for various depths. The solitary-wave results as well as the curve along which the highest solitary wave must lie, $H/d = \frac{1}{2}c^2/gd$, are also shown. This plot represents the region in the two-parameter space in which steady gravity waves can exist. The degree to which an individual curve deviates from constant Froude number as the wave height is increased represents the effect of nonlinearity.

The relatively poor convergence of both a and c^2 for $e^{-d} = 0.9$ has been amplified by division by d. For the high waves in water of this depth a seems to converge to 2 figures with an error of ± 1 in the last figure as shown in column 4 of table 2c. However a smooth curve bounding the highest waves for the other depths in figure 6 would pass about 12% below the highest wave calculated for this depth. We feel that the correct value is most likely that obtained by such a bounding

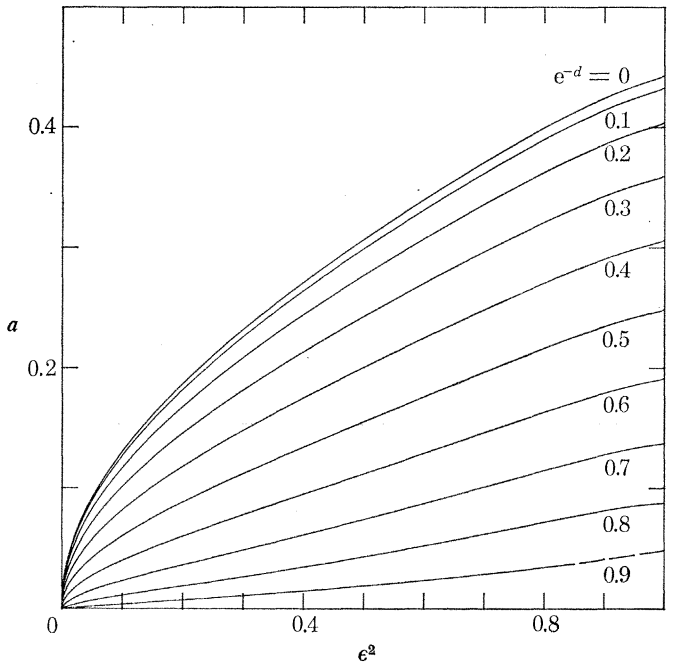

FIGURE 4. The wave amplitude, $a = \frac{1}{2}H$, plotted against the expansion parameter, ϵ^2, for various fluid depths, d. Note that a limiting wave ($\epsilon^2 = 1$) is also a highest wave.

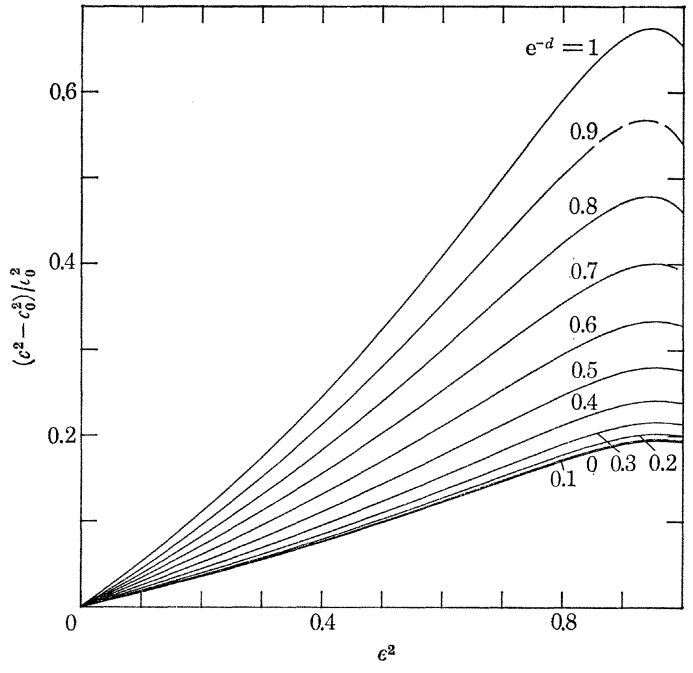

FIGURE 5. The relative increase of the squared wave speed, c^2, to that of infinitesimal waves, c_0^2, plotted against the expansion parameter, ϵ^2. The curve for $e^{-d} = 1$ is from the solitary-wave results of Longuet-Higgins & Fenton (1974). All the wave speeds reach maxima for waves slightly lower than the highest.

curve and that the Padé approximants have not completely converged for $e^{-d} = 0.9$. For his expansions in a Schwartz found that more nonphysical singularities began appearing on the negative real axis in the complex a^2-plane as the depth decreased. The Padé approximants had to use more and more terms to deal with these and had less terms left to accurately represent the series in the region of interest. A similar behaviour can be expected here.

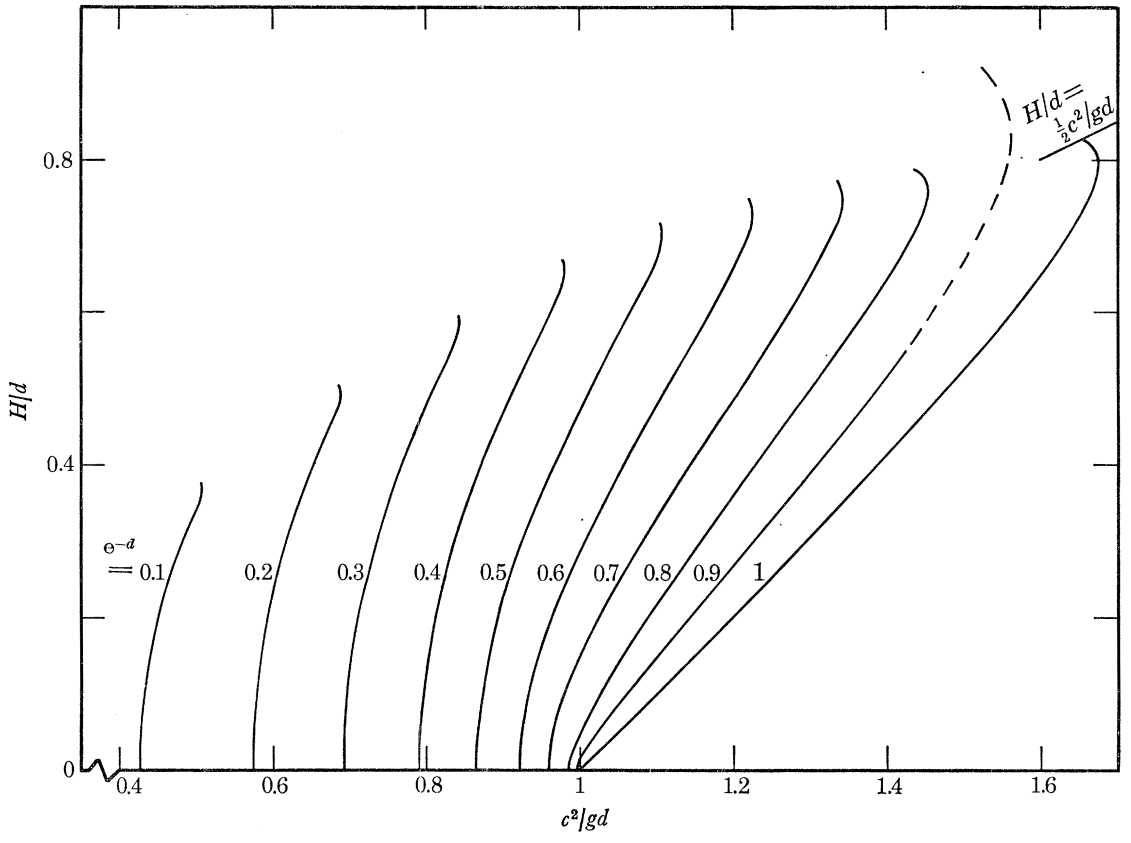

FIGURE 6. The ratio of the wave height to undisturbed fluid depth, H/d, plotted against the squared Froude number, c^2/gd, for a variety of fluid depths. Also plotted are the solitary-wave results of Longuet-Higgins & Fenton (1974) and the line along which the highest solitary wave must lie, $H/d = \frac{1}{2}c^2/gd$.

(*b*) *Comparison with other work*

In the past few years several authors have attempted to determine the characteristics of nonlinear periodic waves. Our technique is closely akin to that of Schwartz (1974) and Longuet-Higgins (1975). Table 3 gives the height of the highest waves for various fluid depths and compares them with Schwartz's results. Agreement is good, but Schwartz's waves are slightly higher than ours. His results do not converge for the two shallower depths. Concerning the wave speed, Schwartz stated that the series for c^2 converged well for waves up to 3% short of the highest, but for higher waves it was necessary to extrapolate. Hence he did not report the wave speed maxima.

Comparing our values of a and c^2 with the highest deep-water waves of Longuet-Higgins we have $a = 0.44313$, $c^2 = 1.1928$ versus his $a = 0.4433$, $c^2 = 1.1931$. These results differ only in the fourth decimal place, and for lower waves both sets of results are identical. It should be pointed out that a solution procedure similar to § 3*b* could be carried out *ab initio* in terms of Longuet-Higgins's

parameter ω. If so the solution scheme outlined in table 1 would be somewhat more complicated in that at the beginning of each odd order, $2M+1$, it would be necessary to solve 7 simultaneous linear equations in the 7 unknowns $\alpha_{1,M-1}$, $\beta_{1,M-1}$, $\alpha_{2,M-1}$, $\beta_{2,M-1}$, $\beta_{0,M}$, Δ_M and γ_M rather than 4 equations in the first 4 unknowns. (One of the equations in Δ_M actually comes from two equations at order $2M+1$. The order $2M+1$ terms are removed with the identity $\delta_1\beta_{00}-\sigma_1\Delta_0=0$.) We have not attempted this calculation, but instead we have expanded ω^2 as a series in ϵ^2, reverted and substituted into the other series. Although there is some loss of significant figures it is not as devastating as changing from a series in a to one in ω. We find that there is little difference between the two parameters; for some depths and some series one parameter may yield slightly better convergence than the other and vice versa.

TABLE 3. THE LIMITING WAVE HEIGHT FOR VARIOUS FLUID DEPTHS. SCHWARTZ'S (1974) RESULTS ARE IN COLUMN 4

e^{-d}	d/λ	H/λ	H/λ (Schwartz)
0	∞	0.141055	0.14118
0.1	0.366468	0.1378	0.1380
0.2	0.256150	0.1285	0.1285
0.3	0.191618	0.11443	0.1145
0.4	0.145832	0.09739	0.0975
0.5	0.110318	0.07910	0.0791
0.6	0.0813004	0.06090	0.0614
0.7	0.0567666	0.04374	0.045
0.8	0.0355144	0.0279	
0.9	0.0167686	0.015	

Dean (1965) has tried a numerical approach to the calculation of nonlinear waves. He expressed the stream function and free-surface elevation as Fourier series in X, truncated after the eleventh harmonic. Due to the truncation, the dynamic free-surface boundary condition is not satisfied exactly. To determine the Fourier coefficients for fixed values of the depth and wave height he minimized the mean-squared error in the dynamic boundary condition over a number of points evenly spaced in X between the wave crest and trough. The highest waves were chosen to satisfy an empirically derived relation between the wave height and depth. Comparing the Padé-approximant deep-water wave results with those of a later paper of Dean (1974, case 10) we find good agreement with his values of ϵ^2, a and c^2 for low to moderately steep waves. However, his values for the wave of greatest height are $\epsilon^2=0.8971$, $a=0.43805$ and $c^2=1.222070$. This is too low a value for ϵ^2, and inspection of table A0 in the appendix indicates that this is too fast a wave for this wave height. Dean's tabulated wave parameters are too widely spaced to detect a maximum in the wave speed. As the highest wave is approached the higher-order harmonics become more important in order to describe the sharply curved wave crest, but Dean's formulation becomes less adequate since the errors are distributed over a small number of Fourier coefficients.

Von Schwind & Reid (1972) have used an approach similar to Dean's. They expressed $Z+id$ as an eighth-order Fourier series in $W-iQ$. Fixing the first Fourier coefficient F_1 (their A_1), they determined the others by an error minimization technique. To find the highest wave for a particular d they increased F_1 until a parameter Γ (their u'/C), associated with the fluid speed

at the wave crest, reached a maximum value and began to fall off erratically. The value of F_1 so obtained was assumed to correspond to the highest wave. In our notation

$$\Gamma = 1 + \frac{q_{\text{crest}}}{c}\left(1 + \frac{\overline{\eta}}{d}\right), \tag{4.7}$$

and its maximum value should be 1 when $q_{\text{crest}} = 0$. Von Schwind & Reid do not mention this, nor do they state what maximum value of Γ they did obtain. However by expressing F_1 in terms of our Fourier coefficient a_1, namely

$$F_1 = \frac{1 - e^{-2d}}{d} \frac{a_1}{1 + \overline{\eta}/d}, \tag{4.8}$$

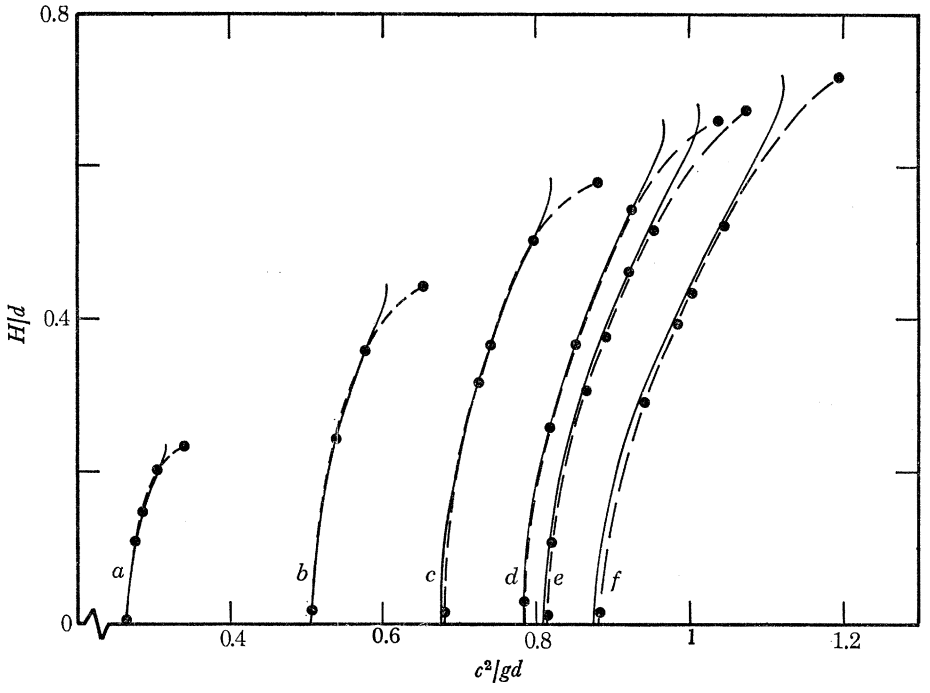

FIGURE 7. A plot of H/d against c^2/gd comparing the Padé-approximant results (——) with those of Thomas (1975) (— ● —) for (*a*) $e^{-d} = 0.0230541$, (*b*) $e^{-d} = 0.151836$, (*c*) $e^{-d} = 0.284610$, (*d*) $e^{-d} = 0.389661$, (*e*) $e^{-d} = 0.42402$, (*f*) $e^{-d} = 0.51272$. Agreement is acceptable except in the case of the highest waves for which Thomas employed a numerical technique *different* from that used for the lower waves.

we can see immediately why their method cannot converge for high waves. For fixed d, a_1 is not a monotonically increasing function of the wave height. Although $\overline{\eta}$ also increases with H and ultimately decreases (as shown in figure 12) the term $1 + \overline{\eta}/d$ will not cancel out the double-valuedness of a_1. Hence F_1 is not monotonic in H. The highest waves calculated by Von Schwind & Reid correspond very closely to the waves for which a_1 achieves a maximum.

Thomas (1975) has solved a nonlinear integral equation iteratively to obtain the relation between the Froude number and the wave height for various depths. His solution involves finding an eigenvalue μ which is related to the reciprocal of the fluid speed at the wave crest and which becomes infinite for highest waves. Our calculations have been performed for the same fluid depths as considered by Thomas, and the results are compared in figure 7. Thomas's curves closely parallel ours for all but the highest waves and differ by at most 1% in the Froude number.

PHILOSOPHICAL TRANSACTIONS OF THE ROYAL SOCIETY A MATHEMATICAL, PHYSICAL & ENGINEERING SCIENCES

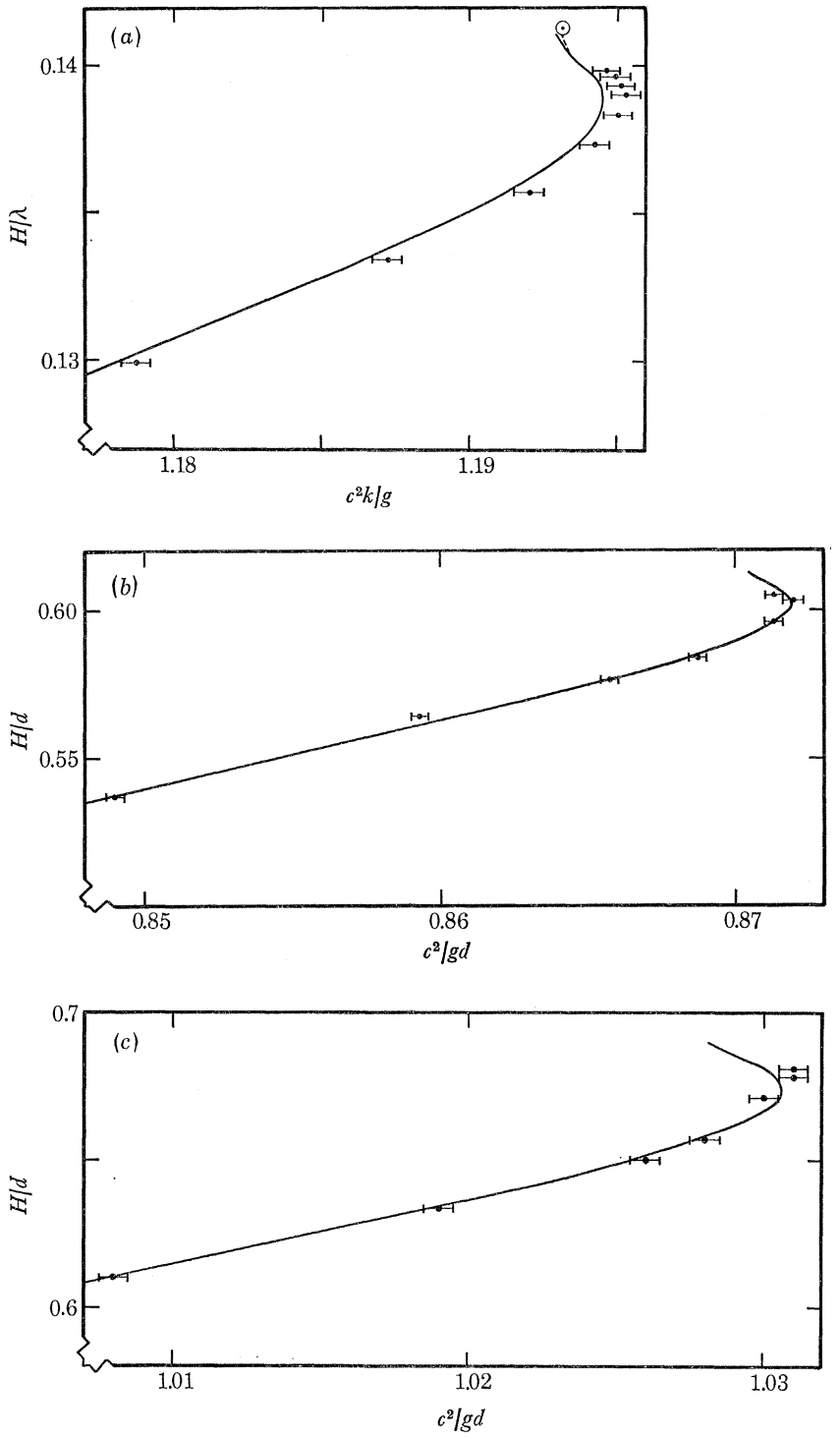

FIGURE 8. Comparison of the Padé-approximant curves (——) of the wave height, H, and speed, c, to Sasaki & Murakami's points with their error bars (⊢●⊣). (*a*) Deep water ($e^{-d} = 0$). Also shown are the curve of Longuet-Higgins (1975) (– – –) where it deviates from our own and the highest wave of Yamada (1957) (⊙). (*b*) $e^{-d} = 0.1813$, (*c*) $e^{-d} = 0.4385$. Notice that the magnitude of Sasaki & Murakami's estimated errors preclude them from identifying the wave speed maxima.

PHILOSOPHICAL TRANSACTIONS OF THE ROYAL SOCIETY A MATHEMATICAL, PHYSICAL & ENGINEERING SCIENCES

However, for waves of greatest height the curves diverge, and Thomas finds a rapid *increase* in wave speed with height. His squared Froude numbers are 7–10% greater than ours, but his highest waves are somewhat lower. Because μ approaches infinity for highest waves Thomas found it necessary to solve a *different* integral equation in this case. He fixed μ at 'some large number' and considered a sequence of iterations different from that of the lower waves. By comparison with our results we feel that this sequence does not converge to the correct answer for highest waves. Thomas's results might be improved by explicitly including the asymptotic form of the crest singularity as the highest wave is approached.

The work of Sasaki & Murakami (1973) tends to support our conclusions. Using an independent numerical method, they solved an integral equation valid for all fluid depths including solitary waves. They do not give results for highest waves, but their near-highest wave results indicate a possible maximum in the wave speed. However, they estimate an error in c of 0.02% which would be enough to obscure the maximum in all but the solitary wave case. We have done our computer calculations for the same three depths as they ($e^{-d} = 0$, 0.3201, 0.4385), and the results are compared in figure 8. Figure 8*a* shows the wave steepness, H/λ, plotted against c^2 for deep-water waves. The solid curve represents our ϵ^{110} results and the points with error bars are those of Sasaki & Murakami. Also displayed are the highest wave results obtained by Yamada (1957) using a numerical method similar to Sasaki & Murakami's and the curve of Longuet-Higgins (1975) which deviates only slightly from ours at highest waves. From the graph we see that Sasaki & Murakami's results parallel our own, but their c^2 values are consistently larger. Figures 8*b* and *c* show H/d against c^2/gd for two intermediate depths. Again, their points fall near our curve, but their error estimates preclude the certain identification of the c^2 maxima. Only in the solitary wave case are their error estimates small enough to detect the maximum, but their wave speeds are consistently 0.4% lower than those of Longuet-Higgins & Fenton (1974). Significantly, Sasaki & Murakami do not mention the maxima in the text of the paper, but they appear in the tabulated results.

A recent confirmation of the solitary wave speed maximum has been given by Byatt-Smith & Longuet-Higgins (1976). They have numerically solved yet a different integral equation and have obtained results for waves up to near the highest. Their solution is important because it is the only approach so far which is both independent of the Padé approximants and convincingly accurate.

5. The integral properties

The integral properties of waves such as the mean momentum and energy and their respective fluxes are of particular interest to hydraulicians and oceanographers. These quantities are readily calculated from the perturbation solutions, and since certain relations exist between them they can be used to provide a cross-check on the Padé approximated results.

(*a*) *Definitions and relations*

Some useful physical quantities can be defined in the (x, y)-frame of reference. Define the mean mass of fluid above the origin per unit horizontal area, M, by

$$M = \frac{1}{\lambda}\int_0^\lambda \rho\eta \,\mathrm{d}x$$
$$= \rho\bar{\eta}, \tag{5.1}$$

PHILOSOPHICAL TRANSACTIONS OF THE ROYAL SOCIETY A MATHEMATICAL, PHYSICAL & ENGINEERING SCIENCES

where the overbar signifies an x-average. Similarly define the circulation per unit length, C, by

$$C = \frac{1}{\lambda}\int_0^\lambda u\,\mathrm{d}x$$
$$= \bar{u}, \tag{5.2}$$

where the integration is to be performed at a level always within the fluid. C is identically zero by the choice of reference frame in § 2. The mean momentum or impulse, I, kinetic energy, T, and potential energy, V, per unit horizontal area are defined by

$$I = \overline{\int_{-d}^{\eta} \rho u\,\mathrm{d}y}, \tag{5.3}$$

$$T = \overline{\int_{-d}^{\eta} \tfrac{1}{2}\rho(u^2+v^2)\,\mathrm{d}y}, \tag{5.4}$$

$$V = \overline{\int_{\bar{\eta}}^{\eta} \rho g y\,\mathrm{d}y}. \tag{5.5}$$

The radiation stress, the excess flux of momentum due to the waves, per unit span denoted S_{xx} is given by

$$S_{xx} = \overline{\int_{-d}^{\eta} (p+\rho u^2)\,\mathrm{d}y} - \int_{-d}^{\bar{\eta}} p_0\,\mathrm{d}y$$
$$= \overline{\int_{-d}^{\eta} (p+\rho u^2)\,\mathrm{d}y} - \tfrac{1}{2}\rho g D^2. \tag{5.6}$$

Here $p_0 = -\rho g(y-\bar{\eta})$ is the (hydrostatic) pressure in the absence of the waves but in a fluid with the same mean depth $D = d+\bar{\eta}$. The mean energy flux per unit span, F, is defined by

$$F = \overline{\int_{-d}^{\eta} [p+\tfrac{1}{2}\rho(u^2+v^2)+\rho g(y-\bar{\eta})]\,u\,\mathrm{d}y}. \tag{5.7}$$

Finally the mean squared velocity at the bottom denoted $\overline{u_b^2}$ is

$$\overline{u_b^2} = \frac{1}{\lambda}\int_0^\lambda [u(x,-d,t)]^2\,\mathrm{d}x. \tag{5.8}$$

In the steady motion (the Z-plane) there are three physical quantities which are independent of X. The first is the mass flux per unit span, $-Q$, defined by

$$-Q = \int_{-d}^{\eta} \rho \mathscr{U}\,\mathrm{d}Y$$
$$= -\rho c d. \tag{5.9}$$

As stated previously, d represents the depth of uniform stream flowing with velocity $-c$ whose mass flux equals that of the wave. A uniform stream with the same *mean* depth and mass flux as the wave will flow with a *different* velocity, $-c_{\mathrm{cm}}$, which is related to c by

$$-c_{\mathrm{cm}} = \overline{\frac{1}{d+\eta}\int_{-d}^{\eta} \mathscr{U}\,\mathrm{d}Y}$$
$$= -c\,d/D. \tag{5.10}$$

$-c_{\rm cm}$ is the velocity of the centre of mass of the fluid with respect to the (X, Y)-frame. For all deep-water and solitary waves $c_{\rm cm}$ equals c, but this is not true in general.

The other two X-independent quantities are the total head, R, defined by

$$R = \frac{p}{\rho g} + \frac{1}{2g}(\mathscr{U}^2 + \mathscr{V}^2) + Y + d \tag{5.11}$$

and the momentum flux per unit span, S, defined by

$$S = \int_{-d}^{\eta} (p + \rho \mathscr{U}^2)\, \mathrm{d}Y. \tag{5.12}$$

We have retained the dimensionless quantities $\rho = g = k = 1$ in the definitions for clarity, but we shall discard them for the remainder of this section. Also we shall drop the words 'per unit horizontal area' and 'per unit span' and refer to T, for example, as the kinetic energy.

Longuet-Higgins (1975) has derived various relations (some previously known) between the integral properties defined above. Since there are minor differences in notation we shall restate these equations but in a slightly more general form which applies when both M and C are non-zero. They are as follows:

$$I = cD - Q, \tag{5.13}$$

$$2T = cI - CQ, \tag{5.14}$$

$$S_{xx} = 4T - 3V + \overline{u_b^2}\, D + 2CQ, \tag{5.15}$$

$$F = c(3T - 2V) + \tfrac{1}{2}\overline{u_b^2}(I + cD) + cCQ, \tag{5.16}$$

$$K = 2M + \overline{u_b^2} + c^2, \tag{5.17}$$

$$R = \tfrac{1}{2}K + d, \tag{5.18}$$

$$S = S_{xx} - 2cI + D(c^2 + \tfrac{1}{2}D). \tag{5.19}$$

Here K is the Bernoulli constant as defined in equation (2.4). The derivations of these relations are omitted here, but they follow closely those of Longuet-Higgins (1975).

We wish to express each integral property as a perturbation series in ϵ. With the definitions of Q and V and the fact that $C = 0$ we have

$$I = c\overline{\eta}, \tag{5.20}$$

$$2T = c^2\overline{\eta}, \tag{5.21}$$

$$2V = \overline{\eta^2} - \overline{\eta}^2. \tag{5.22}$$

These equations relate I, T and V to c^2, $\overline{\eta}$ and $\overline{\eta^2}$. Now we already have perturbation series for c^2 so we only need series for $\overline{\eta}$ and $\overline{\eta^2}$. For the mean displacement of the free surface we have

$$\begin{aligned}
\overline{\eta} &= \frac{1}{2\pi}\int_0^{2\pi} Y(\Phi, 0)\, \mathrm{d}X \\
&= \frac{1}{2\pi}\int_0^{2\pi} \left[\sum_{j=1}^{\infty} \frac{a_j \delta_j}{j} \cos\left(j\frac{\Phi}{c}\right)\right]\left[1 + \sum_{m=1}^{\infty} a_m \sigma_m \cos\left(m\frac{\Phi}{c}\right)\right] \mathrm{d}\frac{\Phi}{c} \\
&= \frac{1}{2}\sum_{n=1}^{\infty} \frac{a_n^2}{n}\delta_n \sigma_n \\
&= \frac{1}{2}\sum_{j=1}^{\infty}\sum_{k=0}^{j-1}\sum_{n=0}^{j-k-1} \frac{\delta_{j-k-n}\sigma_{j-k-n}}{j-k-n}\alpha_{j-k-n,\,k}\alpha_{j-k-n,\,n}\epsilon^{2j},
\end{aligned} \tag{5.23}$$

where we have integrated along the wave profile with the use of equations (2.9) and (3.1a). The mean square of the surface elevation is given by

$$\begin{aligned}
\overline{\eta^2} &= \frac{1}{2\pi}\int_0^{2\pi} Y^2(\Phi, 0)\,\mathrm{d}X \\
&= \frac{1}{2\pi}\int_0^{2\pi}\left[\sum_{n=1}^{\infty}\frac{a_n\delta_n}{n}\cos\left(n\frac{\Phi}{c}\right)\right]^2\left[1+\sum_{m=1}^{\infty}a_m\sigma_m\cos\left(m\frac{\Phi}{c}\right)\right]^2\mathrm{d}\frac{\Phi}{c} \\
&= \frac{1}{2}\sum_{m=1}^{\infty}\frac{a_m^2\delta_m^2}{m^2}+\frac{1}{4}\sum_{l=1}^{\infty}\sum_{m=1}^{\infty}\left(\frac{\delta_m\sigma_{l+m}}{m}+2\frac{\delta_{l+m}\sigma_m}{l+m}\right)\frac{\delta_l}{l}a_l a_m a_{l+m} \\
&= \frac{1}{2}\sum_{j=1}^{\infty}\sum_{k=0}^{j-1}\sum_{l=0}^{j-k-l}\frac{\delta_{j-k-l}}{(j-k-l)^2}\alpha_{j-k-l,k}\alpha_{j-k-l,l}\epsilon^{2j} \\
&\quad+\frac{1}{4}\sum_{j=2}^{\infty}\sum_{m=1}^{j-1}\sum_{k=0}^{j-m-1}\sum_{i=0}^{j-m-k-1}\sum_{n=0}^{j-m-k-i-1}\frac{\delta_{j-m-k-i-n}}{j-m-k-i-n} \\
&\quad\times\left(\frac{\delta_m\sigma_{j-k-i-n}}{m}+2\frac{\delta_{j-k-i-n}\sigma_m}{j-k-i-n}\right)\alpha_{j-m-k-i-n,k}\alpha_{mi}\alpha_{j-k-i-n,n}\epsilon^{2j}. \qquad (5.24)
\end{aligned}$$

Therefore we can use the series (5.23) and (5.24) along with the series (3.1c) and (3.1d) plus the relations (5.15)–(5.22) to express each integral property as a perturbation series in ϵ^2.

(*b*) *The Padé-approximant results*

Taking the complete series solution from §4a and equations (5.23) and (5.24) expanded to order ϵ^{110} we have calculated the various integral properties with the aid of $[N/N]$ Padé approximants. This was done for $\mathrm{e}^{-d} = 0, 0.1, \ldots, 0.9$ and $\epsilon^2 = 0.1, 0.2, \ldots, 0.8, 0.81, 0.82, \ldots, 1$. For a particular depth the computer usage was $5\frac{1}{2}$ min and 124 K bytes in double precision.

On hindsight we feel that a saving in computer time of perhaps a factor of ten but with a subsequent doubling in storage space could be achieved by changing the order in which the calculations are performed. For a particular series at a fixed value of ϵ^2 we computed the coefficients for the $[N/N]$ Padé approximants and summed them for $N = 1, 2, \ldots, 28$. However, the coefficients of the Padé approximants depend on N but not on ϵ^2. Therefore, it would have been wiser to calculate the Padé coefficients, store them for each series (which would require $(N+1)^2$ storage locations) and then sum them for each ϵ^2 rather than to recalculate them. A substantial saving in computer time should result since to calculate each $[N/N]$ Padé approximant requires the solution of a symmetric $N \times N$ system of equations.

The main results are tabulated in the appendix and are presented graphically in figures 9–18. The tabulated results are given to 6 figures where possible. Based on consistency in the Padé approximants we feel they are correct to ± 1 in the last decimal place reported. As with the wave height and speed, the convergence is worse for higher waves and shallower depths, and the effects of this are shown by the dashed lines in the figures.

Figures 9–11 show the momentum, kinetic energy and potential energy plotted against ϵ^2. The important result is that these quantities achieve maxima for waves short of the highest. This is a generalization of the solitary-wave results of Longuet-Higgins & Fenton (1974) and the deep-water results of Longuet-Higgins (1975). It is clear that for a fixed value of ϵ^2 there is an orderly progression of results from deep to shallow water.

Figure 12 is a plot of the mean surface elevation against ϵ^2 for various depths. It shows that $\overline{\eta}$ has an intermediate maximum which is a result also obtained by Schwartz in his thesis (1972). However, he did not make use of the relations (5.20) and (5.21) to obtain the surprising results (at that time, at least) about the wave momentum and energy.

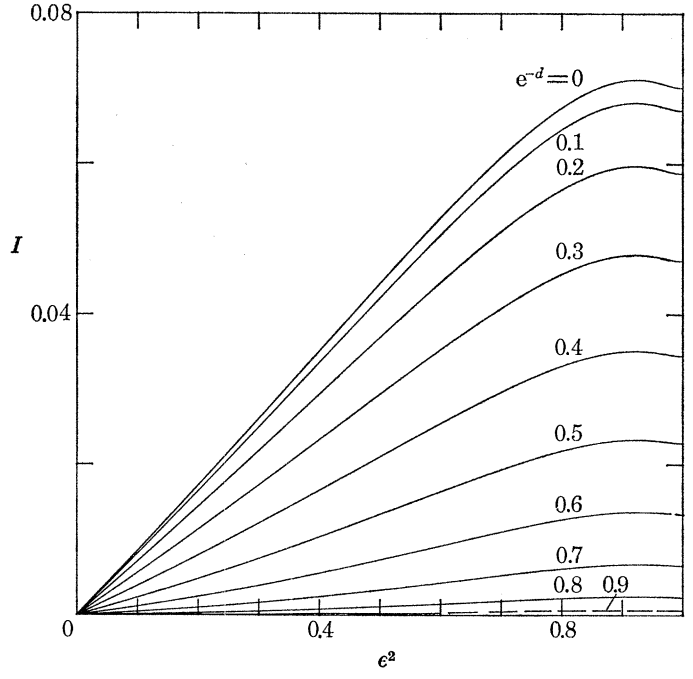

FIGURE 9. The wave momentum, I, plotted against the expansion parameter, ϵ^2, for various depths, d.

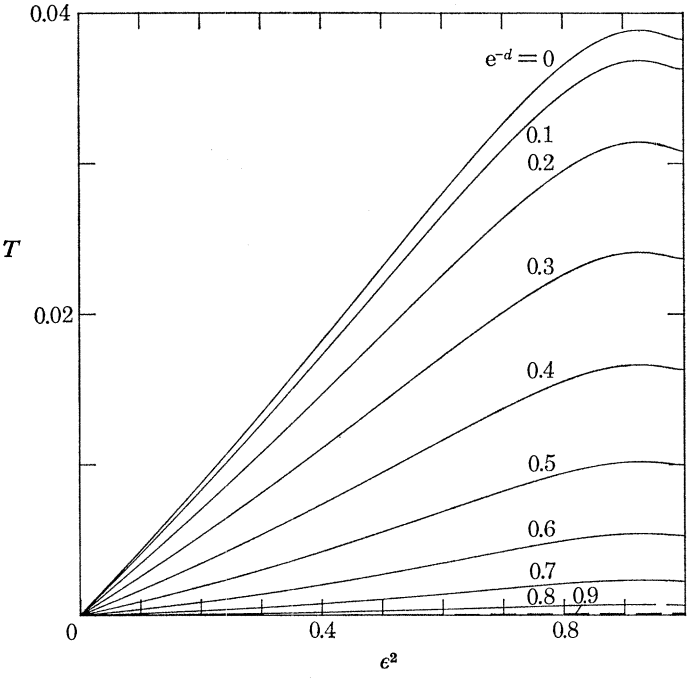

FIGURE 10. The kinetic energy, T, plotted against the expansion parameter, ϵ^2, for various depths, d.

PHILOSOPHICAL TRANSACTIONS OF THE ROYAL SOCIETY A MATHEMATICAL, PHYSICAL & ENGINEERING SCIENCES

The dependence of the mean squared bottom velocity on ϵ^2 and d is illustrated in figure 13. $\overline{u_b^2}$ has the now characteristic dependence on ϵ^2, but its variation with d may at first appear surprising. For $e^{-d} = 0$ the bottom is infinitely far away, and so $u_b = 0$. As d decreases the waves are more influenced by the bottom, and $\overline{u_b^2}$ increases. However, for solitary waves ($e^{-d} = 1$) $\overline{u_b^2}$ must again vanish because although the integral of u_b^2 with respect to x from $-\infty$ to ∞ is finite ($u_b = 0$

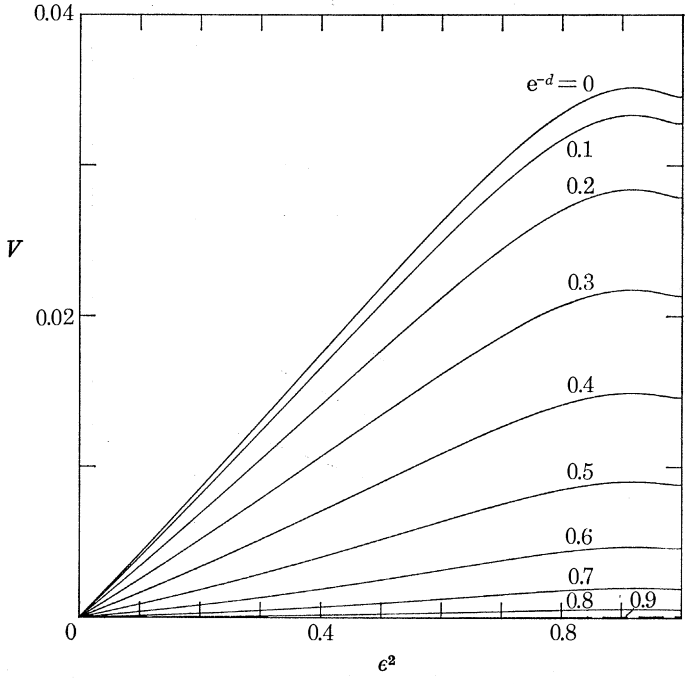

FIGURE 11. The potential energy, V, plotted against the expansion parameter, ϵ^2, for various depths, d.

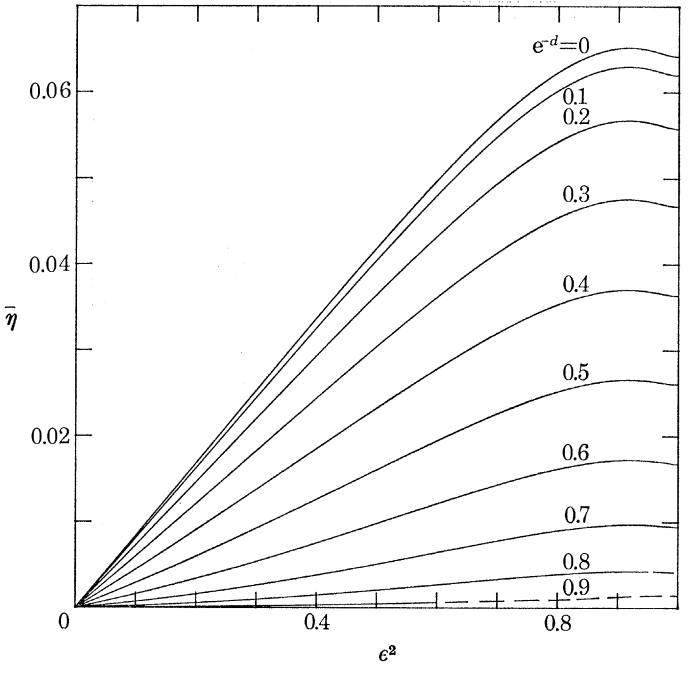

FIGURE 12. The mean free-surface elevation, $\bar{\eta}$, plotted against the expansion parameter, ϵ^2, for various depths, d.

at $\pm\infty$) and nonzero it is divided by ∞, the wavelength of solitary waves. Therefore $\overline{u_b^2}$ must have a maximum (dependent on ϵ) for some intermediate value of d.

The radiation stress and the mean energy flux are plotted in figures 14 and 15. Again each quantitity has an intermediate maximum in ϵ^2, but some of the curves for deeper water intersect those for shallower depths. This effect may be thought of as due to the $\overline{u_b^2}$ terms in equations (5.15) and (5.16).

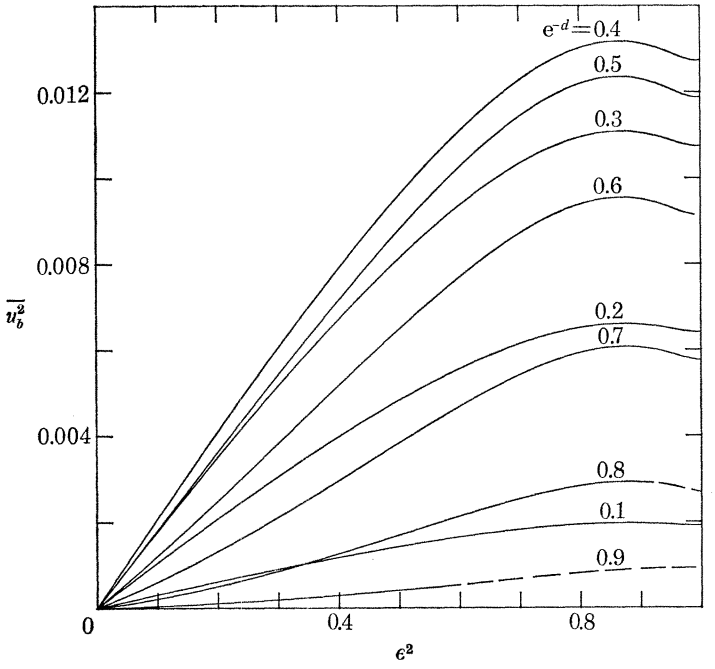

FIGURE 13. The mean squared bottom velocity, $\overline{u_b^2}$, plotted against the expansion parameter, ϵ^2, for various depths, d.

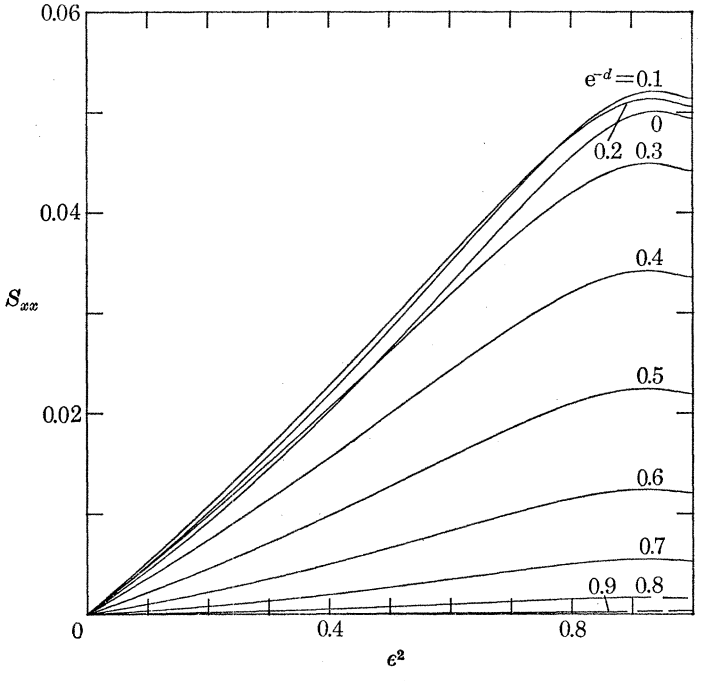

FIGURE 14. The radiation stress, S_{xx}, plotted against the expansion parameter, ϵ^2, for various depths, d.

Assuming no reflexion and constant energy flux, Burnside (1915) showed that small-amplitude waves entering slowly shoaling water first suffer a *decrease* in wave height followed by an increase. The comparison of figures 4 and 15 at constant F appears to confirm this result. However we must caution that these curves are for quantities nondimensionalized with respect to wavenumber. In general, the wavenumber of a shoaling wave will not remain constant, but under certain conditions its frequency will (see Phillips 1966, §3.7). If desired our results can be recast simply in terms

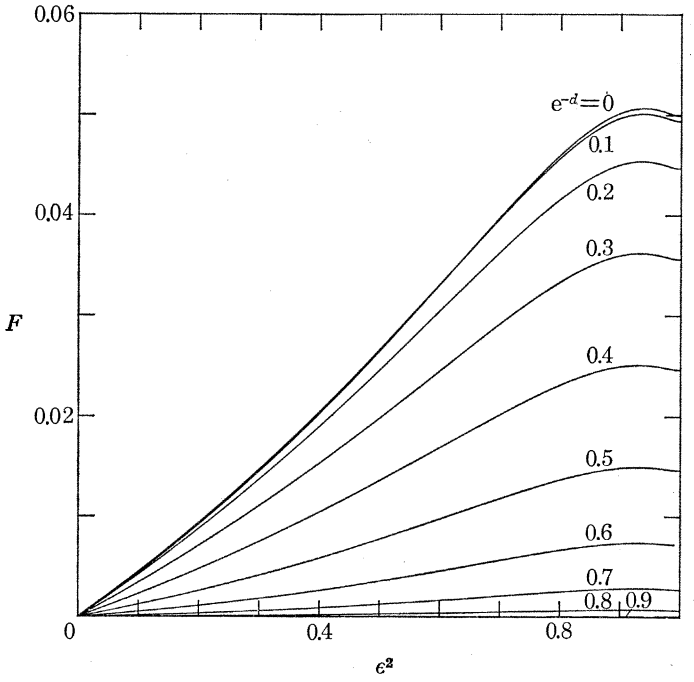

FIGURE 15. The energy flux, F, plotted against the expansion parameter, ϵ^2, for various depths, d. The $e^{-d} = 0.1$ curve lies above the deep-water wave curve for ϵ^2 less than about 0.7.

of frequency, σ, rather than wavenumber, k. If we denote dimensional quantities with a tilde and quantities non-dimensionalized with respect to frequency by a prime we have

$$\left.\begin{aligned} c' &= \tilde{c}\frac{\tilde{\sigma}}{\tilde{g}} = c^2, \\ H' &= \tilde{H}\frac{\tilde{\sigma}^2}{\tilde{g}} = c^2 H, \\ u' &= \tilde{u}\frac{\tilde{\sigma}}{\tilde{g}} = cu, \\ I' &= \tilde{I}\frac{\tilde{\sigma}^3}{\tilde{\rho}\tilde{g}^2} = c^3 I, \\ T' &= \tilde{T}\frac{\tilde{\sigma}^4}{\tilde{\rho}\tilde{g}^3} = c^4 T, \\ S' &= \tilde{S}\frac{\tilde{\sigma}^4}{\tilde{\rho}\tilde{g}^3} = c^4 S, \\ F' &= \tilde{F}\frac{\tilde{\sigma}^5}{\tilde{\rho}\tilde{g}^4} = c^5 F, \end{aligned}\right\} \qquad (5.25)$$

where we have used the identity $$\tilde{c} = \frac{\tilde{\sigma}}{\tilde{k}}. \tag{5.26}$$

In order to emphasize some of the shallower-water results, we have chosen to subtract from the mass flux, total head and momentum flux their respective zero-order values, and then to divide by them. The solitary-wave results of Longuet-Higgins & Fenton can be compared with these since by the definitions of Q, R and S we have

$$\begin{aligned} Q &= -\int_{-d}^{\eta} \mathscr{U}\,\mathrm{d}Y \\ &= cd \quad \text{at} \quad X = \infty, \end{aligned} \tag{5.27}$$

$$\begin{aligned} R &= p + \tfrac{1}{2}(\mathscr{U}^2 + \mathscr{V}^2) + Y + d \\ &= \tfrac{1}{2}c^2 + d \quad \text{at} \quad X = \infty,\ Y = 0, \end{aligned} \tag{5.28}$$

$$\begin{aligned} S &= \int_{-d}^{\eta} (p + \mathscr{U}^2)\,\mathrm{d}Y \\ &= \int_{-d}^{0} (-Y + c^2)\,\mathrm{d}Y \quad \text{at} \quad X = \infty \\ &= \tfrac{1}{2}d^2 + c^2 d. \end{aligned} \tag{5.29}$$

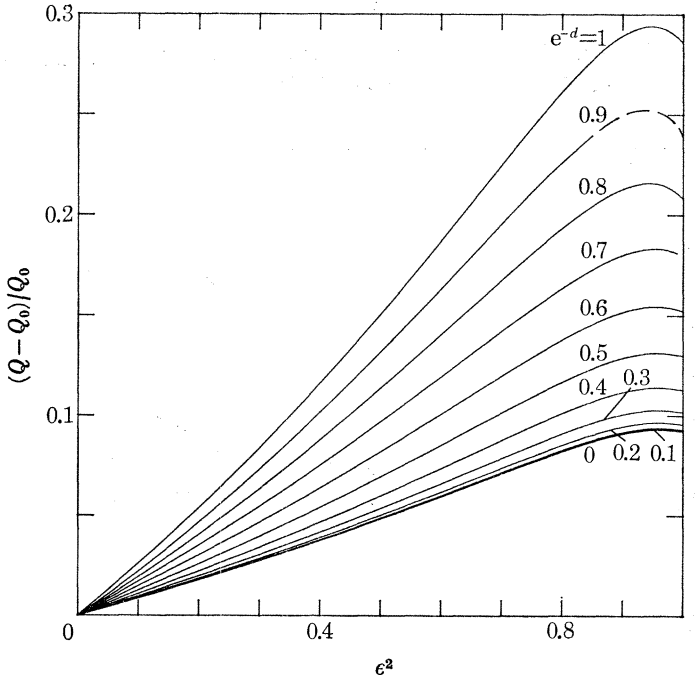

FIGURE 16. The relative increase of the mass flux, Q, over that of linear waves, Q_0, plotted against the expansion parameter, ϵ^2, for the entire range of fluid depths.

Figures 16–18 show $(Q-Q_0)/Q_0$, $(R-R_0)/R_0$ and $(S-S_0)/S_0$ plotted against ϵ^2 for various depths where the subscript zero refers to linear waves. We see that the solitary-wave curves represent upper bounds and that all but one of the curves reach maxima for $\epsilon^2 < 1$. The exception is the $(R-R_0)/R_0$ curve for $\mathrm{e}^{-d} = 0.9$ which is too uncertain to plot for $\epsilon^2 \geqslant 0.91$ owing to incomplete convergence of the Padé approximants.

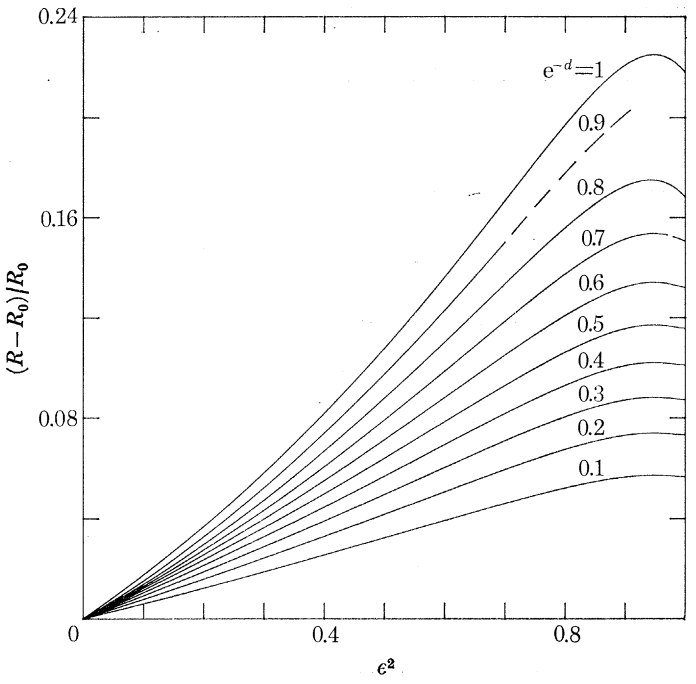

FIGURE 17. The relative increase of the total head, R, over that of linear waves, R_0, plotted against the expansion parameter, ϵ^2, for various depths, d.

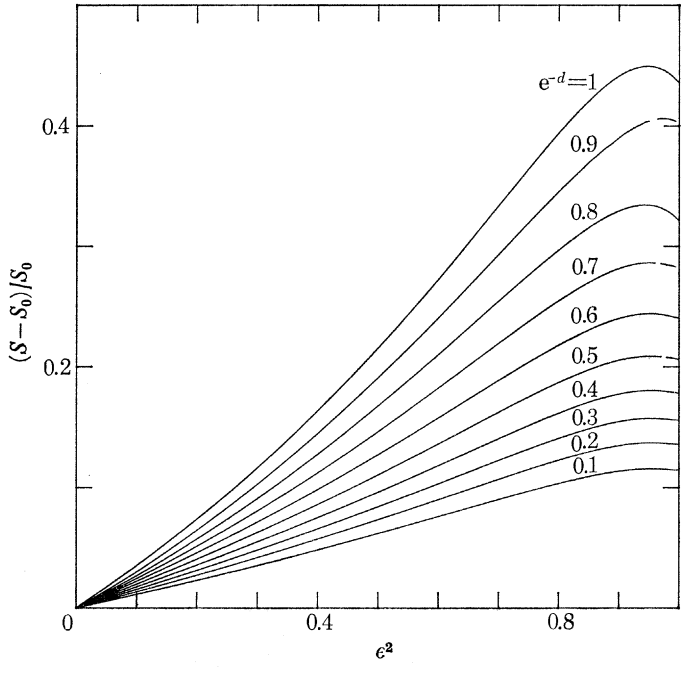

FIGURE 18. The relative increase of the momentum flux, S, over that of linear waves, S_0, plotted against the expansion parameter, ϵ^2, for various depths, d.

PHILOSOPHICAL TRANSACTIONS OF THE ROYAL SOCIETY A MATHEMATICAL, PHYSICAL & ENGINEERING SCIENCES

In a celebrated paper, Benjamin & Lighthill (1954) parameterized finite-depth surface waves in terms of Q, R and S. Using cnoidal wave theory, they calculated the positions of two barriers in the R–S plane beyond which no steady waves can exist. One barrier consists of waves of zero height and the other of solitary waves and uniform supercritical flows. They were not able to calculate the position of the third barrier which was thought to consist of waves of greatest height. From our results we find that this third barrier consists of waves of greatest total head and momentum flux but does not exactly correspond to waves of greatest height. From the tabulated values in the appendix the coordinates of some points along this barrier can be determined.

As a check on the behaviour of the Padé approximants the integral properties were calculated in two different ways, and the results were compared. Using the relations (5.15)–(5.22), we combined the series for the individual terms and then Padé approximated the resulting series. We also Padé approximated the individual terms and then combined them. Comparing the results, we find that for deep water they differ by between 10^{-19} and 10^{-4} depending on the value of ϵ^2 and the integral property in question. Usually the comparisons are very good and only deteriorate for waves very near the highest. They are still good enough to confirm that all of the integral properties achieve maxima for waves short of the highest. The same is generally true for finite depths, but the agreement worsens as the depth decreases. Excluding the $e^{-d} = 0.9$ case which did not converge completely, the differences range from 10^{-21} to 10^{-3}. Since the results of calculating the same physical quantity by Padé approximating different series agree, it is unlikely that this is due to spurious behaviour of the Padé approximants.

In general the series for properties with a basic physical meaning, such as momentum and energy, converged better than those which were just individual terms in the equations. Therefore the results given in the appendix are those for which the series were first combined and then Padé approximated.

6. The wave profile

It is useful to determine the shape of the wave profile. An irregular profile is a visual indication that all is not well in the calculations. Also it is possible to integrate along the wave profile numerically to find the mean free-surface elevation and the potential energy thus providing another check on the results of §5.

We shall use Schwartz's (1972) method of calculating the stream lines. The basic idea is to calculate the Fourier coefficients a_j as series in ϵ and Padé approximate them. With these in hand we then Padé approximate the Fourier series itself and thereby mimic the behaviour of the unknown higher harmonics.

From equation (2.8) we have

$$\begin{aligned} Z &= -\frac{W}{c} + \mathrm{i}\sum_{j=1}^{\infty}\frac{a_j}{j}\mathrm{e}^{\mathrm{i}jW/c} - \mathrm{i}\sum_{j=1}^{\infty}\frac{a_j}{j}\mathrm{e}^{-2jd}\,\mathrm{e}^{-\mathrm{i}jW/c} \\ &\cong -\frac{W}{c} + \mathrm{i}\mathrm{e}^{\mathrm{i}W/c}\frac{p_0 + p_1\mathrm{e}^{\mathrm{i}W/c} + \ldots + p_N\mathrm{e}^{\mathrm{i}NW/c}}{1 + q_1\mathrm{e}^{\mathrm{i}W/c} + \ldots + q_N\mathrm{e}^{\mathrm{i}NW/c}} \\ &\quad - \mathrm{i}\mathrm{e}^{-(\mathrm{i}W/c+2d)}\frac{p_0 + p_1\mathrm{e}^{-(\mathrm{i}W/c+2d)} + \ldots + p_N\mathrm{e}^{-N(\mathrm{i}W/c+2d)}}{1 + q_1\mathrm{e}^{-(\mathrm{i}W/c+2d)} + \ldots + q_N\mathrm{e}^{-N(\mathrm{i}W/c+2d)}}, \end{aligned} \tag{6.1}$$

where the p_j and q_j are related to the a_j by the definition of the $[N/N]$ Padé approximants. Along a streamline Ψ/c is constant and Φ/c varies between 0 and 2π.

It is convenient to define two intermediate variables, r and $\bar{z}$, by

$$r = e^{-\Psi/c}, \tag{6.2a}$$

$$\bar{z} = e^{(\Psi/c)-2d}. \tag{6.2b}$$

By equating real and imaginary parts of (6.1), it can be shown that

$$X = -\frac{\Phi}{c} - r\frac{\mathscr{F}(\Phi,r)}{\mathscr{H}(\Phi,r)} - \bar{z}\frac{\mathscr{F}(\Phi,\bar{z})}{\mathscr{H}(\Phi,\bar{z})}, \tag{6.3a}$$

$$Y = -\frac{\Psi}{c} + r\frac{\mathscr{G}(\Phi,r)}{\mathscr{H}(\Phi,r)} - \bar{z}\frac{\mathscr{G}(\Phi,\bar{z})}{\mathscr{H}(\Phi,\bar{z})}, \tag{6.3b}$$

where

$$\mathscr{F}(\Phi,r) = \sum_{m=-N}^{N} d_m(r)\sin\left[(m+1)\frac{\Phi}{c}\right], \tag{6.4a}$$

$$\mathscr{G}(\Phi,r) = \sum_{m=-N}^{N} d_m(r)\cos\left[(m+1)\frac{\Phi}{c}\right], \tag{6.4b}$$

$$\mathscr{H}(\Phi,r) = \sum_{m=0}^{N} h_m(r)\cos\left(m\frac{\Phi}{c}\right), \tag{6.4c}$$

$$d_m(r) = \begin{cases} \sum_{k=m}^{N} p_k q_{k-m} r^{2k-m} & (m = 0, 1, \ldots, N), \quad (6.5a) \\ \sum_{k=0}^{N+m} p_k q_{k-m} r^{2k-m} & (m = -N, -N+1, \ldots, 0), \quad (6.5b) \end{cases}$$

$$h_0(r) = \sum_{k=0}^{N} q_k^2 r^{2k}, \tag{6.5c}$$

$$h_m(r) = 2\sum_{k=m}^{N} q_k q_{k-m} r^{2k-m} \quad (m = 1, 2, \ldots, N). \tag{6.5d}$$

There is a conflict between the need for the higher harmonics to define the wave profile adequately and the fact that their Fourier coefficients converge less well due to fewer terms in the perturbation series. For a given maximum order of the perturbation expansion, M, and a particular Fourier coefficient, a_j, only $\{\frac{1}{2}(M-j)+1\}$ terms are known in the series expansion since from equation (3.1a)

$$a_j \cong \epsilon^j \sum_{k=0}^{\{\frac{1}{2}(M-j)\}} \alpha_{jk}\epsilon^{2k}. \tag{6.6}$$

Here we use the notation '$\{\ \}$' to mean 'the integer part of'. Therefore the highest-order $[N/N]$ Padé approximant that can be calculated is $\{\frac{1}{4}(M-j)\}$. For the lower harmonics (small j) this is often of sufficiently high order to converge to several figures, but for the higher harmonics convergence is not as good. However, since the Fourier coefficients contribute to Z like a_j/j the higher harmonics need not be as well converged to obtain acceptable accuracy. We have used a simple technique to determine the highest-order Fourier coefficient which is sufficiently converged. For a particular j, $j = 1, 2, \ldots, M$, we calculate

$$\mathscr{E} = \frac{[L/L]\,a_j - [L-1/L-1]\,a_j}{ja}, \tag{6.7}$$

PHILOSOPHICAL TRANSACTIONS OF THE ROYAL SOCIETY A MATHEMATICAL, PHYSICAL & ENGINEERING SCIENCES

with $L = 1, 2, \ldots$ until either $\mathscr{E} \leqslant 10^{-5}$ or $L = \{\frac{1}{4}(M-j)\}$. If the first criterion is satisfied we take $[L/L]\, a_j$ for the jth Fourier coefficient and try the same procedure on a_{j+1}. If the second criterion is satisfied then a_{j-1} is taken as the largest usable Fourier coefficient. By experimentation we have found that increasing or decreasing the convergence criterion for $\mathscr{E}$ by an order of magnitude produces less accurate wave profiles.

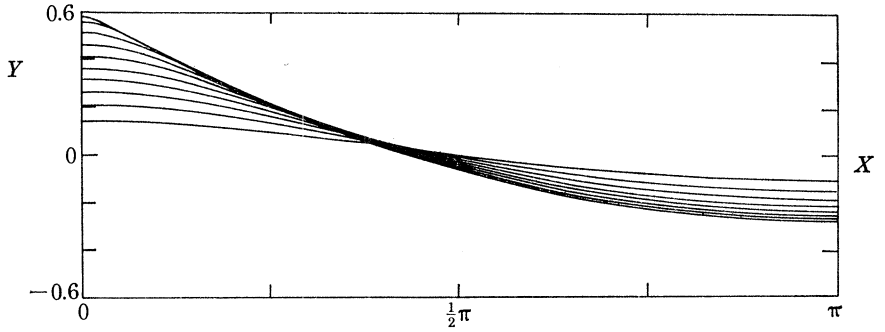

FIGURE 19. The wave profiles from crest to trough of deep-water waves for $\epsilon^2 = 0.1, 0.2, \ldots, 0.8, 0.9, 0.95$.

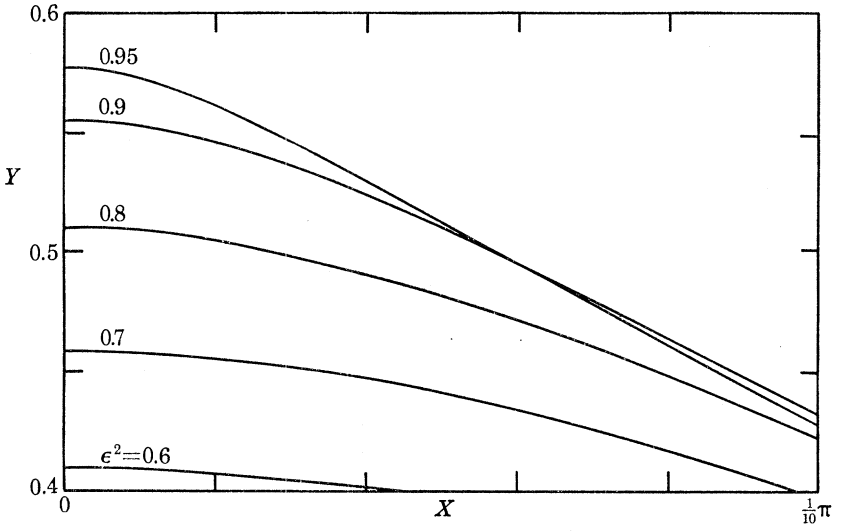

FIGURE 20. A small portion of the deep-water wave profiles near the crests of the higher waves ($\epsilon^2 = 0.6, 0.7, 0.8, 0.9, 0.95$). Notice that the $\epsilon^2 = 0.95$ wave profile intersects that of the lower $\epsilon^2 = 0.9$ wave very near the crest so that it is on average less extreme. This accounts for the intermediate maxima in the wave properties considered as a function of ϵ^2.

The surface streamlines were calculated for various wave heights and depths with the perturbation expansion carried to order ϵ^{110}. Figure 19 shows the deep-water wave profiles from crest to trough adjusted to the same mean level for $\epsilon^2 = 0.1, 0.2, \ldots, 0.8, 0.9, 0.95$. The $\epsilon^2 = 0.95$ profile intersects the $\epsilon^2 = 0.9$ profile twice between crest and trough, once near the wave crest and again near the mean level. A magnified portion of the profiles near the crests is shown in figure 20. We can see that the $\epsilon^2 = 0.95$ wave is higher than the $\epsilon^2 = 0.9$ wave at its crest but soon becomes lower. Over most of the profile the $\epsilon^2 = 0.9$ wave is higher above the mean level and lower beneath it; therefore it is, in an average sense, more extreme. For solitary waves this behaviour was guessed by Longuet-Higgins & Fenton (1974, §6) and confirmed by Byatt-Smith & Longuet-Higgins (1976).

The maxima in the wave energy and other physical properties may be explained in terms of the behaviour of the wave profile. Initially the integral properties increase with the wave height. But as the limiting wave is approached (which also corresponds to the highest wave) the crest stagnation point forces the rounded profile to conform to a sharp 120° angle as shown by Stokes (1880*a*). In so doing the crest narrows, and the wave becomes on average less extreme. Hence the integral properties decrease.

Schwartz found that as the wave height increases the successive Fourier coefficients first increase and then decrease so that the high waves have relatively more high-harmonic content. This is necessary to produce the sharp 120° angle at the highest wave crest. As ϵ^2 ranges between 0.1 and 0.95 we have been able to calculate between 105 and 83 Fourier coefficients using the method of equation (6.7). For larger ϵ^2 the profiles begin to diverge because the a_j fail to converge adequately at order ϵ^{110}. Grant (1973) has shown that the wave crest is not a regular singular point; therefore the Padé approximants have an increasingly difficult time as the highest wave is approached.

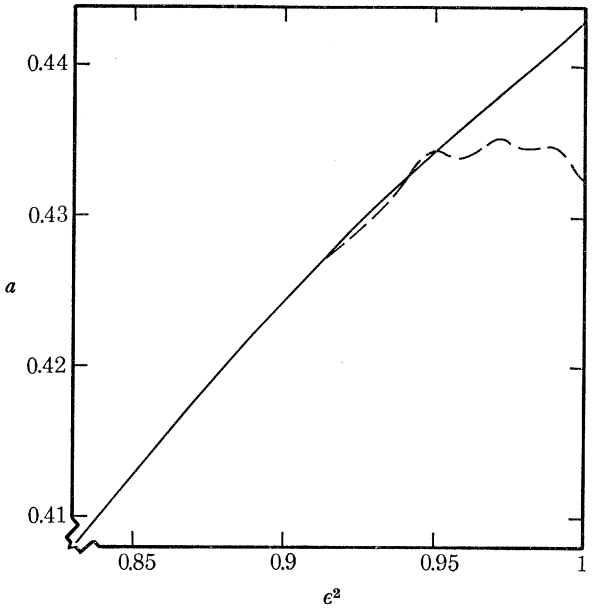

FIGURE 21. A comparison of the Padé-approximated series results (——) and the profile results (– – –) for a small portion of the wave amplitude, a, against expansion parameter, ϵ^2, curve near the highest deep-water wave.

In order to provide an independent check on the results of §§4–5 we have calculated a, $\overline{\eta}$ and V directly from the wave profile. The wave amplitude is simply one-half the vertical distance from crest to trough. $\overline{\eta}$ and V were calculated from their definitions by numerically integrating along the wave profile by the Clemshaw–Curtis quadrature technique (which involves integrating Chebyshev series) over 64 and 128 integration intervals between crest and trough.

Figure 21 shows part of the a against ϵ^2 curve for high waves in deep water. The solid line represents the Padé-approximated series results of §4 and the dashed line those obtained directly from the profile. The two curves are indistinguishable for $\epsilon^2 \leqslant 0.91$ and are still within 0.1% of one another up until $\epsilon^2 = 0.95$. Beyond this point the profile-determined values of a begin to deviate due to the inability of the Padé approximants to represent the sharp crest, but the maximum deviation at $\epsilon^2 = 1$ is still only 2%.

Figures 22 and 23 show portions of the mean surface elevation and potential energy curves

plotted against ϵ^2. The important result here is that the profile results confirm the existence of the maxima. The results disagree by at most 0.5% for high waves even though the high-harmonic content is not adequately represented. Similar calculations have been done for the shallower depths, and the presence of the maxima are confirmed for $e^{-d} \leqslant 0.5$. For depths shallower than this, accurate representations of the wave profiles are not obtainable.

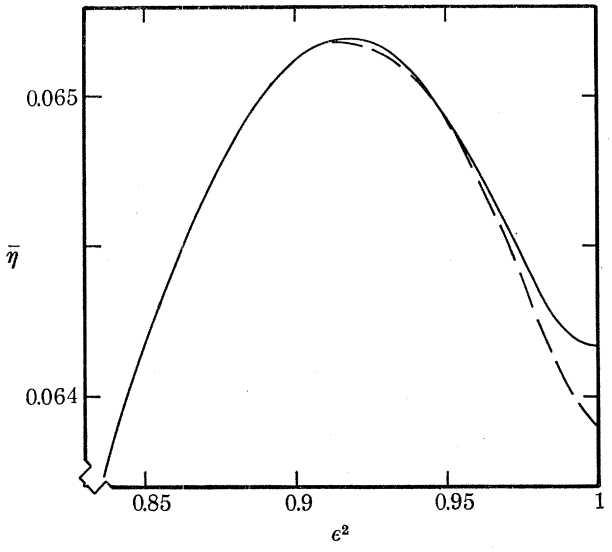

FIGURE 22. A comparison of the Padé-approximated series results (——) and the profile results (– –) for a small portion of the mean free-surface elevation, $\bar{\eta}$, against expansion parameter, ϵ^2, curve near the highest deep-water wave.

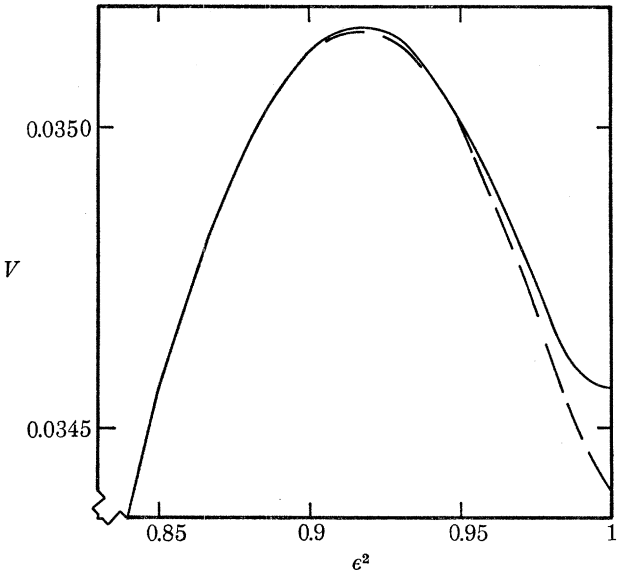

FIGURE 23. A comparison of the Padé-approximated series results (——) and the profile results (– –) for a small portion of the potential energy, V, against expansion parameter, ϵ^2, curve near the highest deep-water wave.

PHILOSOPHICAL TRANSACTIONS OF THE ROYAL SOCIETY A MATHEMATICAL, PHYSICAL & ENGINEERING SCIENCES

7. Discussion

The properties of steady, periodic gravity waves from the lowest to the highest have been determined by a perturbation technique. We have carried the expansion out to a very high order in terms of a parameter whose range is known *ab initio*, and the resulting series have been accurately summed with Padé approximants. The most significant result is that the wave speed, momentum and energy attain maxima for waves which are lower than the highest in water of any uniform depth. By calculating the wave profile we have shown that a very high wave intersects a lower wave near the wave crest. Therefore along most of the profile the very high wave is less extreme. The intermediate maximum in the potential energy has been confirmed by numerically integrating along the wave profile.

We know that small-amplitude waves are unstable to disturbances of slightly different wavelength by the Benjamin & Feir (1967) mechanism of instability, but this requires many wave periods to develop. As pointed out by Longuet-Higgins & Fenton (1974), the non-monotonicity of the integral properties as functions of wave height raises certain questions about the stability of very high waves. For instance, in water of the same depth it is possible for two waves of equal wavelength and frequency to exist, but with the lower one having more energy than the higher one. If disturbed might one of these waves tend to the other perhaps losing energy but gaining in height? Alternatively might a wave become unstable when its height first becomes a double-valued function of another of its properties, its momentum, say? Such instabilities occurring on a short time-scale might explain why it is difficult to generate very high waves in the laboratory.

To date no experimental observations have been made of steady waves whose heights near those at which the wave speed, etc., first become non-monotonic. Such waves may become unstable and break, but even that would be a useful observation to make. A careful measurement of the wave profile in time and space and of the fluid velocity at a fixed point would provide enough information to calculate the wave height, speed and potential energy. The waves should be as long as possible to scale down the effects of surface tension and viscosity. Also the wave-speed maximum becomes more pronounced as the wavelength to depth ratio increases, but it must be remembered that even for solitary waves the speed difference between the fastest and highest waves is only 0.6 %. Therefore precise measurements need to be made. Because of the difficulty in generating very high waves it might be better to generate lower waves and then build up their energy density by sending them into a slowly converging channel.

The existence of the stagnation point at the crest of a highest wave forces the flow to become singular there and for the free surface to conform to a sharp 120° angle. This in turn causes the highest wave to be less extreme than a slightly lower wave. In reality, the effect of surface tension will become important at the wave crest. Our calculations are valid strictly only in the limit of large-scale waves, when gravity dominates surface tension except in a limited region near the wave crest. For waves of finite length, surface tension will become important at some wave amplitude, near the crest. It would be interesting to see how the surface tension affects the relation between wave height and wave energy.

The existence of periodic waves has been proven by Krasovskii (1961) for wave slopes up to 30° from the horizontal. His proof does not consider steeper waves although Stokes's (1880*a*) *local* solution at the crest of a wave with a stagnation point in the Z-plane does have this limiting slope. However, Sasaki & Murakami (1973) have suggested that the maximum slope exceeds 30°, and in a recent paper Longuet-Higgins & Fox (1977) have shown it to be equal to 30.37°.

PHILOSOPHICAL TRANSACTIONS OF THE ROYAL SOCIETY A MATHEMATICAL, PHYSICAL & ENGINEERING SCIENCES

Therefore it would be better to have an existence proof whose validity is limited by the presence of a stagnation point rather than by a maximum slope.

Nekrasov (1921), Levi-Civita (1925) and Struik (1926) have proven that series expansions similar to Stokes's do converge for sufficiently small wave amplitudes. However they were not able to determine the maximum radius of convergence. We have not proven that our series converge, but we have relied on physical reasoning and consistency of the Padé approximants in several different series to obtain what we feel are reliable results. The final resolution of this problem lies in the proper identification and removal of the singularities near the wave crest as the highest wave is approached.

A complete dynamical description of wave breaking has long eluded investigators because the wave motion is time-dependent and fully nonlinear. A recent numerical method (Longuet-Higgins & Cokelet 1976) has been developed which allows the fluid surface to be followed as it bends over on itself. Such techniques probably will help to unravel what happens in the irrotational part of a breaking wave, but any numerical method must be tested to prove that it gives reliable answers. The results of the present investigation have already provided an accurate and exact nonlinear wave which was used as a check for those calculations.

8. Appendix

The properties of the waves as a function of the expansion parameter, $\epsilon^2 = 1 - (q^2_{\text{crest}} q^2_{\text{trough}}/c^4)$, as determined by $[N/N]$ Padé approximating the various perturbation series are given in the following tables labelled A 0 to A 9 corresponding to $e^{-d} = 0, 0.1, \ldots, 0.9$ respectively. The various symbols are defined in the main text of the paper.

The numerical values are given to 6 significant figures where the convergence of the Padé approximants allows. The consistency of the Padé approximants indicates that for a particular numerical value the least significant figure given is correct to ± 1. However, as we have indicated in §4*a* and §5*b*, this may not be true for the shallowest depth ($e^{-d} = 0.9$).

For the purposes of interpolation we find that a cubic spline (Ahlberg, Nilson & Walsh 1967) with its third derivative equal over its first pair and last pair of endpoints works well along lines of constant e^{-d}. Indeed many of the figures were computer-drawn using splines.

I wish to acknowledge with gratitude the guidance of Professor M. S. Longuet-Higgins, F.R.S., who acted as my Ph.D. thesis supervisor during the course of this research (Cokelet 1976) in the Department of Applied Mathematics and Theoretical Physics, Cambridge University.

I was supported for two years by a National Science Foundation Graduate Fellowship from the United States of America and for a third year by a Research Studentship from the Cambridge Philosophical Society. During my final year of research, fees were remitted by Trinity College and Cambridge University. I also received support from the Departments of Energy and Industry during the preparation of this manuscript. I express thanks and appreciation to all of these bodies.

PHILOSOPHICAL TRANSACTIONS OF THE ROYAL SOCIETY A MATHEMATICAL, PHYSICAL & ENGINEERING SCIENCES

PHILOSOPHICAL TRANSACTIONS OF THE ROYAL SOCIETY A MATHEMATICAL, PHYSICAL & ENGINEERING SCIENCES

TABLE A 0. THE PROPERTIES OF THE STEADY WAVE AS A FUNCTION OF THE EXPANSION PARAMETER ϵ^2 FOR $\epsilon^{-d} = 0$

ϵ^2	a	c^2	I	T	V	$\bar{\eta}$	K	S_{xx}	F
0.0	0.0	1.00000	0.0	0.0	0.0	0.0	1.00000	0.0	0.0
0.10	1.30622×10^{-1}	1.01721	8.45446×10^{-3}	4.26345×10^{-3}	4.22707×10^{-3}	8.38264×10^{-3}	1.03397	4.37259×10^{-3}	4.37336×10^{-3}
0.20	1.86957×10^{-1}	1.03557	1.71367×10^{-2}	8.71942×10^{-3}	8.56686×10^{-3}	1.68398×10^{-2}	1.06925	9.17713×10^{-3}	9.18368×10^{-3}
0.30	2.31791×10^{-1}	1.05520	2.60090×10^{-2}	1.33586×10^{-2}	1.29987×10^{-2}	2.53196×10^{-2}	1.10584	1.44384×10^{-2}	1.44618×10^{-2}
0.40	2.70970×10^{-1}	1.07619	3.50007×10^{-2}	1.81548×10^{-2}	1.74844×10^{-2}	3.37390×10^{-2}	1.14367	2.01659×10^{-2}	2.02246×10^{-2}
0.50	3.06684×10^{-1}	1.09858	4.39839×10^{-2}	2.30505×10^{-2}	2.19555×10^{-2}	4.19640×10^{-2}	1.18251	2.63353×10^{-2}	2.64552×10^{-2}
0.60	3.39924×10^{-1}	1.12229	5.27280×10^{-2}	2.79296×10^{-2}	2.62900×10^{-2}	4.97724×10^{-2}	1.22184	3.28487×10^{-2}	3.30623×10^{-2}
0.70	3.71029×10^{-1}	1.14688	6.08108×10^{-2}	3.25619×10^{-2}	3.02660×10^{-2}	5.67834×10^{-2}	1.26045	3.94496×10^{-2}	3.97888×10^{-2}
0.80	3.99671×10^{-1}	1.17093	6.74309×10^{-2}	3.64834×10^{-2}	3.34698×10^{-2}	6.23151×10^{-2}	1.29556	4.55242×10^{-2}	4.60006×10^{-2}
0.81	4.02358×10^{-1}	1.17319	6.79621×10^{-2}	3.68062×10^{-2}	3.37220×10^{-2}	6.27455×10^{-2}	1.29868	4.60586×10^{-2}	4.65473×10^{-2}
0.82	4.05006×10^{-1}	1.17540	6.84620×10^{-2}	3.71118×10^{-2}	3.39582×10^{-2}	6.31477×10^{-2}	1.30169	4.65726×10^{-2}	4.70731×10^{-2}
0.83	4.07612×10^{-1}	1.17755	6.89285×10^{-2}	3.73988×10^{-2}	3.41771×10^{-2}	6.35198×10^{-2}	1.30459	4.70640×10^{-2}	4.75754×10^{-2}
0.84	4.10172×10^{-1}	1.17963	6.93591×10^{-2}	3.76658×10^{-2}	3.43776×10^{-2}	6.38601×10^{-2}	1.30735	4.75301×10^{-2}	4.80517×10^{-2}
0.85	4.12684×10^{-1}	1.18164	6.97512×10^{-2}	3.79110×10^{-2}	3.45585×10^{-2}	6.41665×10^{-2}	1.30998	4.79684×10^{-2}	4.84991×10^{-2}
0.86	4.15145×10^{-1}	1.18357	7.01022×10^{-2}	3.81328×10^{-2}	3.47184×10^{-2}	6.44370×10^{-2}	1.31244	4.83759×10^{-2}	4.89145×10^{-2}
0.87	4.17550×10^{-1}	1.18540	7.04094×10^{-2}	3.83294×10^{-2}	3.48561×10^{-2}	6.46694×10^{-2}	1.31473	4.87494×10^{-2}	4.92947×10^{-2}
0.88	4.19897×10^{-1}	1.18711	7.06698×10^{-2}	3.84989×10^{-2}	3.49701×10^{-2}	6.48617×10^{-2}	1.31683	4.90855×10^{-2}	4.96360×10^{-2}
0.89	4.22181×10^{-1}	1.18870	7.08804×10^{-2}	3.86395×10^{-2}	3.50592×10^{-2}	6.50116×10^{-2}	1.31872	4.93806×10^{-2}	4.99348×10^{-2}
0.90	4.24397×10^{-1}	1.19014	7.10386×10^{-2}	3.87492×10^{-2}	3.51219×10^{-2}	6.51172×10^{-2}	1.32037	4.96310×10^{-2}	5.01871×10^{-2}
0.91	4.26542×10^{-1}	1.19142	7.11415×10^{-2}	3.88262×10^{-2}	3.51573×10^{-2}	6.51765×10^{-2}	1.32177	4.98328×10^{-2}	5.03888×10^{-2}
0.92	4.28611×10^{-1}	1.19251	7.11868×10^{-2}	3.88687×10^{-2}	3.51642×10^{-2}	6.51882×10^{-2}	1.32288	4.99820×10^{-2}	5.05361×10^{-2}
0.93	4.30602×10^{-1}	1.19339	7.11729×10^{-2}	3.88755×10^{-2}	3.51423×10^{-2}	6.51514×10^{-2}	1.32369	5.00752×10^{-2}	5.06250×10^{-2}
0.94	4.32512×10^{-1}	1.19404	7.10996×10^{-2}	3.88459×10^{-2}	3.50916×10^{-2}	6.50665×10^{-2}	1.32417	5.01089×10^{-2}	5.06527×10^{-2}
0.95	4.34342×10^{-1}	1.19443	7.09686×10^{-2}	3.87806×10^{-2}	3.50137×10^{-2}	6.49358×10^{-2}	1.32430	5.00818×10^{-2}	5.06172×10^{-2}
0.96	4.36098×10^{-1}	1.19454	7.07859×10^{-2}	3.86824×10^{-2}	3.49119×10^{-2}	6.4765×10^{-2}	1.32407	4.99941×10^{-2}	5.05199×10^{-2}
0.97	4.37795×10^{-1}	1.19436	7.0563×10^{-2}	3.8557×10^{-2}	3.47935×10^{-2}	6.4566×10^{-2}	1.32349	4.9852×10^{-2}	5.03671×10^{-2}
0.98	4.39467×10^{-1}	1.19391	7.0333×10^{-2}	3.8421×10^{-2}	3.4673×10^{-2}	6.4363×10^{-2}	1.32264	4.9671×10^{-2}	5.01762×10^{-2}
0.99	4.41190×10^{-1}	1.19329	7.016×10^{-2}	3.8303×10^{-2}	3.457×10^{-2}	6.4201×10^{-2}	1.32169	4.9491×10^{-2}	4.99882×10^{-2}
1.00	4.4313×10^{-1}	1.1928	7.01×10^{-2}	3.827×10^{-2}	3.457×10^{-2}	6.417×10^{-2}	1.3212	4.941×10^{-2}	4.9903×10^{-2}

TABLE A 1. THE PROPERTIES OF THE STEADY WAVE AS A FUNCTION OF THE EXPANSION PARAMETER ϵ^2 FOR $e^{-d} = 0.1$

ϵ^2	a	c^2	I	T	V	$\bar{\eta}$
0.0	0.0	9.80198×10^{-1}	0.0	0.0	0.0	0.0
0.10	1.27189×10^{-1}	9.97193×10^{-1}	8.09195×10^{-3}	4.04029×10^{-3}	4.00620×10^{-3}	8.10334×10^{-3}
0.20	1.82094×10^{-1}	1.01533	1.64013×10^{-2}	8.26329×10^{-3}	8.12016×10^{-3}	1.62770×10^{-2}
0.30	2.25827×10^{-1}	1.03472	2.48923×10^{-2}	1.26604×10^{-2}	1.23224×10^{-2}	2.44710×10^{-2}
0.40	2.64080×10^{-1}	1.05546	3.34974×10^{-2}	1.72068×10^{-2}	1.65766×10^{-2}	3.26054×10^{-2}
0.50	2.98985×10^{-1}	1.07759	4.20945×10^{-2}	2.18485×10^{-2}	2.08180×10^{-2}	4.05508×10^{-2}
0.60	3.31510×10^{-1}	1.10103	5.04632×10^{-2}	2.64755×10^{-2}	2.49305×10^{-2}	4.80924×10^{-2}
0.70	3.61984×10^{-1}	1.12534	5.81986×10^{-2}	3.08691×10^{-2}	2.87032×10^{-2}	5.48620×10^{-2}
0.80	3.90091×10^{-1}	1.14912	6.45322×10^{-2}	3.45883×10^{-2}	3.17417×10^{-2}	6.01996×10^{-2}
0.81	3.92730×10^{-1}	1.15135	6.50400×10^{-2}	3.48943×10^{-2}	3.19808×10^{-2}	6.06145×10^{-2}
0.82	3.95332×10^{-1}	1.15354	6.55179×10^{-2}	3.51840×10^{-2}	3.22045×10^{-2}	6.10021×10^{-2}
0.83	3.97893×10^{-1}	1.15566	6.59637×10^{-2}	3.54561×10^{-2}	3.24118×10^{-2}	6.13606×10^{-2}
0.84	4.00410×10^{-1}	1.15772	6.63750×10^{-2}	3.57090×10^{-2}	3.26016×10^{-2}	6.16882×10^{-2}
0.85	4.02880×10^{-1}	1.15971	6.67495×10^{-2}	3.59412×10^{-2}	3.27727×10^{-2}	6.19830×10^{-2}
0.86	4.05300×10^{-1}	1.16162	6.70845×10^{-2}	3.61513×10^{-2}	3.29239×10^{-2}	6.22431×10^{-2}
0.87	4.07666×10^{-1}	1.16342	6.73774×10^{-2}	3.63373×10^{-2}	3.30538×10^{-2}	6.24663×10^{-2}
0.88	4.09975×10^{-1}	1.16512	6.76254×10^{-2}	3.64976×10^{-2}	3.31613×10^{-2}	6.26506×10^{-2}
0.89	4.12223×10^{-1}	1.16668	6.78257×10^{-2}	3.66304×10^{-2}	3.32450×10^{-2}	6.27940×10^{-2}
0.90	4.14405×10^{-1}	1.16811	6.79756×10^{-2}	3.67337×10^{-2}	3.33037×10^{-2}	6.28943×10^{-2}
0.91	4.16518×10^{-1}	1.16937	6.80722×10^{-2}	3.68059×10^{-2}	3.33363×10^{-2}	6.29500×10^{-2}
0.92	4.18557×10^{-1}	1.17045	6.81114×10^{-2}	3.68454×10^{-2}	3.33418×10^{-2}	6.29595×10^{-2}
0.93	4.20519×10^{-1}	1.17132	6.80991×10^{-2}	3.68510×10^{-2}	3.33199×10^{-2}	6.29222×10^{-2}
0.94	4.22403×10^{-1}	1.17196	6.80270×10^{-2}	3.68220×10^{-2}	3.32708×10^{-2}	6.28384×10^{-2}
0.95	4.24208×10^{-1}	1.17234	6.78997×10^{-2}	3.67591×10^{-2}	3.31957×10^{-2}	6.27104×10^{-2}
0.96	4.25941×10^{-1}	1.17245	6.77229×10^{-2}	3.66650×10^{-2}	3.30981×10^{-2}	6.25442×10^{-2}
0.97	4.27616×10^{-1}	1.17227	6.7508×10^{-2}	3.65463×10^{-2}	3.29850×10^{-2}	6.2351×10^{-2}
0.98	4.2927×10^{-1}	1.17182	6.7286×10^{-2}	3.6418×10^{-2}	3.28702×10^{-2}	6.2153×10^{-2}
0.99	4.3097×10^{-1}	1.1712	6.710×10^{-2}	3.631×10^{-2}	3.2783×10^{-2}	6.200×10^{-2}
1.00	4.329×10^{-1}	1.1708	6.706×10^{-2}	3.630×10^{-2}	3.280×10^{-2}	6.200×10^{-2}

ϵ^2	K	S_{xx}	F	$\overline{u_b^2}$	R	S
0.0	9.80198×10^{-1}	0.0	0.0	0.0	2.79268	4.90794
0.10	1.01371	4.86378×10^{-3}	4.46407×10^{-3}	3.12111×10^{-4}	2.80944	4.96254
0.20	1.04850	1.01187×10^{-2}	9.33834×10^{-3}	6.14972×10^{-4}	2.82683	5.02004
0.30	1.08457	1.57814×10^{-2}	1.46488×10^{-2}	9.05476×10^{-4}	2.84487	5.08059
0.40	1.12185	2.18515×10^{-2}	2.04069×10^{-2}	1.17938×10^{-3}	2.86351	5.14428
0.50	1.16012	2.82923×10^{-2}	2.65898×10^{-2}	1.43073×10^{-3}	2.88264	5.21098
0.60	1.19886	3.49914×10^{-2}	3.31007×10^{-2}	1.65101×10^{-3}	2.90202	5.28009
0.70	1.23689	4.16754×10^{-2}	3.96803×10^{-2}	1.82761×10^{-3}	2.92103	5.34990
0.80	1.27146	4.77157×10^{-2}	4.57022×10^{-2}	1.94162×10^{-3}	2.93832	5.41587
0.81	1.27453	4.82400×10^{-2}	4.62285×10^{-2}	1.94861×10^{-3}	2.93985	5.42190
0.82	1.27749	4.87428×10^{-2}	4.67340×10^{-2}	1.95467×10^{-3}	2.94133	5.42776
0.83	1.28034	4.92217×10^{-2}	4.72160×10^{-2}	1.95979×10^{-3}	2.94276	5.43344
0.84	1.28306	4.96744×10^{-2}	4.76721×10^{-2}	1.96392×10^{-3}	2.94412	5.43891
0.85	1.28565	5.00981×10^{-2}	4.80996×10^{-2}	1.96704×10^{-3}	2.94541	5.44414
0.86	1.28807	5.04901×10^{-2}	4.84955×10^{-2}	1.96913×10^{-3}	2.94662	5.44911
0.87	1.29032	5.08473×10^{-2}	4.88567×10^{-2}	1.97015×10^{-3}	2.94775	5.45378
0.88	1.29239	5.11663×10^{-2}	4.91797×10^{-2}	1.97010×10^{-3}	2.94878	5.45812
0.89	1.29424	5.14438×10^{-2}	4.94609×10^{-2}	1.96896×10^{-3}	2.94971	5.46208
0.90	1.29586	5.16761×10^{-2}	4.96967×10^{-2}	1.96674×10^{-3}	2.95052	5.46562
0.91	1.29723	5.18596×10^{-2}	4.98832×10^{-2}	1.96344×10^{-3}	2.95120	5.46870
0.92	1.29832	5.19906×10^{-2}	5.00166×10^{-2}	1.95912×10^{-3}	2.95175	5.47126
0.93	1.29912	5.20659×10^{-2}	5.00936×10^{-2}	1.95384×10^{-3}	2.95214	5.47324
0.94	1.29958	5.20829×10^{-2}	5.01114×10^{-2}	1.94773×10^{-3}	2.95238	5.47459
0.95	1.29970	5.20403×10^{-2}	5.00685×10^{-2}	1.94098×10^{-3}	2.95244	5.47525
0.96	1.29947	5.1939×10^{-2}	4.9967×10^{-2}	1.93390×10^{-3}	2.95232	5.47519
0.97	1.29890	5.1789×10^{-2}	4.9812×10^{-2}	1.92699×10^{-3}	2.95203	5.47440
0.98	1.29805	5.160×10^{-2}	4.9623×10^{-2}	1.9211×10^{-3}	2.95161	5.47298
0.99	1.29713	5.143×10^{-2}	4.945×10^{-2}	1.9176×10^{-3}	2.95115	5.47123
1.00	1.29670	5.14×10^{-2}	4.936×10^{-2}	1.919×10^{-3}	2.9509	5.47016

PHILOSOPHICAL TRANSACTIONS OF THE ROYAL SOCIETY A MATHEMATICAL, PHYSICAL & ENGINEERING SCIENCES

TABLE A 2. THE PROPERTIES OF THE STEADY WAVE AS A FUNCTION OF THE EXPANSION PARAMETER ϵ^2 FOR $e^{-d} = 0.2$

ϵ^2	a	c^2	I	T	V	$\bar{\eta}$
0.0	0.0	9.23077×10^{-1}	0.0	0.0	0.0	0.0
0.10	1.17156×10^{-1}	9.39572×10^{-1}	7.06286×10^{-3}	3.42307×10^{-3}	3.39470×10^{-3}	7.28645×10^{-3}
0.20	1.67926×10^{-1}	9.57179×10^{-1}	1.43239×10^{-2}	7.00692×10^{-3}	6.88749×10^{-3}	1.46408×10^{-2}
0.30	2.08508×10^{-1}	9.76003×10^{-1}	2.17525×10^{-2}	1.07450×10^{-2}	1.04621×10^{-2}	2.20183×10^{-2}
0.40	2.44136×10^{-1}	9.96136×10^{-1}	2.92906×10^{-2}	1.46170×10^{-2}	1.40880×10^{-2}	2.93473×10^{-2}
0.50	2.76769×10^{-1}	1.01763	3.68315×10^{-2}	1.85774×10^{-2}	1.77097×10^{-2}	3.65111×10^{-2}
0.60	3.07303×10^{-1}	1.04039	4.41818×10^{-2}	2.25326×10^{-2}	2.12275×10^{-2}	4.33156×10^{-2}
0.70	3.36041×10^{-1}	1.06401	5.09836×10^{-2}	2.62950×10^{-2}	2.44591×10^{-2}	4.94261×10^{-2}
0.80	3.62685×10^{-1}	1.08713	5.65549×10^{-2}	2.94836×10^{-2}	2.70626×10^{-2}	5.42413×10^{-2}
0.81	3.65196×10^{-1}	1.08929	5.70012×10^{-2}	2.97459×10^{-2}	2.72671×10^{-2}	5.46149×10^{-2}
0.82	3.67671×10^{-1}	1.09141	5.74211×10^{-2}	2.99941×10^{-2}	2.74584×10^{-2}	5.49638×10^{-2}
0.83	3.70110×10^{-1}	1.09348	5.78125×10^{-2}	3.02272×10^{-2}	2.76355×10^{-2}	5.52862×10^{-2}
0.84	3.72509×10^{-1}	1.09584	5.81734×10^{-2}	3.04437×10^{-2}	2.77976×10^{-2}	5.55804×10^{-2}
0.85	3.74864×10^{-1}	1.09741	5.85017×10^{-2}	3.06425×10^{-2}	2.79434×10^{-2}	5.58449×10^{-2}
0.86	3.77174×10^{-1}	1.09926	5.87950×10^{-2}	3.08220×10^{-2}	2.80720×10^{-2}	5.60777×10^{-2}
0.87	3.79434×10^{-1}	1.10101	5.90510×10^{-2}	3.09808×10^{-2}	2.81823×10^{-2}	5.62770×10^{-2}
0.88	3.81642×10^{-1}	1.10265	5.92671×10^{-2}	3.11174×10^{-2}	2.82732×10^{-2}	5.64409×10^{-2}
0.89	3.83792×10^{-1}	1.10418	5.94410×10^{-2}	3.12302×10^{-2}	2.83434×10^{-2}	5.65675×10^{-2}
0.90	3.85882×10^{-1}	1.10556	5.95701×10^{-2}	3.13176×10^{-2}	2.83920×10^{-2}	5.66550×10^{-2}
0.91	3.87906×10^{-1}	1.10678	5.96521×10^{-2}	3.13781×10^{-2}	2.84181×10^{-2}	5.67018×10^{-2}
0.92	3.89863×10^{-1}	1.10782	5.96853×10^{-2}	3.14102×10^{-2}	2.84207×10^{-2}	5.67066×10^{-2}
0.93	3.91747×10^{-1}	1.10866	5.96681×10^{-2}	3.14131×10^{-2}	2.83997×10^{-2}	5.66688×10^{-2}
0.94	3.93558×10^{-1}	1.10927	5.96003×10^{-2}	3.13861×10^{-2}	2.83551×10^{-2}	5.65888×10^{-2}
0.95	3.95295×10^{-1}	1.10963	5.94838×10^{-2}	3.13300×10^{-2}	2.82883×10^{-2}	5.64689×10^{-2}
0.96	3.96964×10^{-1}	1.10972	5.9323×10^{-2}	3.12471×10^{-2}	2.8202×10^{-2}	5.6314×10^{-2}
0.97	3.98578×10^{-1}	1.10954	5.9130×10^{-2}	3.1144×10^{-2}	2.8102×10^{-2}	5.6136×10^{-2}
0.98	4.0017×10^{-1}	1.10910	5.8925×10^{-2}	3.103×10^{-2}	2.800×10^{-2}	5.595×10^{-2}
0.99	4.0181×10^{-1}	1.1085	5.876×10^{-2}	3.09×10^{-2}	2.79×10^{-2}	5.581×10^{-2}
1.00	4.037×10^{-1}	1.1080	5.872×10^{-2}	3.08×10^{-2}	2.79×10^{-2}	5.57×10^{-2}

ϵ^2	K	S_{xx}	F	$\overline{u_b^2}$	R	S
0.0	9.23077×10^{-1}	0.0	0.0	0.0	2.07098	2.78078
0.10	9.55202×10^{-1}	5.21690×10^{-3}	4.20491×10^{-3}	1.05690×10^{-3}	2.08704	2.81745
0.20	9.88540×10^{-1}	1.07425×10^{-2}	8.75593×10^{-3}	2.07950×10^{-3}	2.10371	2.85606
0.30	1.02310	1.65818×10^{-2}	1.36714×10^{-2}	3.05758×10^{-3}	2.12099	2.89673
0.40	1.05880	2.27214×10^{-2}	1.89653×10^{-2}	3.97706×10^{-3}	2.13884	2.93952
0.50	1.09547	2.91109×10^{-2}	2.45797×10^{-2}	4.81820×10^{-3}	2.15717	2.98434
0.60	1.13258	3.56251×10^{-2}	3.04487×10^{-2}	5.55256×10^{-3}	2.17573	3.03081
0.70	1.16900	4.19851×10^{-2}	3.63192×10^{-2}	6.13803×10^{-3}	2.19394	3.07778
0.80	1.20212	4.75794×10^{-3}	4.16213×10^{-2}	6.51137×10^{-3}	2.21050	3.12219
0.81	1.20506	4.80548×10^{-2}	4.20797×10^{-2}	6.53378×10^{-3}	2.21197	3.12625
0.82	1.20790	4.85083×10^{-2}	4.25187×10^{-2}	6.55310×10^{-3}	2.21338	3.13020
0.83	1.21062	4.89378×10^{-2}	4.29362×10^{-2}	6.56920×10^{-3}	2.21475	3.13403
0.84	1.21323	4.93412×10^{-2}	4.33298×10^{-2}	6.58199×10^{-3}	2.21605	3.13771
0.85	1.21569	4.97160×10^{-2}	4.36973×10^{-2}	6.59138×10^{-3}	2.21728	3.14123
0.86	1.21801	5.00597×10^{-2}	4.40360×10^{-2}	6.59729×10^{-3}	2.21844	3.14458
0.87	1.22016	5.03694×10^{-2}	4.43431×10^{-2}	6.59964×10^{-3}	2.21952	3.14772
0.88	1.22214	5.06423×10^{-2}	4.46158×10^{-2}	6.59837×10^{-3}	2.22051	3.15064
0.89	1.22390	5.08754×10^{-2}	4.48508×10^{-2}	6.59346×10^{-3}	2.22139	3.15330
0.90	1.22545	5.10654×10^{-2}	4.50451×10^{-2}	6.58492×10^{-3}	2.22216	3.15568
0.91	1.22675	5.12094×10^{-2}	4.51954×10^{-2}	6.57282×10^{-3}	2.22281	3.15775
0.92	1.22779	5.13042×10^{-2}	4.52986×10^{-2}	6.55729×10^{-3}	2.22333	3.15946
0.93	1.22853	5.13474×10^{-2}	4.53518×10^{-2}	6.53861×10^{-3}	2.22370	3.16079
0.94	1.22896	5.13370×10^{-2}	4.53531×10^{-2}	6.51719×10^{-3}	2.22392	3.16168
0.95	1.22906	5.12730×10^{-2}	4.53017×10^{-2}	6.49374×10^{-3}	2.22397	3.16212
0.96	1.22882	5.11579×10^{-2}	4.5199×10^{-2}	6.45933×10^{-3}	2.22385	3.16206
0.97	1.22826	5.1000×10^{-2}	4.5053×10^{-2}	6.4457×10^{-3}	2.22357	3.16152
0.98	1.22744	5.0820×10^{-2}	4.488×10^{-2}	6.4256×10^{-3}	2.22316	3.16055
0.99	1.22656	5.066×10^{-2}	4.472×10^{-2}	6.4138×10^{-3}	2.22272	3.15936
1.00	1.2262	5.06×10^{-2}	4.47×10^{-2}	6.418×10^{-3}	2.2225	3.15862

PHILOSOPHICAL TRANSACTIONS OF THE ROYAL SOCIETY A MATHEMATICAL, PHYSICAL & ENGINEERING SCIENCES

TABLE A 3. THE PROPERTIES OF THE STEADY WAVE AS A FUNCTION OF THE EXPANSION PARAMETER ϵ^2 FOR $e^{-d} = 0.3$

ϵ^2	a	c^2	I	T	V	$\bar{\eta}$
0.0	0.0	8.34862×10^{-1}	0.0	0.0	0.0	0.0
0.10	1.01407×10^{-1}	8.50859×10^{-1}	5.54793×10^{-3}	2.55876×10^{-3}	2.53722×10^{-3}	6.01453×10^{-3}
0.20	1.45806×10^{-1}	8.67918×10^{-1}	1.12878×10^{-2}	5.25780×10^{-3}	5.16699×10^{-3}	1.21163×10^{-2}
0.30	1.81613×10^{-1}	8.86141×10^{-1}	1.71966×10^{-2}	8.09400×10^{-3}	7.87762×10^{-3}	1.82680×10^{-2}
0.40	2.13322×10^{-1}	9.05617×10^{-1}	2.32284×10^{-2}	1.10525×10^{-2}	1.06642×10^{-2}	2.44088×10^{-2}
0.50	2.42619×10^{-1}	9.26393×10^{-1}	2.92979×10^{-2}	1.40995×10^{-2}	1.34302×10^{-2}	3.04396×10^{-2}
0.60	2.70271×10^{-1}	9.48390×10^{-1}	3.52476×10^{-2}	1.71630×10^{-2}	1.61518×10^{-2}	3.61940×10^{-2}
0.70	2.96534×10^{-1}	9.71196×10^{-1}	4.07832×10^{-2}	2.00958×10^{-2}	1.86670×10^{-2}	4.13835×10^{-2}
0.80	3.21119×10^{-1}	9.93490×10^{-1}	4.53378×10^{-2}	2.25950×10^{-2}	2.07209×10^{-2}	4.54861×10^{-2}
0.81	3.23450×10^{-1}	9.95578×10^{-1}	4.57033×10^{-2}	2.28011×10^{-2}	2.08631×10^{-2}	4.58048×10^{-2}
0.82	3.25750×10^{-1}	9.97621×10^{-1}	4.60472×10^{-2}	2.29962×10^{-2}	2.10123×10^{-2}	4.61020×10^{-2}
0.83	3.28018×10^{-1}	9.99610×10^{-1}	4.63676×10^{-2}	2.31793×10^{-2}	2.11515×10^{-2}	4.63767×10^{-2}
0.84	3.30252×10^{-1}	1.00153	4.66631×10^{-2}	2.33495×10^{-2}	2.12783×10^{-2}	4.66273×10^{-2}
0.85	3.32448×10^{-1}	1.00339	4.69317×10^{-2}	2.35056×10^{-2}	2.13923×10^{-2}	4.68522×10^{-2}
0.86	3.34604×10^{-1}	1.00517	4.71715×10^{-2}	2.36466×10^{-2}	2.14927×10^{-2}	4.70500×10^{-2}
0.87	3.36717×10^{-1}	1.00685	4.73804×10^{-2}	2.37712×10^{-2}	2.15786×10^{-2}	4.72189×10^{-2}
0.88	3.38782×10^{-1}	1.00843	4.75565×10^{-2}	2.38782×10^{-2}	2.16490×10^{-2}	4.73573×10^{-2}
0.89	3.40797×10^{-1}	1.00989	4.76976×10^{-2}	2.39664×10^{-2}	2.17032×10^{-2}	4.74635×10^{-2}
0.90	3.42757×10^{-1}	1.01121	4.78016×10^{-2}	2.40344×10^{-2}	2.17403×10^{-2}	4.75360×10^{-2}
0.91	3.44658×10^{-1}	1.01237	4.78667×10^{-2}	2.40810×10^{-2}	2.17593×10^{-2}	4.75733×10^{-2}
0.92	3.46498×10^{-1}	1.01336	4.78912×10^{-2}	2.41051×10^{-2}	2.17599×10^{-2}	4.75744×10^{-2}
0.93	3.48272×10^{-1}	1.01416	4.78741×10^{-2}	2.41059×10^{-2}	2.17416×10^{-2}	4.75387×10^{-2}
0.94	3.49978×10^{-1}	1.01473	4.78150×10^{-2}	2.40830×10^{-2}	2.17046×10^{-2}	4.74666×10^{-2}
0.95	3.51617×10^{-1}	1.01507	4.77154×10^{-2}	2.40368×10^{-2}	2.16499×10^{-2}	4.73600×10^{-2}
0.96	3.53193×10^{-1}	1.01514	4.75796×10^{-2}	2.39692×10^{-2}	2.15800×10^{-2}	4.72236×10^{-2}
0.97	3.54717×10^{-1}	1.01494	4.74172×10^{-2}	2.38850×10^{-2}	2.14995×10^{-2}	4.70668×10^{-2}
0.98	3.56219×10^{-1}	1.01450	4.7246×10^{-2}	2.37937×10^{-2}	2.1418×10^{-2}	4.69079×10^{-2}
0.99	3.57760×10^{-1}	1.01391	4.7105×10^{-2}	2.3716×10^{-2}	2.1353×10^{-2}	4.6784×10^{-2}
1.00	3.5948×10^{-1}	1.01349	4.708×10^{-2}	2.3698×10^{-2}	2.1346×10^{-2}	4.6772×10^{-2}

ϵ^2	K	S_{xx}	F	$\overline{u_b^2}$	R	S
0.0	8.34862×10^{-1}	0.0	0.0	0.0	1.62140	1.72993
0.10	8.64670×10^{-1}	4.77967×10^{-3}	3.39944×10^{-3}	1.78208×10^{-3}	1.63631	1.75611
0.20	8.95656×10^{-1}	9.79464×10^{-3}	7.07385×10^{-3}	3.50601×10^{-3}	1.65180	1.78366
0.30	9.27831×10^{-1}	1.50432×10^{-2}	1.10362×10^{-2}	5.15450×10^{-3}	1.66788	1.81268
0.40	9.61139×10^{-1}	2.05061×10^{-2}	1.52874×10^{-2}	6.70368×10^{-3}	1.68454	1.84320
0.50	9.95392×10^{-1}	2.61307×10^{-2}	1.98017×10^{-2}	8.11989×10^{-3}	1.70167	1.87517
0.60	1.03013	3.17976×10^{-2}	2.44974×10^{-2}	9.35441×10^{-3}	1.71904	1.90831
0.70	1.06430	3.72525×10^{-2}	2.91729×10^{-2}	1.03348×10^{-2}	1.73612	1.94181
0.80	1.09541	4.19552×10^{-2}	3.33611×10^{-2}	1.09519×10^{-2}	1.75168	1.97347
0.81	1.09818	4.23477×10^{-2}	3.37202×10^{-2}	1.09880×10^{-2}	1.75306	1.97637
0.82	1.10084	4.27204×10^{-2}	3.40633×10^{-2}	1.10188×10^{-2}	1.75439	1.97918
0.83	1.10341	4.30716×10^{-2}	3.43887×10^{-2}	1.10441×10^{-2}	1.75568	1.98190
0.84	1.10586	4.33993×10^{-2}	3.46946×10^{-2}	1.10637×10^{-2}	1.75690	1.98452
0.85	1.10818	4.37016×10^{-2}	3.49790×10^{-2}	1.10774×10^{-2}	1.75806	1.98703
0.86	1.11035	4.39764×10^{-2}	3.52400×10^{-2}	1.10852×10^{-2}	1.75915	1.98941
0.87	1.11238	4.42212×10^{-2}	3.54752×10^{-2}	1.10869×10^{-2}	1.76016	1.99164
0.88	1.11423	4.44337×10^{-2}	3.56824×10^{-2}	1.10825×10^{-2}	1.76109	1.99371
0.89	1.11589	4.46115×10^{-2}	3.58592×10^{-2}	1.10717×10^{-2}	1.76192	1.99560
0.90	1.11733	4.47520×10^{-2}	3.60031×10^{-2}	1.10548×10^{-2}	1.76264	1.99729
0.91	1.11855	4.48528×10^{-2}	3.61115×10^{-2}	1.10319×10^{-2}	1.76325	1.99875
0.92	1.11952	4.49116×10^{-2}	3.61821×10^{-2}	1.10031×10^{-2}	1.76373	1.99995
0.93	1.12021	4.49266×10^{-2}	3.62128×10^{-2}	1.09690×10^{-2}	1.76408	2.00088
0.94	1.12060	4.48967×10^{-2}	3.62022×10^{-2}	1.09304×10^{-2}	1.76427	2.00149
0.95	1.12068	4.48224×10^{-2}	3.61501×10^{-2}	1.08885×10^{-2}	1.76431	2.00178
0.96	1.12043	4.47065×10^{-2}	3.60584×10^{-2}	1.08452×10^{-2}	1.76419	2.00172
0.97	1.11988	4.4557×10^{-2}	3.59334×10^{-2}	1.08035×10^{-2}	1.76392	2.00131
0.98	1.11909	4.4391×10^{-2}	3.5789×10^{-2}	1.07685×10^{-2}	1.76352	2.00059
0.99	1.11822	4.4246×10^{-2}	3.5657×10^{-2}	1.07484×10^{-2}	1.76309	1.99974
1.00	1.1178	4.420×10^{-2}	3.561×10^{-2}	1.07585×10^{-2}	1.76287	1.99923

PHILOSOPHICAL TRANSACTIONS OF THE ROYAL SOCIETY A MATHEMATICAL, PHYSICAL & ENGINEERING SCIENCES

TABLE A 4. THE PROPERTIES OF THE STEADY WAVE AS A FUNCTION OF THE EXPANSION PARAMETER ϵ^2 FOR $\epsilon^{-d} = 0.4$

ϵ^2	a	c^2	I	T	V	$\bar{\eta}$
0.0	0.0	7.24138×10^{-1}	0.0	0.0	0.0	0.0
0.10	8.16165×10^{-2}	7.39745×10^{-1}	3.84088×10^{-3}	1.65174×10^{-3}	1.63656×10^{-3}	4.46570×10^{-3}
0.20	1.18154×10^{-1}	7.56364×10^{-1}	7.88489×10^{-3}	3.42871×10^{-3}	3.36430×10^{-3}	9.06630×10^{-3}
0.30	1.48160×10^{-1}	7.74088×10^{-1}	1.21161×10^{-2}	5.33003×10^{-3}	5.17620×10^{-3}	1.37711×10^{-2}
0.40	1.75182×10^{-1}	7.93000×10^{-1}	1.65018×10^{-2}	7.34745×10^{-3}	7.05728×10^{-3}	1.85308×10^{-2}
0.50	2.00545×10^{-1}	8.13140×10^{-1}	2.09784×10^{-2}	9.45857×10^{-3}	8.97835×10^{-3}	2.32643×10^{-2}
0.60	2.24848×10^{-1}	8.34428×10^{-1}	2.54266×10^{-2}	1.16132×10^{-2}	1.08843×10^{-2}	2.78352×10^{-2}
0.70	2.48271×10^{-1}	8.56460×10^{-1}	2.96191×10^{-2}	1.37055×10^{-2}	1.26708×10^{-2}	3.20050×10^{-2}
0.80	2.70520×10^{-1}	8.77946×10^{-1}	3.31113×10^{-2}	1.55124×10^{-2}	1.41363×10^{-2}	3.53380×10^{-2}
0.81	2.72647×10^{-1}	8.79954×10^{-1}	3.33934×10^{-2}	1.56625×10^{-2}	1.42524×10^{-2}	3.55984×10^{-2}
0.82	2.74749×10^{-1}	8.81918×10^{-1}	3.36592×10^{-2}	1.58048×10^{-2}	1.43612×10^{-2}	3.58418×10^{-2}
0.83	2.76826×10^{-1}	8.83828×10^{-1}	3.39072×10^{-2}	1.59384×10^{-2}	1.44620×10^{-2}	3.60668×10^{-2}
0.84	2.78873×10^{-1}	8.85679×10^{-1}	3.41361×10^{-2}	1.60628×10^{-2}	1.45543×10^{-2}	3.62723×10^{-2}
0.85	2.80889×10^{-1}	8.87460×10^{-1}	3.43444×10^{-2}	1.61771×10^{-2}	1.46374×10^{-2}	3.64570×10^{-2}
0.86	2.82871×10^{-1}	8.89162×10^{-1}	3.45305×10^{-2}	1.62803×10^{-2}	1.47106×10^{-2}	3.66195×10^{-2}
0.87	2.84816×10^{-1}	8.90772×10^{-1}	3.46929×10^{-2}	1.63717×10^{-2}	1.47733×10^{-2}	3.67585×10^{-2}
0.88	2.86720×10^{-1}	8.92280×10^{-1}	3.48299×10^{-2}	1.64502×10^{-2}	1.48249×10^{-2}	3.68724×10^{-2}
0.89	2.88580×10^{-1}	8.93670×10^{-1}	3.49397×10^{-2}	1.65150×10^{-2}	1.48645×10^{-2}	3.69599×10^{-2}
0.90	2.90392×10^{-1}	8.94927×10^{-1}	3.50207×10^{-2}	1.65649×10^{-2}	1.48916×10^{-2}	3.70196×10^{-2}
0.91	2.92152×10^{-1}	8.96033×10^{-1}	3.50714×10^{-2}	1.65991×10^{-2}	1.49055×10^{-2}	3.70502×10^{-2}
0.92	2.93856×10^{-1}	8.96969×10^{-1}	3.50903×10^{-2}	1.66168×10^{-2}	1.49058×10^{-2}	3.70509×10^{-2}
0.93	2.95501×10^{-1}	8.97713×10^{-1}	3.50766×10^{-2}	1.66172×10^{-2}	1.48923×10^{-2}	3.70211×10^{-2}
0.94	2.97085×10^{-1}	8.98244×10^{-1}	3.50301×10^{-2}	1.66000×10^{-2}	1.48649×10^{-2}	3.69610×10^{-2}
0.95	2.98606×10^{-1}	8.98542×10^{-1}	3.49518×10^{-2}	1.65656×10^{-2}	1.48244×10^{-2}	3.68723×10^{-2}
0.96	3.00069×10^{-1}	8.98588×10^{-1}	3.4845×10^{-2}	1.65155×10^{-2}	1.47726×10^{-2}	3.67588×10^{-2}
0.97	3.01485×10^{-1}	8.98377×10^{-1}	3.4717×10^{-2}	1.6453×10^{-2}	1.47130×10^{-2}	3.6628×10^{-2}
0.98	3.02877×10^{-1}	8.9793×10^{-1}	3.4582×10^{-2}	1.6385×10^{-2}	1.4652×10^{-2}	3.6495×10^{-2}
0.99	3.0431×10^{-1}	8.9735×10^{-1}	3.4471×10^{-2}	1.6327×10^{-2}	1.4604×10^{-2}	3.639×10^{-2}
1.00	3.059×10^{-1}	8.9693×10^{-1}	3.445×10^{-2}	1.631×10^{-2}	1.460×10^{-2}	3.638×10^{-2}

ϵ^2	K	S_{xx}	F	$\overline{u_b^2}$	R	S
0.0	7.24138×10^{-1}	0.0	0.0	0.0	1.27836	1.08332
0.10	7.50747×10^{-1}	3.60328×10^{-3}	2.27038×10^{-3}	2.07004×10^{-3}	1.29166	1.10202
0.20	7.78588×10^{-1}	7.40763×10^{-3}	4.75628×10^{-3}	4.09106×10^{-3}	1.30558	1.12174
0.30	8.07671×10^{-1}	1.14095×10^{-2}	7.46818×10^{-3}	6.04048×10^{-3}	1.32013	1.14255
0.40	8.37949×10^{-1}	1.55193×10^{-2}	1.04078×10^{-2}	7.88740×10^{-3}	1.33526	1.16446
0.50	8.69257×10^{-1}	1.99081×10^{-2}	1.35577×10^{-2}	9.58845×10^{-3}	1.35092	1.18745
0.60	9.01180×10^{-1}	2.42618×10^{-2}	1.68592×10^{-2}	1.10808×10^{-2}	1.36688	1.21130
0.70	9.32742×10^{-1}	2.84465×10^{-2}	2.01654×10^{-2}	1.22712×10^{-2}	1.38266	1.23543
0.80	9.61640×10^{-1}	3.20295×10^{-2}	2.31333×10^{-2}	1.30183×10^{-2}	1.39711	1.25826
0.81	9.64213×10^{-1}	3.23257×10^{-2}	2.33873×10^{-2}	1.30613×10^{-2}	1.39840	1.26034
0.82	9.66699×10^{-1}	3.26062×10^{-2}	2.36297×10^{-2}	1.30978×10^{-2}	1.39964	1.26237
0.83	9.69090×10^{-1}	3.28696×10^{-2}	2.38593×10^{-2}	1.31273×10^{-2}	1.40084	1.26433
0.84	9.71373×10^{-1}	3.31144×10^{-2}	2.40748×10^{-2}	1.31498×10^{-2}	1.40198	1.26622
0.85	9.73539×10^{-1}	3.33391×10^{-2}	2.42747×10^{-2}	1.31649×10^{-2}	1.40306	1.26802
0.86	9.75573×10^{-1}	3.35418×10^{-2}	2.44575×10^{-2}	1.31726×10^{-2}	1.40408	1.26973
0.87	9.77462×10^{-1}	3.37210×10^{-2}	2.46217×10^{-2}	1.31727×10^{-2}	1.40502	1.27134
0.88	9.79190×10^{-1}	3.38747×10^{-2}	2.47656×10^{-2}	1.31650×10^{-2}	1.40588	1.27282
0.89	9.80739×10^{-1}	3.40011×10^{-2}	2.48873×10^{-2}	1.31494×10^{-2}	1.40666	1.27418
0.90	9.82093×10^{-1}	3.40981×10^{-2}	2.49851×10^{-2}	1.31262×10^{-2}	1.40734	1.27538
0.91	9.83229×10^{-1}	3.41641×10^{-2}	2.50572×10^{-2}	1.30953×10^{-2}	1.40791	1.27642
0.92	9.84128×10^{-1}	3.41974×10^{-2}	2.51019×10^{-2}	1.30571×10^{-2}	1.40835	1.27728
0.93	9.84768×10^{-1}	3.41967×10^{-2}	2.51178×10^{-2}	1.30124×10^{-2}	1.40867	1.27793
0.94	9.85130×10^{-1}	3.41614×10^{-2}	2.51040×10^{-2}	1.29620×10^{-2}	1.40886	1.27836
0.95	9.85196×10^{-1}	3.40921×10^{-2}	2.50604×10^{-2}	1.29075×10^{-2}	1.40889	1.27855
0.96	9.8496×10^{-1}	3.39917×10^{-2}	2.49887×10^{-2}	1.28515×10^{-2}	1.40877	1.27848
0.97	9.8444×10^{-1}	3.3867×10^{-2}	2.48937×10^{-2}	1.27979×10^{-2}	1.40851	1.27816
0.98	9.8371×10^{-1}	3.3732×10^{-2}	2.4786×10^{-2}	1.27530×10^{-2}	1.40815	1.2776
0.99	9.830×10^{-1}	3.3617×10^{-2}	2.4690×10^{-2}	1.27276×10^{-2}	1.4078	1.2770
1.00	9.829×10^{-1}	3.359×10^{-2}	2.465×10^{-2}	1.2741×10^{-2}	1.4077	1.276

PHILOSOPHICAL TRANSACTIONS OF THE ROYAL SOCIETY A MATHEMATICAL, PHYSICAL & ENGINEERING SCIENCES

TABLE A 5. THE PROPERTIES OF THE STEADY WAVE AS A FUNCTION OF THE EXPANSION PARAMETER ϵ^2 FOR $e^{-d} = 0.5$

ϵ^2	a	c^2	I	T	V	$\bar{\eta}$
0.0	0.0	6.00000×10^{-1}	0.0	0.0	0.0	0.0
0.10	6.02076×10^{-2}	6.15059×10^{-1}	2.27828×10^{-3}	8.93380×10^{-4}	8.83775×10^{-4}	2.90502×10^{-3}
0.20	8.83127×10^{-2}	6.31112×10^{-1}	4.76432×10^{-3}	1.89245×10^{-3}	1.85131×10^{-3}	5.99719×10^{-3}
0.30	1.12137×10^{-1}	6.48237×10^{-1}	7.44898×10^{-3}	2.99870×10^{-3}	2.89960×10^{-3}	9.25188×10^{-3}
0.40	1.34191×10^{-1}	6.66501×10^{-1}	1.03114×10^{-2}	4.20911×10^{-3}	4.02062×10^{-3}	1.26305×10^{-2}
0.50	1.55402×10^{-1}	6.85933×10^{-1}	1.33093×10^{-2}	5.51145×10^{-3}	5.19710×10^{-3}	1.60699×10^{-2}
0.60	1.76177×10^{-1}	7.06443×10^{-1}	1.63593×10^{-2}	6.87501×10^{-3}	6.39438×10^{-3}	1.94637×10^{-2}
0.70	1.96607×10^{-1}	7.27629×10^{-1}	1.92985×10^{-2}	8.23092×10^{-3}	7.54417×10^{-3}	2.26240×10^{-2}
0.80	2.16384×10^{-1}	7.48230×10^{-1}	2.18008×10^{-2}	9.42888×10^{-3}	8.51053×10^{-3}	2.52032×10^{-2}
0.81	2.18293×10^{-1}	7.50151×10^{-1}	2.20058×10^{-2}	9.52974×10^{-3}	8.58833×10^{-3}	2.54075×10^{-2}
0.82	2.20184×10^{-1}	7.52028×10^{-1}	2.21993×10^{-2}	9.62558×10^{-3}	8.66141×10^{-3}	2.55990×10^{-2}
0.83	2.22054×10^{-1}	7.53853×10^{-1}	2.23805×10^{-2}	9.71559×10^{-3}	8.72937×10^{-3}	2.57766×10^{-2}
0.84	2.23901×10^{-1}	7.55618×10^{-1}	2.25481×10^{-2}	9.80014×10^{-3}	8.79180×10^{-3}	2.59394×10^{-2}
0.85	2.25723×10^{-1}	7.57316×10^{-1}	2.27012×10^{-2}	9.87776×10^{-3}	8.84823×10^{-3}	2.60862×10^{-2}
0.86	2.27518×10^{-1}	7.58937×10^{-1}	2.28386×10^{-2}	9.94813×10^{-3}	8.89823×10^{-3}	2.62160×10^{-2}
0.87	2.29281×10^{-1}	7.60469×10^{-1}	2.29589×10^{-2}	1.00106×10^{-2}	8.94130×10^{-3}	2.63276×10^{-2}
0.88	2.31009×10^{-1}	7.61900×10^{-1}	2.30609×10^{-2}	1.00646×10^{-2}	8.97694×10^{-3}	2.64197×10^{-2}
0.89	2.32700×10^{-1}	7.63217×10^{-1}	2.31434×10^{-2}	1.01093×10^{-2}	9.00467×10^{-3}	2.64913×10^{-3}
0.90	2.34349×10^{-1}	7.64403×10^{-1}	2.32049×10^{-2}	1.01440×10^{-2}	9.02400×10^{-3}	2.65411×10^{-2}
0.91	2.35952×10^{-1}	7.65444×10^{-1}	2.32444×10^{-2}	1.01682×10^{-2}	9.03450×10^{-3}	2.65681×10^{-2}
0.92	2.37505×10^{-1}	7.66318×10^{-1}	2.32605×10^{-2}	1.01811×10^{-2}	9.03579×10^{-3}	2.65714×10^{-2}
0.93	2.39005×10^{-1}	7.67008×10^{-1}	2.32527×10^{-2}	1.01822×10^{-2}	9.02767×10^{-3}	2.65505×10^{-2}
0.94	2.40448×10^{-1}	7.67492×10^{-1}	2.32206×10^{-2}	1.01714×10^{-2}	9.0101×10^{-3}	2.65055×10^{-2}
0.95	2.41832×10^{-1}	7.67748×10^{-1}	2.3165×10^{-2}	1.01487×10^{-2}	8.9836×10^{-3}	2.64376×10^{-2}
0.96	2.4316×10^{-1}	7.67764×10^{-1}	2.3087×10^{-2}	1.0114×10^{-2}	8.9491×10^{-3}	2.6349×10^{-2}
0.97	2.4443×10^{-1}	7.6754×10^{-1}	2.2993×10^{-2}	1.0073×10^{-2}	8.909×10^{-3}	2.6246×10^{-2}
0.98	2.457×10^{-1}	7.6707×10^{-1}	2.290×10^{-2}	1.0027×10^{-2}	8.868×10^{-3}	2.614×10^{-2}
0.99	2.469×10^{-1}	7.6648×10^{-1}	2.281×10^{-2}	9.987×10^{-3}	8.835×10^{-3}	2.606×10^{-2}
1.00	2.484×10^{-1}	7.660×10^{-1}	2.28×10^{-2}	9.97×10^{-3}	8.83×10^{-3}	2.606×10^{-2}

ϵ^2	K	S_{xx}	F	$\overline{u_b^2}$	R	S
0.0	6.00000×10^{-1}	0.0	0.0	0.0	9.93147×10^{-1}	6.56115×10^{-1}
0.10	6.22675×10^{-1}	2.17915×10^{-3}	1.21065×10^{-3}	1.80583×10^{-3}	1.00448	6.68936×10^{-1}
0.20	6.46724×10^{-1}	4.54525×10^{-3}	2.58210×10^{-3}	3.61783×10^{-3}	1.01651	6.82615×10^{-1}
0.30	6.72150×10^{-1}	7.09579×10^{-3}	4.12374×10^{-3}	5.40970×10^{-3}	1.02922	6.97104×10^{-1}
0.40	6.98909×10^{-1}	9.81850×10^{-3}	5.83983×10^{-3}	7.14661×10^{-3}	1.04260	7.12445×10^{-1}
0.50	7.26854×10^{-1}	1.26818×10^{-2}	7.72253×10^{-3}	8.78050×10^{-3}	1.05657	7.28606×10^{-1}
0.60	7.55613×10^{-1}	1.56158×10^{-2}	9.73756×10^{-3}	1.02425×10^{-2}	1.07095	7.45442×10^{-1}
0.70	7.84307×10^{-1}	1.84728×10^{-2}	1.17925×10^{-2}	1.14306×10^{-2}	1.08530	7.62529×10^{-1}
0.80	8.10826×10^{-1}	2.09403×10^{-2}	1.36648×10^{-2}	1.21896×10^{-2}	1.09856	7.78730×10^{-1}
0.81	8.13200×10^{-1}	2.11447×10^{-2}	1.38260×10^{-2}	1.22339×10^{-2}	1.09975	7.80211×10^{-1}
0.82	8.15497×10^{-1}	2.13381×10^{-2}	1.39800×10^{-2}	1.22714×10^{-2}	1.10090	7.81651×10^{-1}
0.83	8.17708×10^{-1}	2.15196×10^{-2}	1.41260×10^{-2}	1.23019×10^{-2}	1.10200	7.83044×10^{-1}
0.84	8.19822×10^{-1}	2.16880×10^{-2}	1.42630×10^{-2}	1.23252×10^{-2}	1.10306	7.84385×10^{-1}
0.85	8.21830×10^{-1}	2.18424×10^{-2}	1.43901×10^{-2}	1.23410×10^{-2}	1.10406	7.85667×10^{-1}
0.86	8.23718×10^{-1}	2.19813×10^{-2}	1.45063×10^{-2}	1.23491×10^{-2}	1.10501	7.86882×10^{-1}
0.87	8.25473×10^{-1}	2.21037×10^{-2}	1.46106×10^{-2}	1.23493×10^{-2}	1.10588	7.88021×10^{-1}
0.88	8.27081×10^{-1}	2.22080×10^{-2}	1.47019×10^{-2}	1.23414×10^{-2}	1.10669	7.89076×10^{-1}
0.89	8.28525×10^{-1}	2.22930×10^{-2}	1.47788×10^{-2}	1.23255×10^{-2}	1.10741	7.90036×10^{-1}
0.90	8.29787×10^{-1}	2.23574×10^{-2}	1.48404×10^{-2}	1.23014×10^{-2}	1.10804	7.90890×10^{-1}
0.91	8.30849×10^{-1}	2.23997×10^{-2}	1.48853×10^{-2}	1.22693×10^{-2}	1.10857	7.91623×10^{-1}
0.92	8.31691×10^{-1}	2.24188×10^{-2}	1.49125×10^{-2}	1.22296×10^{-2}	1.10899	7.92226×10^{-1}
0.93	8.32292×10^{-1}	2.24140×10^{-2}	1.49210×10^{-2}	1.21829×10^{-2}	1.10929	7.92681×10^{-1}
0.94	8.32633×10^{-1}	2.23847×10^{-2}	1.49102×10^{-2}	1.21302×10^{-2}	1.10946	7.92977×10^{-1}
0.95	8.32699×10^{-1}	2.23316×10^{-2}	1.48800×10^{-2}	1.20731×10^{-2}	1.10949	7.93099×10^{-1}
0.96	8.3248×10^{-1}	2.2256×10^{-2}	1.48318×10^{-2}	1.20143×10^{-2}	1.10939	7.9304×10^{-1}
0.97	8.3199×10^{-1}	2.2165×10^{-2}	1.47686×10^{-2}	1.19577×10^{-2}	1.10914	7.9279×10^{-1}
0.98	8.313×10^{-1}	2.206×10^{-2}	1.46975×10^{-2}	1.1910×10^{-2}	1.10878	7.924×10^{-1}
0.99	8.305×10^{-1}	2.198×10^{-2}	1.4634×10^{-2}	1.1883×10^{-2}	1.1084	7.919×10^{-1}
1.00	8.303×10^{-1}	2.19×10^{-2}	1.4613×10^{-2}	1.189×10^{-2}	1.1082	7.92×10^{-1}

PHILOSOPHICAL TRANSACTIONS OF THE ROYAL SOCIETY A MATHEMATICAL, PHYSICAL & ENGINEERING SCIENCES

TABLE A 6. THE PROPERTIES OF THE STEADY WAVE AS A FUNCTION OF THE EXPANSION PARAMETER ϵ^2 FOR $e^{-d} = 0.6$

ϵ^2	a	c^2	I	T	V	$\bar{\eta}$
0.0	0.0	4.70588×10^{-1}	0.0	0.0	0.0	0.0
0.10	3.99211×10^{-2}	4.84437×10^{-1}	1.11395×10^{-3}	3.87661×10^{-4}	3.82663×10^{-4}	1.60046×10^{-3}
0.20	5.99596×10^{-2}	4.99333×10^{-1}	2.40760×10^{-3}	8.50650×10^{-4}	8.28720×10^{-4}	3.40714×10^{-3}
0.30	7.77954×10^{-2}	5.15320×10^{-1}	3.87720×10^{-3}	1.39163×10^{-3}	1.33768×10^{-3}	5.40107×10^{-3}
0.40	9.49578×10^{-2}	5.32433×10^{-1}	5.51241×10^{-3}	2.01115×10^{-3}	1.90660×10^{-3}	7.55455×10^{-3}
0.50	1.12000×10^{-1}	5.50678×10^{-1}	7.28956×10^{-3}	2.70471×10^{-3}	2.52746×10^{-3}	9.82319×10^{-3}
0.60	1.29152×10^{-1}	5.69948×10^{-1}	9.15842×10^{-3}	3.45707×10^{-3}	3.18215×10^{-3}	1.21312×10^{-2}
0.70	1.46424×10^{-1}	5.89843×10^{-1}	1.10153×10^{-2}	4.22993×10^{-3}	3.83222×10^{-3}	1.43426×10^{-2}
0.80	1.63500×10^{-1}	6.09151×10^{-1}	1.26445×10^{-2}	4.93439×10^{-3}	4.39736×10^{-3}	1.62009×10^{-2}
0.81	1.65166×10^{-1}	6.10947×10^{-1}	1.27805×10^{-2}	4.99483×10^{-3}	4.44389×10^{-3}	1.63511×10^{-2}
0.82	1.66818×10^{-1}	6.12701×10^{-1}	1.29095×10^{-2}	5.05247×10^{-3}	4.48780×10^{-3}	1.64924×10^{-2}
0.83	1.68456×10^{-1}	6.14405×10^{-1}	1.30307×10^{-2}	5.10700×10^{-3}	4.52885×10^{-3}	1.66242×10^{-2}
0.84	1.70076×10^{-1}	6.16053×10^{-1}	1.31434×10^{-2}	5.15808×10^{-3}	4.56676×10^{-3}	1.67456×10^{-2}
0.85	1.71677×10^{-1}	6.17635×10^{-1}	1.32469×10^{-2}	5.20536×10^{-3}	4.60127×10^{-3}	1.68558×10^{-2}
0.86	1.73256×10^{-1}	6.19144×10^{-1}	1.33403×10^{-2}	5.24845×10^{-3}	4.63208×10^{-3}	1.69539×10^{-2}
0.87	1.74809×10^{-1}	6.20568×10^{-1}	1.34227×10^{-2}	5.28694×10^{-3}	4.65887×10^{-3}	1.70390×10^{-2}
0.88	1.76333×10^{-1}	6.21896×10^{-1}	1.34932×10^{-2}	5.32040×10^{-3}	4.68134×10^{-3}	1.71102×10^{-2}
0.89	1.77825×10^{-1}	6.23115×10^{-1}	1.35509×10^{-2}	5.34840×10^{-3}	4.69916×10^{-3}	1.71666×10^{-2}
0.90	1.79282×10^{-1}	6.24210×10^{-1}	1.35950×10^{-2}	5.37046×10^{-3}	4.71202×10^{-3}	1.72071×10^{-2}
0.91	1.80698×10^{-1}	6.25165×10^{-1}	1.36244×10^{-2}	5.38617×10^{-3}	4.71962×10^{-3}	1.72310×10^{-2}
0.92	1.82071×10^{-1}	6.25964×10^{-1}	1.36383×10^{-2}	5.39509×10^{-3}	4.72172×10^{-3}	1.7237×10^{-2}
0.93	1.83395×10^{-1}	6.26585×10^{-1}	1.36363×10^{-2}	5.39689×10^{-3}	4.7181×10^{-3}	1.7226×10^{-2}
0.94	1.84666×10^{-1}	6.27010×10^{-1}	1.36182×10^{-2}	5.3913×10^{-3}	4.7088×10^{-3}	1.7196×10^{-2}
0.95	1.8588×10^{-1}	6.2722×10^{-1}	1.35845×10^{-2}	5.3784×10^{-3}	4.6941×10^{-3}	1.715×10^{-2}
0.96	1.8704×10^{-1}	6.2720×10^{-1}	1.3538×10^{-2}	5.3586×10^{-3}	4.675×10^{-3}	1.708×10^{-2}
0.97	1.8815×10^{-1}	6.2693×10^{-1}	1.3485×10^{-2}	5.3333×10^{-3}	4.652×10^{-3}	1.700×10^{-2}
0.98	1.8921×10^{-1}	6.2643×10^{-1}	1.3449×10^{-2}	5.305×10^{-3}	4.631×10^{-3}	1.693×10^{-2}
0.99	1.902×10^{-1}	6.257×10^{-1}	1.35×10^{-2}	5.279×10^{-3}	4.62×10^{-3}	1.68×10^{-2}
1.00	1.914×10^{-1}	6.249×10^{-1}	1.32×10^{-2}	5.26×10^{-3}	4.65×10^{-3}	1.68×10^{-2}

ϵ^2	K	S_{xx}	F	$\overline{u_b^2}$	R	S
0.0	4.70588×10^{-1}	0.0	0.0	0.0	7.46120×10^{-1}	3.70860×10^{-1}
0.10	4.88845×10^{-1}	1.02113×10^{-3}	4.92681×10^{-4}	1.20695×10^{-3}	7.55248×10^{-1}	3.78999×10^{-1}
0.20	5.08636×10^{-1}	2.19612×10^{-3}	1.08722×10^{-3}	2.48852×10^{-3}	7.65144×10^{-1}	3.87785×10^{-1}
0.30	5.29939×10^{-1}	3.52432×10^{-3}	1.79125×10^{-3}	3.81773×10^{-3}	7.75795×10^{-1}	3.97224×10^{-1}
0.40	5.52703×10^{-1}	4.99993×10^{-3}	2.61029×10^{-3}	5.16057×10^{-3}	7.87177×10^{-1}	4.07317×10^{-1}
0.50	5.76796×10^{-1}	6.60573×10^{-3}	3.54388×10^{-3}	6.47135×10^{-3}	7.99224×10^{-1}	4.18034×10^{-1}
0.60	6.01896×10^{-1}	8.30086×10^{-3}	4.57729×10^{-3}	7.68517×10^{-3}	8.11773×10^{-1}	4.29273×10^{-1}
0.70	6.27234×10^{-1}	9.99494×10^{-3}	5.66311×10^{-3}	8.70555×10^{-3}	8.24443×10^{-1}	4.40743×10^{-1}
0.80	6.50937×10^{-1}	1.14914×10^{-2}	6.67891×10^{-3}	9.38466×10^{-3}	8.36294×10^{-1}	4.51671×10^{-1}
0.81	6.53076×10^{-1}	1.16168×10^{-2}	6.76763×10^{-3}	9.42602×10^{-3}	8.37363×10^{-1}	4.52672×10^{-1}
0.82	6.55147×10^{-1}	1.17357×10^{-2}	6.85257×10^{-3}	9.46157×10^{-3}	8.38399×10^{-1}	4.53646×10^{-1}
0.83	6.57145×10^{-1}	1.18475×10^{-2}	6.93324×10^{-3}	9.49108×10^{-3}	8.39398×10^{-1}	4.54589×10^{-1}
0.84	6.59058×10^{-1}	1.19515×10^{-2}	7.00915×10^{-3}	9.51428×10^{-3}	8.40355×10^{-1}	4.55497×10^{-1}
0.85	6.60878×10^{-1}	1.20469×10^{-2}	7.07977×10^{-3}	9.53090×10^{-3}	8.41265×10^{-1}	4.56364×10^{-1}
0.86	6.62592×10^{-1}	1.21330×10^{-2}	7.14448×10^{-3}	9.54074×10^{-3}	8.42122×10^{-1}	4.57186×10^{-1}
0.87	6.64190×10^{-1}	1.22089×10^{-2}	7.20270×10^{-3}	9.54358×10^{-3}	8.42920×10^{-1}	4.57958×10^{-1}
0.88	6.65656×10^{-1}	1.22737×10^{-2}	7.25374×10^{-3}	9.53924×10^{-3}	8.43653×10^{-1}	4.58671×10^{-1}
0.89	6.66976×10^{-1}	1.23266×10^{-2}	7.29692×10^{-3}	9.52761×10^{-3}	8.44314×10^{-1}	4.59321×10^{-1}
0.90	6.68133×10^{-1}	1.23667×10^{-2}	7.33157×10^{-3}	9.5086×10^{-3}	8.44892×10^{-1}	4.59897×10^{-1}
0.91	6.69110×10^{-1}	1.23931×10^{-2}	7.3569×10^{-3}	9.4824×10^{-3}	8.45380×10^{-1}	4.60393×10^{-1}
0.92	6.69889×10^{-1}	1.2405×10^{-2}	7.3724×10^{-3}	9.4490×10^{-3}	8.45770×10^{-1}	4.60798×10^{-1}
0.93	6.70448×10^{-1}	1.2402×10^{-2}	7.3774×10^{-3}	9.4092×10^{-3}	8.46049×10^{-1}	4.61103×10^{-1}
0.94	6.7077×10^{-1}	1.2383×10^{-2}	7.3715×10^{-3}	9.3636×10^{-3}	8.46209×10^{-1}	4.61299×10^{-1}
0.95	6.7083×10^{-1}	1.2349×10^{-2}	7.354×10^{-3}	9.314×10^{-3}	8.4624×10^{-1}	4.6137×10^{-1}
0.96	6.7063×10^{-1}	1.230×10^{-2}	7.327×10^{-3}	9.262×10^{-3}	8.4614×10^{-1}	4.6131×10^{-1}
0.97	6.7018×10^{-1}	1.224×10^{-2}	7.293×10^{-3}	9.211×10^{-3}	8.4591×10^{-1}	4.6113×10^{-1}
0.98	6.694×10^{-1}	1.218×10^{-2}	7.25×10^{-3}	9.17×10^{-3}	8.455×10^{-1}	4.6082×10^{-1}
0.99	6.686×10^{-1}	1.21×10^{-2}	7.21×10^{-3}	9.14×10^{-3}	8.451×10^{-1}	4.604×10^{-1}
1.00	6.677×10^{-1}	1.21×10^{-2}	7.2×10^{-3}	9.1×10^{-3}	8.447×10^{-1}	4.600×10^{-1}

PHILOSOPHICAL TRANSACTIONS OF THE ROYAL SOCIETY A MATHEMATICAL, PHYSICAL & ENGINEERING SCIENCES

TABLE A 7. THE PROPERTIES OF THE STEADY WAVE AS A FUNCTION OF THE EXPANSION PARAMETER ϵ^2 FOR $e^{-d} = 0.7$

ϵ^2	a	c^2	I	T	V	$\bar{\eta}$
0.0	0.0	3.42282×10^{-1}	0.0	0.0	0.0	0.0
0.10	2.30969×10^{-2}	3.53910×10^{-1}	4.22398×10^{-4}	1.25643×10^{-4}	1.23741×10^{-4}	7.10029×10^{-4}
0.20	3.61956×10^{-2}	3.66691×10^{-1}	9.64986×10^{-4}	2.92174×10^{-4}	2.83384×10^{-4}	1.59357×10^{-3}
0.30	4.86378×10^{-2}	3.80583×10^{-1}	1.62559×10^{-3}	5.01426×10^{-4}	4.78885×10^{-4}	2.63504×10^{-3}
0.40	6.11638×10^{-2}	3.95576×10^{-1}	2.40086×10^{-3}	7.55010×10^{-4}	7.09813×10^{-4}	3.81727×10^{-3}
0.50	7.40387×10^{-2}	4.11646×10^{-1}	3.28155×10^{-3}	1.05272×10^{-3}	9.73850×10^{-4}	5.11467×10^{-3}
0.60	8.73675×10^{-2}	4.28680×10^{-1}	4.24442×10^{-3}	1.38949×10^{-3}	1.26413×10^{-3}	6.48263×10^{-3}
0.70	1.01119×10^{-1}	4.46301×10^{-1}	5.23600×10^{-3}	1.74897×10^{-3}	1.56388×10^{-3}	7.83765×10^{-3}
0.80	1.15005×10^{-1}	4.63400×10^{-1}	6.13736×10^{-3}	2.08896×10^{-3}	1.83503×10^{-3}	9.01579×10^{-3}
0.81	1.16374×10^{-1}	4.64988×10^{-1}	6.21434×10^{-3}	2.11878×10^{-3}	1.85794×10^{-3}	9.11328×10^{-3}
0.82	1.17735×10^{-1}	4.66538×10^{-1}	6.28767×10^{-3}	2.14735×10^{-3}	1.87969×10^{-3}	9.20547×10^{-3}
0.83	1.19085×10^{-1}	4.68044×10^{-1}	6.35692×10^{-3}	2.17450×10^{-3}	1.90014×10^{-3}	9.29189×10^{-3}
0.84	1.20423×10^{-1}	4.69498×10^{-1}	6.42167×10^{-3}	2.20006×10^{-3}	1.91915×10^{-3}	9.37200×10^{-3}
0.85	1.21747×10^{-1}	4.70893×10^{-1}	6.4815×10^{-3}	2.22385×10^{-3}	1.93360×10^{-3}	9.44524×10^{-3}
0.86	1.23054×10^{-1}	4.72222×10^{-1}	6.5358×10^{-3}	2.2456×10^{-3}	1.9523×10^{-3}	9.51101×10^{-3}
0.87	1.24341×10^{-1}	4.73474×10^{-1}	6.5842×10^{-3}	2.2653×01^{-3}	1.9661×10^{-3}	9.56870×10^{-3}
0.88	1.25606×10^{-1}	4.74641×10^{-1}	6.6260×10^{-3}	2.2824×10^{-3}	1.9778×10^{-3}	9.61767×10^{-3}
0.89	1.2684×10^{-1}	4.7571×10^{-1}	6.6606×10^{-3}	2.2969×10^{-3}	1.9873×10^{-3}	9.65722×10^{-3}
0.90	1.2805×10^{-1}	4.7666×10^{-1}	6.6876×10^{-3}	2.3085×10^{-3}	1.9944×10^{-3}	9.68671×10^{-3}
0.91	1.2923×10^{-1}	4.7749×10^{-1}	6.706×10^{-3}	2.3171×10^{-3}	1.9989×10^{-3}	9.70549×10^{-3}
0.92	1.3036×10^{-1}	4.7818×10^{-1}	6.716×10^{-3}	2.322×01^{-3}	2.0007×10^{-3}	9.71296×10^{-3}
0.93	1.3146×10^{-1}	4.7871×10^{-1}	6.717×10^{-3}	2.324×10^{-3}	1.999×10^{-3}	9.7086×10^{-3}
0.94	1.3250×10^{-1}	4.790×10^{-1}	6.708×10^{-3}	2.321×10^{-3}	1.996×10^{-3}	9.6922×10^{-3}
0.95	1.3349×10^{-1}	4.792×10^{-1}	6.689×10^{-3}	2.315×10^{-3}	1.988×10^{-3}	9.6639×10^{-3}
0.96	1.344×10^{-1}	4.792×10^{-1}	6.66×10^{-3}	2.305×10^{-3}	1.978×10^{-3}	9.6243×10^{-3}
0.97	1.353×10^{-1}	4.789×10^{-1}	6.62×10^{-3}	2.291×10^{-3}	1.966×10^{-3}	9.575×10^{-3}
0.98	1.361×10^{-1}	4.783×10^{-1}	6.58×10^{-3}	2.274×10^{-3}	1.951×10^{-3}	9.519×10^{-3}
0.99	1.368×10^{-1}	4.775×10^{-1}	6.53×10^{-3}	2.25×10^{-3}	1.94×10^{-3}	9.464×10^{-3}
1.00	1.374×10^{-1}	4.76×10^{-1}	6.48×10^{-3}	2.24×10^{-3}	1.92×10^{-3}	9.421×10^{-3}

ϵ^2	K	S_{xx}	F	$\overline{u_b^2}$	R	S
0.0	3.42282×10^{-1}	0.0	0.0	0.0	5.27816×10^{-1}	1.85692×10^{-1}
0.10	3.55936×10^{-1}	3.48087×10^{-4}	1.41606×10^{-4}	6.06452×10^{-4}	5.34643×10^{-1}	1.90190×10^{-1}
0.20	3.71197×10^{-1}	7.91006×10^{-4}	3.31257×10^{-4}	1.31874×10^{-3}	5.42273×10^{-1}	1.95174×10^{-1}
0.30	3.87965×10^{-1}	1.32808×10^{-3}	5.72994×10^{-4}	2.11247×10^{-3}	5.50658×10^{-1}	2.00621×10^{-1}
0.40	4.06171×10^{-1}	1.95800×10^{-3}	8.70939×10^{-4}	2.96095×10^{-3}	5.59761×10^{-1}	2.06517×10^{-1}
0.50	4.25706×10^{-1}	2.67496×10^{-3}	1.22742×10^{-3}	3.82997×10^{-3}	5.69528×10^{-1}	2.12839×10^{-1}
0.60	4.46316×10^{-1}	3.46180×10^{-3}	1.63911×10^{-3}	4.67079×10^{-3}	5.79833×10^{-1}	2.19524×10^{-1}
0.70	4.67385×10^{-1}	4.27599×10^{-3}	2.08850×10^{-2}	5.40924×10^{-3}	5.90368×10^{-1}	2.26397×10^{-1}
0.80	4.87360×10^{-1}	5.01870×10^{-3}	2.52384×10^{-3}	5.92840×10^{-3}	6.00355×10^{-1}	2.32989×10^{-1}
0.81	4.89177×10^{-1}	5.08211×10^{-3}	2.56260×10^{-3}	5.96194×10^{-3}	6.01263×10^{-1}	2.33595×10^{-1}
0.82	4.90940×10^{-1}	5.14245×10^{-3}	2.59985×10^{-3}	5.99134×10^{-3}	6.02145×10^{-1}	2.34184×10^{-1}
0.83	4.92644×10^{-1}	5.19939×10^{-3}	2.63535×10^{-3}	6.01638×10^{-3}	6.02997×10^{-1}	2.34756×10^{-1}
0.84	4.94279×10^{-1}	5.2525×10^{-3}	2.66888×10^{-3}	6.03682×10^{-3}	6.03814×10^{-1}	2.35306×10^{-1}
0.85	4.95837×10^{-1}	5.3015×10^{-3}	2.70020×10^{-3}	6.0525×10^{-3}	6.04593×10^{-1}	2.35832×10^{-1}
0.86	4.97308×10^{-1}	5.3459×10^{-3}	2.7290×10^{-3}	6.0631×10^{-3}	6.05329×10^{-1}	2.36330×10^{-1}
0.87	4.98682×10^{-1}	5.3853×10^{-3}	2.7550×10^{-3}	6.0684×10^{-3}	6.0601×10^{-1}	2.36798×10^{-1}
0.88	4.9994×10^{-1}	5.4191×10^{-3}	2.7779×10^{-3}	6.0685×10^{-3}	6.0665×10^{-1}	2.37232×10^{-1}
0.89	5.0108×10^{-1}	5.4468×10^{-3}	2.7974×10^{-3}	6.0630×10^{-3}	6.0722×10^{-1}	2.3763×10^{-1}
0.90	5.0209×10^{-1}	5.468×10^{-3}	2.813×10^{-3}	6.0519×10^{-3}	6.0772×10^{-1}	2.3797×10^{-1}
0.91	5.029×10^{-1}	5.482×10^{-3}	2.825×10^{-3}	6.035×10^{-3}	6.0814×10^{-1}	2.3828×10^{-1}
0.92	5.036×10^{-1}	5.489×10^{-3}	2.832×10^{-3}	6.013×10^{-3}	6.0848×10^{-1}	2.3852×10^{-1}
0.93	5.041×10^{-1}	5.488×10^{-3}	2.834×10^{-3}	5.985×10^{-3}	6.087×10^{-1}	2.3871×10^{-1}
0.94	5.044×10^{-1}	5.479×10^{-3}	2.832×10^{-3}	5.952×10^{-3}	6.089×10^{-1}	2.3882×10^{-1}
0.95	5.045×10^{-1}	5.46×10^{-3}	2.824×10^{-3}	5.916×10^{-3}	6.089×10^{-1}	2.3886×10^{-1}
0.96	5.04×10^{-1}	5.43×10^{-3}	2.81×10^{-3}	5.876×10^{-3}	6.088×10^{-1}	2.3883×10^{-1}
0.97	5.04×10^{-1}	5.40×10^{-3}	2.79×10^{-3}	5.836×10^{-3}	6.086×10^{-1}	2.386×10^{-1}
0.98	5.03×10^{-1}	5.37×10^{-3}	2.77×10^{-3}	5.801×10^{-3}	6.08×10^{-1}	2.385×10^{-1}
0.99	5.02×10^{-1}	5.32×10^{-3}	2.74×10^{-3}	5.77×10^{-3}	6.08×10^{-1}	2.383×10^{-1}
1.00	5.0×10^{-1}	5.28×10^{-3}	2.72×10^{-3}	5.76×10^{-3}	6.07×10^{-1}	2.380×10^{-1}

PHILOSOPHICAL TRANSACTIONS OF THE ROYAL SOCIETY A MATHEMATICAL, PHYSICAL & ENGINEERING SCIENCES

TABLE A 8. THE PROPERTIES OF THE STEADY WAVE AS A FUNCTION OF THE EXPANSION PARAMETER ϵ^2 FOR $e^{-d} = 0.8$

ϵ^2	a	c^2	I	T	V	$\overline{\eta}$
0.0	0.0	2.19512×10^{-1}	0.0	0.0	0.0	0.0
0.10	1.10585×10^{-2}	2.27975×10^{-1}	1.09966×10^{-4}	2.62526×10^{-5}	2.58047×10^{-5}	2.30316×10^{-4}
0.20	1.86852×10^{-2}	2.37587×10^{-1}	2.74402×10^{-4}	6.68759×10^{-5}	6.46052×10^{-5}	5.62959×10^{-4}
0.30	2.64278×10^{-2}	2.48167×10^{-1}	4.90670×10^{-4}	1.22217×10^{-4}	1.16017×10^{-4}	9.84957×10^{-4}
0.40	3.45424×10^{-2}	2.59680×10^{-1}	7.58669×10^{-4}	1.93305×10^{-4}	1.80270×10^{-4}	1.48789×10^{-3}
0.50	4.31421×10^{-2}	2.72109×10^{-1}	1.07720×10^{-3}	2.80956×10^{-4}	2.57319×10^{-4}	2.06503×10^{-3}
0.60	5.22822×10^{-2}	2.85369×10^{-1}	1.44002×10^{-3}	3.84628×10^{-4}	3.45816×10^{-4}	2.69566×10^{-3}
0.70	6.19407×10^{-2}	2.99161×10^{-1}	1.82848×10^{-3}	5.00048×10^{-4}	4.41159×10^{-4}	3.34302×10^{-3}
0.80	7.1910×10^{-2}	3.12589×10^{-1}	2.1956×10^{-3}	6.1373×10^{-4}	5.312×10^{-4}	3.927×10^{-3}
0.81	7.2903×10^{-2}	3.13836×10^{-1}	2.2277×10^{-3}	6.239×10^{-4}	5.390×10^{-4}	3.976×10^{-3}
0.82	7.3892×10^{-2}	3.15053×10^{-1}	2.2583×10^{-3}	6.337×10^{-4}	5.465×10^{-4}	4.023×10^{-3}
0.83	7.4876×10^{-2}	3.16233×10^{-1}	2.2875×10^{-3}	6.431×10^{-4}	5.535×10^{-4}	4.067×10^{-3}
0.84	7.5851×10^{-2}	3.17371×10^{-1}	2.314×10^{-3}	6.519×10^{-4}	5.601×10^{-4}	4.108×10^{-3}
0.85	7.6818×10^{-2}	3.18462×10^{-1}	2.340×10^{-3}	6.602×10^{-4}	5.661×10^{-4}	4.146×10^{-3}
0.86	7.777×10^{-2}	3.19498×10^{-1}	2.363×10^{-3}	6.677×10^{-4}	5.716×10^{-4}	4.181×10^{-3}
0.87	7.871×10^{-2}	3.2047×10^{-1}	2.384×10^{-3}	6.745×10^{-4}	5.764×10^{-4}	4.212×10^{-3}
0.88	7.963×10^{-2}	3.2137×10^{-1}	2.402×10^{-3}	6.805×10^{-4}	5.805×10^{-4}	4.238×10^{-3}
0.89	8.055×10^{-2}	3.2219×10^{-1}	2.417×10^{-3}	6.854×10^{-4}	5.84×10^{-4}	4.26×10^{-3}
0.90	8.143×10^{-2}	3.2291×10^{-1}	2.429×10^{-3}	6.894×10^{-4}	5.86×10^{-4}	4.27×10^{-3}
0.91	8.228×10^{-2}	3.2352×10^{-1}	2.436×10^{-3}	6.922×10^{-4}	5.87×10^{-4}	4.28×10^{-3}
0.92	8.311×10^{-2}	3.2402×10^{-1}	2.44×10^{-3}	6.935×10^{-4}	5.88×10^{-4}	4.29×10^{-3}
0.93	8.390×10^{-2}	3.2437×10^{-1}	2.43×10^{-3}	6.934×10^{-4}	5.87×10^{-4}	4.28×10^{-3}
0.94	8.464×10^{-2}	3.2454×10^{-1}	2.43×10^{-3}	6.916×10^{-4}	5.85×10^{-4}	4.27×10^{-3}
0.95	8.534×10^{-2}	3.245×10^{-1}	2.42×10^{-3}	6.87×10^{-4}	5.81×10^{-4}	4.26×10^{-3}
0.96	8.598×10^{-2}	3.243×10^{-1}	2.40×10^{-3}	6.82×10^{-4}	5.76×10^{-4}	4.2×10^{-3}
0.97	8.65×10^{-2}	3.238×10^{-1}	2.38×10^{-3}	6.74×10^{-4}	5.70×10^{-4}	4.2×10^{-3}
0.98	8.70×10^{-2}	3.230×10^{-1}	2.35×10^{-3}	6.63×10^{-4}	5.6×10^{-4}	4.1×10^{-3}
0.99	8.74×10^{-2}	3.219×10^{-1}	2.31×10^{-3}	6.50×10^{-4}	5.5×10^{-4}	4.1×10^{-3}
1.00	8.77×10^{-2}	3.205×10^{-1}	2.27×10^{-3}	6.34×10^{-4}	5.4×10^{-4}	4.0×10^{-3}

ϵ^2	K	S_{xx}	F	$\overline{r_b^2}$	R	S
0.0	2.19512×10^{-1}	0.0	0.0	0.0	3.32900×10^{-1}	7.38793×10^{-2}
0.10	2.28648×10^{-1}	7.50472×10^{-5}	2.43023×10^{-5}	2.12428×10^{-4}	3.37468×10^{-1}	7.58416×10^{-2}
0.20	2.39218×10^{-1}	1.86659×10^{-4}	6.24129×10^{-5}	5.04997×10^{-4}	3.42753×10^{-1}	7.80912×10^{-2}
0.30	2.50996×10^{-1}	3.33424×10^{-4}	1.15247×10^{-4}	8.59365×10^{-4}	3.48642×10^{-1}	8.05827×10^{-2}
0.40	2.63920×10^{-1}	5.15787×10^{-4}	1.84472×10^{-4}	1.26152×10^{-3}	3.55103×10^{-1}	8.33050×10^{-2}
0.50	2.77934×10^{-1}	7.33549×10^{-4}	2.71682×10^{-4}	1.69478×10^{-3}	3.62111×10^{-1}	8.62505×10^{-2}
0.60	2.92894×10^{-1}	9.83053×10^{-4}	3.77210×10^{-4}	2.13422×10^{-3}	3.69591×10^{-1}	8.93937×10^{-2}
0.70	3.08387×10^{-1}	1.2518×10^{-3}	4.9751×10^{-4}	2.5391×10^{-3}	3.77337×10^{-1}	9.26557×10^{-2}
0.80	3.23286×10^{-1}	1.506×10^{-3}	6.1888×10^{-4}	2.841×10^{-3}	3.84786×10^{-1}	9.58120×10^{-2}
0.81	3.24653×10^{-1}	1.528×10^{-3}	6.2992×10^{-4}	2.862×10^{-3}	3.85470×10^{-1}	9.61034×10^{-2}
0.82	3.25982×10^{-1}	1.55×10^{-3}	6.4056×10^{-4}	2.880×10^{-3}	3.86135×10^{-1}	9.63871×10^{-2}
0.83	3.27268×10^{-1}	1.57×10^{-3}	6.5073×10^{-4}	2.896×10^{-3}	3.86777×10^{-1}	9.66620×10^{-2}
0.84	3.28504×10^{-1}	1.59×10^{-3}	6.603×10^{-4}	2.91×10^{-3}	3.87395×10^{-1}	9.69268×10^{-2}
0.85	3.29682×10^{-1}	1.60×10^{-3}	6.693×10^{-4}	2.92×10^{-3}	3.87984×10^{-1}	9.7180×10^{-2}
0.86	3.30796×10^{-1}	1.62×10^{-3}	6.776×10^{-4}	2.93×10^{-3}	3.88542×10^{-1}	9.7420×10^{-2}
0.87	3.31836×10^{-1}	1.63×10^{-3}	6.851×10^{-4}	2.93×10^{-3}	3.89062×10^{-1}	9.7644×10^{-2}
0.88	3.3279×10^{-1}	1.65×10^{-3}	6.916×10^{-4}	2.93×10^{-3}	3.89540×10^{-1}	9.7851×10^{-2}
0.89	3.3365×10^{-1}	1.66×10^{-3}	6.971×10^{-4}	2.93×10^{-3}	3.89971×10^{-1}	9.8039×10^{-2}
0.90	3.3441×10^{-1}	1.67×10^{-3}	7.014×10^{-4}	2.92×10^{-3}	3.9035×10^{-1}	9.8204×10^{-2}
0.91	3.3504×10^{-1}	1.67×10^{-3}	7.044×10^{-4}	2.92×10^{-3}	3.9066×10^{-1}	9.8343×10^{-2}
0.92	3.3554×10^{-1}	1.67×10^{-3}	7.059×10^{-4}	2.91×10^{-3}	3.9091×10^{-1}	9.8453×10^{-2}
0.93	3.3587×10^{-1}	1.67×10^{-3}	7.057×10^{-4}	2.9×10^{-3}	3.9108×10^{-1}	9.8530×10^{-2}
0.94	3.3603×10^{-1}	1.6×10^{-3}	7.037×10^{-4}	2.9×10^{-3}	3.9116×10^{-1}	9.857×10^{-2}
0.95	3.3598×10^{-1}	1.6×10^{-3}	6.996×10^{-4}	2.8×10^{-3}	3.9113×10^{-1}	9.856×10^{-2}
0.96	3.3570×10^{-1}	1.6×10^{-3}	6.93×10^{-4}	2.8×10^{-3}	3.9099×10^{-1}	9.851×10^{-2}
0.97	3.3515×10^{-1}	1.6×10^{-3}	6.84×10^{-4}	2.7×10^{-3}	3.9071×10^{-1}	9.839×10^{-2}
0.98	3.3429×10^{-1}	1.6×10^{-3}	6.72×10^{-4}	2.7×10^{-3}	3.9029×10^{-1}	9.821×10^{-2}
0.99	3.3309×10^{-1}	1.5×10^{-3}	6.57×10^{-4}	2.6×10^{-3}	3.8969×10^{-1}	9.796×10^{-2}
1.00	3.315×10^{-1}	$1. \times 10^{-3}$	6.38×10^{-4}	$2. \times 10^{-3}$	3.889×10^{-1}	9.761×10^{-2}

PHILOSOPHICAL TRANSACTIONS OF THE ROYAL SOCIETY A MATHEMATICAL, PHYSICAL & ENGINEERING SCIENCES

TABLE A 9. THE PROPERTIES OF THE STEADY WAVE AS A FUNCTION OF THE EXPANSION PARAMETER ϵ^2 FOR $e^{-d} = 0.9$

ϵ^2	a	c^2	I	T	V	$\bar{\eta}$
0.0	0.0	1.04972×10^{-1}	0.0	0.0	0.0	0.0
0.10	3.80037×10^{-3}	1.09612×10^{-1}	1.34267×10^{-5}	2.22264×10^{-6}	2.18126×10^{-6}	4.05547×10^{-5}
0.20	7.16574×10^{-3}	1.14960×10^{-1}	3.75001×10^{-5}	6.35734×10^{-6}	6.12048×10^{-6}	1.10601×10^{-4}
0.30	1.07501×10^{-2}	1.20861×10^{-1}	7.1385×10^{-5}	1.24086×10^{-5}	1.1716×10^{-5}	2.05336×10^{-4}
0.40	1.463×10^{-2}	1.27330×10^{-1}	1.9552×10^{-4}	2.061×10^{-5}	1.908×10^{-5}	3.238×10^{-4}
0.50	1.88×10^{-2}	1.34381×10^{-1}	1.703×10^{-4}	3.123×10^{-5}	2.83×10^{-5}	4.65×10^{-4}
0.60	2.36×10^{-2}	1.41983×10^{-1}	2.36×10^{-4}	4.44×10^{-5}	3.98×10^{-5}	6.26×10^{-4}
0.70	2.87×10^{-2}	1.4998×10^{-1}	3.1×10^{-4}	6.0×10^{-5}	5.32×10^{-5}	8.0×10^{-4}
0.80	3.44×10^{-2}	1.578×10^{-1}	3.9×10^{-4}	7.8×10^{-5}	6.8×10^{-5}	9.9×10^{-4}
0.81	3.50×10^{-2}	1.585×10^{-1}	4.0×10^{-4}	8.0×10^{-5}	7.0×10^{-5}	9.9×10^{-4}
0.82	3.56×10^{-2}	1.592×10^{-1}	4.1×10^{-4}	8.2×10^{-5}	7.2×10^{-5}	1.0×10^{-3}
0.83	3.62×10^{-2}	1.599×10^{-1}	4.1×10^{-4}	8.4×10^{-5}	7.3×10^{-5}	1.0×10^{-3}
0.84	3.68×10^{-2}	1.606×10^{-1}	4.2×10^{-4}	8.6×10^{-5}	7.5×10^{-5}	1.0×10^{-3}
0.85	3.76×10^{-2}	1.613×10^{-1}	4.4×10^{-4}	$9. \times 10^{-5}$	7.7×10^{-5}	1.0×10^{-3}
0.86	3.8×10^{-2}	1.619×10^{-1}	4.4×10^{-4}	$9. \times 10^{-5}$	7.8×10^{-5}	1.1×10^{-3}
0.87	3.9×10^{-2}	1.624×10^{-1}	4.5×10^{-4}	$9. \times 10^{-5}$	$8. \times 10^{-5}$	1.1×10^{-3}
0.88	3.9×10^{-2}	1.630×10^{-1}	4.6×10^{-4}	$9. \times 10^{-5}$	$8. \times 10^{-5}$	1.1×10^{-3}
0.89	4.0×10^{-2}	1.634×10^{-1}	4.7×10^{-4}	$9. \times 10^{-5}$	$8. \times 10^{-5}$	1.1×10^{-3}
0.90	4.1×10^{-2}	1.638×10^{-1}	4.8×10^{-4}	1.0×10^{-4}	$8. \times 10^{-5}$	1.1×10^{-3}
0.91	4.1×10^{-2}	1.642×10^{-1}	$5. \times 10^{-4}$	1.0×10^{-4}	$9. \times 10^{-5}$	1.2×10^{-3}
0.92	4.2×10^{-2}	1.645×10^{-1}	$5. \times 10^{-4}$	1.0×10^{-4}	$9. \times 10^{-5}$	1.2×10^{-3}
0.93	4.3×10^{-2}	1.64×10^{-1}	$5. \times 10^{-4}$	1.0×10^{-4}	$9. \times 10^{-5}$	1.2×10^{-3}
0.94	4.3×10^{-2}	1.64×10^{-1}	$5. \times 10^{-4}$	1.0×10^{-4}	$9. \times 10^{-5}$	1.2×10^{-3}
0.95	4.4×10^{-2}	1.64×10^{-1}	$5. \times 10^{-4}$	1.1×10^{-4}	$9. \times 10^{-5}$	1.2×10^{-3}
0.96	4.5×10^{-2}	1.64×10^{-1}	$5. \times 10^{-4}$	1.1×10^{-4}	1.0×10^{-4}	1.3×10^{-3}
0.97	4.6×10^{-2}	1.64×10^{-1}	$5. \times 10^{-4}$	1.1×10^{-4}	1.0×10^{-4}	1.3×10^{-3}
0.98	4.6×10^{-2}	1.63×10^{-1}	$5. \times 10^{-4}$	1.1×10^{-4}	1.0×10^{-4}	1.3×10^{-3}
0.99	4.7×10^{-2}	1.62×10^{-1}	$6. \times 10^{-4}$	1.1×10^{-4}	1.0×10^{-4}	1.3×10^{-3}
1.00	4.8×10^{-2}	1.61×10^{-1}	$6. \times 10^{-4}$	1.1×10^{-4}	1.0×10^{-4}	1.3×10^{-3}

ϵ^2	K	S_{xx}	F	$\overline{u_b^2}$	R	S
0.0	1.04972×10^{-1}	0.0	0.0	0.0	1.57847×10^{-1}	1.66104×10^{-2}
0.10	1.09732×10^{-1}	6.47033×10^{-6}	1.44613×10^{-6}	3.91227×10^{-5}	1.60226×10^{-1}	1.71055×10^{-2}
0.20	1.15285×10^{-1}	1.80889×10^{-5}	4.18645×10^{-6}	1.04493×10^{-4}	1.63003×10^{-1}	1.76796×10^{-2}
0.30	1.21462×10^{-1}	3.4526×10^{-5}	8.2856×10^{-6}	1.8984×10^{-4}	1.66092×10^{-1}	1.83158×10^{-2}
0.40	1.28270×10^{-1}	5.609×10^{-5}	1.3976×10^{-5}	2.923×10^{-4}	1.69496×10^{-1}	1.90150×10^{-2}
0.50	1.35720×10^{-1}	8.32×10^{-5}	2.153×10^{-5}	4.08×10^{-4}	1.73221×10^{-1}	1.97787×10^{-2}
0.60	1.4378×10^{-1}	1.159×10^{-4}	3.12×10^{-5}	5.34×10^{-4}	1.7725×10^{-1}	2.06039×10^{-2}
0.70	1.5230×10^{-1}	1.54×10^{-4}	4.32×10^{-5}	6.6×10^{-4}	1.8152×10^{-1}	2.1475×10^{-2}
0.80	1.609×10^{-1}	1.96×10^{-4}	5.7×10^{-5}	7.8×10^{-4}	1.858×10^{-1}	2.2346×10^{-2}
0.81	1.617×10^{-1}	2.00×10^{-4}	5.9×10^{-5}	7.9×10^{-4}	1.862×10^{-1}	2.243×10^{-2}
0.82	1.625×10^{-1}	2.05×10^{-4}	6.0×10^{-5}	8.0×10^{-4}	1.866×10^{-1}	2.251×10^{-2}
0.83	1.633×10^{-1}	2.09×10^{-4}	6.2×10^{-5}	8.1×10^{-4}	1.871×10^{-1}	2.259×10^{-2}
0.84	1.641×10^{-1}	2.14×10^{-4}	6.3×10^{-5}	8.2×10^{-4}	1.875×10^{-1}	2.267×10^{-2}
0.85	1.649×10^{-1}	2.18×10^{-4}	6.5×10^{-5}	8.3×10^{-4}	1.878×10^{-1}	2.275×10^{-2}
0.86	1.657×10^{-1}	2.23×10^{-4}	6.6×10^{-5}	8.4×10^{-4}	1.882×10^{-1}	2.282×10^{-2}
0.87	1.664×10^{-1}	2.27×10^{-4}	6.8×10^{-5}	8.5×10^{-4}	1.886×10^{-1}	2.289×10^{-2}
0.88	1.671×10^{-1}	2.33×10^{-4}	6.9×10^{-5}	8.7×10^{-4}	1.890×10^{-1}	2.296×10^{-2}
0.89	1.678×10^{-1}	2.36×10^{-4}	7.1×10^{-5}	$9. \times 10^{-4}$	1.893×10^{-1}	2.302×10^{-2}
0.90	1.686×10^{-1}	2.4×10^{-4}	7.3×10^{-5}	$9. \times 10^{-4}$	1.897×10^{-1}	2.309×10^{-2}
0.91	1.691×10^{-1}	2.4×10^{-4}	7.4×10^{-5}	$9. \times 10^{-4}$	1.900×10^{-1}	2.315×10^{-2}
0.92	1.69×10^{-1}	2.5×10^{-4}	7.6×10^{-5}	$9. \times 10^{-4}$	1.90×10^{-1}	2.320×10^{-2}
0.93	1.70×10^{-1}	2.5×10^{-4}	7.7×10^{-5}	$9. \times 10^{-4}$	1.91×10^{-1}	2.325×10^{-2}
0.94	1.71×10^{-1}	2.6×10^{-4}	7.9×10^{-5}	$9. \times 10^{-4}$	1.91×10^{-1}	2.329×10^{-2}
0.95	1.71×10^{-1}	2.6×10^{-4}	8.0×10^{-5}	$9. \times 10^{-4}$	1.91×10^{-1}	2.332×10^{-2}
0.96	1.71×10^{-1}	2.7×10^{-4}	8.3×10^{-5}	$9. \times 10^{-4}$	1.91×10^{-1}	2.33×10^{-2}
0.97	1.72×10^{-1}	2.7×10^{-4}	8.4×10^{-5}	$9. \times 10^{-4}$	1.91×10^{-1}	2.336×10^{-2}
0.98	1.72×10^{-1}	2.8×10^{-4}	8.5×10^{-5}	$9. \times 10^{-4}$	1.92×10^{-1}	2.34×10^{-2}
0.99	1.73×10^{-1}	2.8×10^{-4}	8.7×10^{-5}	$9. \times 10^{-4}$	1.92×10^{-1}	2.34×10^{-2}
1.00	1.73×10^{-1}	2.8×10^{-4}	8.9×10^{-5}	$9. \times 10^{-4}$	1.92×10^{-1}	2.33×10^{-2}

PHILOSOPHICAL TRANSACTIONS OF THE ROYAL SOCIETY A MATHEMATICAL, PHYSICAL & ENGINEERING SCIENCES

References

Ahlberg, J. H., Nilson, E. N. & Walsh, J. L. 1967 *The theory of splines and their applications*. New York: Academic Press.

Airy, G. B. 1845 Tides and waves. In *Encyclopedia Metropolitan*. London.

Baker, G. A. 1965 The theory and application of the Padé approximant method. *Advances in theoretical physics* (ed. K. Brueckner), vol. 1, pp. 1–58. New York: Academic Press.

Benjamin, T. B. & Feir, J. E. 1967 The disintegration of wave trains on deep water. *J. Fluid Mech.* **27**, 417–430.

Benjamin, T. B. & Lighthill, M. J. 1954 On cnoidal waves and bores. *Proc. R. Soc. Lond.* A **224**, 448–460.

Burnside, W. 1915 On the modification of a train of waves as it advances into shallow water. *Proc. Lond. Math. Soc.* Series 2, **14** (1221), 131–133.

Byatt-Smith, J. G. B. & Longuet-Higgins, M. S. 1976 On the speed and profile of steep solitary waves. *Proc. R. Soc. Lond.* A **350**, 175–189.

Cokelet, E. D. 1976 Steady and unsteady nonlinear water waves. Ph.D. dissertation, Cambridge University.

De, S. C. 1955 Contributions to the theory of Stokes waves. *Proc. Camb. Phil. Soc.* **51**, 713–736.

Dean, R. G. 1965 Stream function representation of nonlinear ocean waves. *J. geophys. Res.* **70**, 4561–4572.

Dean, R. G. 1974 Evolution and development of water wave theories for engineering application. Vols. I and II. *Special report No.* 1, U.S. Army Coastal Engin. Res. Center, Fort Belvoir, Virginia.

Fenton, J. 1972 A ninth-order solution for the solitary wave. *J. Fluid Mech.* **53**, 257–271.

Grant, M. A. 1973 The singularity at the crest of a finite amplitude progressive Stokes wave. *J. Fluid Mech.* **59** 257–262.

Graves-Morris, P. R. (ed.) 1973 *Padé approximants and their applications*. London: Academic Press.

Krasovskii, Yu. P. 1961 On the theory of steady-state waves of finite amplitude. *Zh. Vych. Mat.* **1**, no. 5, 836–855. English translation: *USSR Comp. Math. & Math. Phys.* **4**, 996–1018.

Levi-Civita, T. 1925 Détermination rigoureuse des ondes permanentes d'ampleur finie. *Math. Ann.* **93**, 264–314.

Longuet-Higgins, M. S. 1975 Integral properties of periodic gravity waves of finite amplitude. *Proc. R. Soc. Lond.* A **342**, 157–174.

Longuet-Higgins, M. S. & Cokelet, E. D. 1976 The deformation of steep surface waves on water. I. A numerical method of computation. *Proc. R. Soc. Lond.* A **350**, 1–26.

Longuet-Higgins, M. S. & Fenton, J. D. 1974 On the mass, momentum, energy and circulation of a solitary wave. II. *Proc. R. Soc. Lond.* A **340**, 471–493.

Longuet-Higgins, M. S. & Fox, M. J. H. 1977 Theory of the almost-highest wave: The inner solution. *J. Fluid Mech.* **80**, 721–742.

Monkmeyer, P. L. & Kutzbach, J. E. 1966 A higher order theory for deep water waves. *Coastal Engineering, Santa Barbara Specialty Conference*, October 1965, pp. 301–326. American Society of Civil Engineers, New York.

Nekrasov, A. I. 1921 On waves of permanent type I. *Izv. Ivanovo-Voznesensk, Politekhn. Inst.* **3**, 52–65.

Phillips, O. M. 1966 *The dynamics of the upper ocean*. Cambridge University Press.

Rayleigh, Lord 1876 On waves. *Phil. Mag.* **1**, 257–279.

Sasaki, K. & Murakami, T. 1973 Irrotational progressive, surface gravity waves near the limiting height. *J. Ocean. Soc. Japan* **29**, 94–105.

Schwartz, L. W. 1972 Analytic continuation of Stokes' expansion for gravity waves. Ph.D. dissertation, Stanford University.

Schwartz, L. W. 1974 Computer extension and analytic continuation of Stokes' expansion for gravity waves. *J. Fluid Mech.* **62**, 553–578.

Stokes, G. G. 1847 On the theory of oscillatory waves. *Trans. Camb. Phil. Soc.* **8**, 441–455.

Stokes, G. G. 1880*a* Considerations relative to the greatest height of oscillatory waves which can be propagated without change of form. *Mathematical and physical papers*, vol. I, pp. 225–228, Cambridge University Press.

Stokes, G. G. 1880*b* Supplement to a paper on the theory of oscillatory waves. *Mathematical and physical papers*, vol. I, pp. 314–326. Cambridge University Press.

Struik, D. J. 1926 Détermination rigoureuse des ondes irrotationelles periodiques dans un canal à profondeur finie. *Math. Ann.* **95**, 595–634.

Thomas, J. W. 1975 A numerical study of the relationship between the dimensionless parameters in the problem of periodic waves of permanent type in a liquid of finite depth. *Q. appl. Math.* **32**, 403–410.

Van Dyke, M. 1974 Analysis and improvement of perturbation series. *Q. J. Mech. appl. Math.* **27**, 423–450.

Von Schwind, J. J. & Reid, R. O. 1972 Characteristics of gravity waves of permanent form. *J. geophys. Res.* **77**, 420–433.

Yamada, H. 1957 Highest waves of permanent type on the surface of deep water. *Rep. Res. Inst. appl. Mech., Kyushu Univ.* **5**, 37–52.

PHILOSOPHICAL TRANSACTIONS OF THE ROYAL SOCIETY A MATHEMATICAL, PHYSICAL & ENGINEERING SCIENCES